Structural Characterization of Vapor-deposited Organic Glasses

By

Ankit Gujral

A dissertation submitted in partial fulfillment of

the requirement for the degree of

Doctor of Philosophy

(Chemistry)

at the

UNIVERSITY OF WISCONSIN-MADISON

2017

Date of final oral examination: August 18, 2017.

The dissertation is approved by the following members of the Final Oral Committee:

Lian Yu, Professor, Pharmaceutical Sciences
Paul Evans, Professor, Materials Science and Engineering
Paul Voyles, Professor, Materials Science and Engineering
Nick Abbott, Professor, Chemical and Biological Engineering
Mark D. Ediger, Professor, Chemistry

To my family,

For their unconditional support through all my choices in life, no matter how absurd.

(Is there time to still become a musician?)

Acknowledgements

I would like to thank Professor Mark Ediger, my advisor, for his years of support. Mark has been a thoughtful and passionate advisor and leader. His leadership is commendable in, both, its effectiveness and humanity. It has been a privilege working with Mark, and I have grown professionally and personally because of it.

I am grateful to the members of my committee; I have learnt much from each of you over the years. I am fortunate to have counted Professor Lian Yu as a teacher, mentor and co-author for the last few years. Lian's careful analysis always makes me rethink assumptions in my work, leading to more thorough investigations. Professor Paul Evans was integral in helping incorporate X-ray scattering studies into our materials characterization toolkit. X-ray scattering, as can be seen by the content of this thesis, has played a crucial role in characterizing the materials discussed here. Professor Paul Voyles, who spearheaded the glass supergroup bringing together researchers from across campus, has helped broaden my understanding and appreciation for the field at large. Aside from the very useful conversations about liquid crystalline systems with Professor Nick Abbott, it has been inspiring watching him lead the UW MRSEC center through numerous site visits and grant renewals. My time involved in the MRSEC executive committee was perhaps the biggest learning experience outside of lab during my graduate school career.

The grazing incidence X-ray scattering work would not have been possible without the assistance of Dr. Michael F. Toney at the Stanford Synchrotron Radiation Lightsource, and Professor Michael Chabinyc along with his student Katie O'Hara at the University of California Santa Barbara. I am indebted to the Chabinyc group for sharing beamtime, a precious commodity, with us so we could collect preliminary data for our own proposals, and for their continued guidance in collecting and interpreting data.

I am very thankful to the Stanford Synchrotron community for the welcoming environment they have fostered that leads to open scientific exchanges. Casual conversations with Dennis Nordlund, Tim

Dunn, Badri Shyam and Chris Takacs led to numerous investigations and hopefully future collaborations with the Ediger group. The X-ray absorption spectroscopy results shared in this dissertation would not have been possible without Dennis' generosity with his time and expertise.

Closer to home, I was lucky enough to work with brilliant colleagues, Jaritza Gomez and Jing Jiang. The liquid crystal projects (parts of which are included in this body of work) would not have been a success without the coordinated effort of Jaritza and Jing. I am thankful to them for their openness in sharing results and their sense of humor that made coming to work a pleasure.

The Ediger research group has been a fun, safe, and productive place to work. I am very grateful to wonderful colleagues who made working together so enjoyable. Keep it glassy!

Table of Contents

Abstract

Physical vapor deposition, a common route of thin film fabrication for organic electronic devices, has recently been shown to produce organic glassy films with enhanced kinetic stability and anisotropic structure. Anisotropic structures are of interest in the organic electronics community as it has been shown that certain structures lead to enhanced device performance, such as higher carrier mobility and better light outcoupling. A mechanism proposed to explain the origin of the stability and anisotropy of vapor-deposited glasses relies on two parameters: 1) enhanced molecular mobility at the free surface (vacuum interface) of a glass, and 2) anisotropic molecular packing at the free surface of the supercooled liquid of the glass-forming system. By vapor-depositing onto a substrate maintained at $T_{substrate} < T_g$ (where T_g is the glass transition temperature), the enhanced molecular mobility at the free surface allows every molecule that lands on the surface to at least partially equilibrate to the preferred anisotropic molecular packing motifs before being buried by further deposition. The extent of equilibration depends on the mobility at the surface, controlled by $T_{substrate}$, and the residence time on the free surface, controlled by the rate of deposition. This body of work deals with the optimization of deposition conditions and system chemistry to prepare and characterize films with functional anisotropic structures.

Films of TPD, a rod-shaped molecule used as an organic semiconductor, were prepared by vapor deposition across a range of $T_{substrate}$, and grazing incidence X-ray scattering (GIXS) was used to characterize the molecular packing anisotropy in the films. It was determined that for films prepared at $T_{substrate} \sim .75\ T_g$ the molecules pack face-on while at $T_{substrate} \sim 0.95\ T_g$, the molecules have a slight preference for edge-on packing. Amorphous films resulted when deposited at $T_{substrate} \sim T_g$. These results not only confirmed recent optical measurements that could be used to infer average molecular orientation in films, but also extended the characterization by combining the optical and scattering observables to propose a molecular model of glass structure (with nearest-neighbor distance and average molecular orientations).

Liquid crystalline moieties were used to extend the range of structures accessible by vapor deposition, using both calamitic (rod-shaped) and discotic (disc-shaped) mesogens. Itraconazole, a calamitic mesogen that forms a smectic phase (molecular layers) above the glass transition temperature, T_g = 330 K, was used to prepare glasses by depositing at a range of $T_{substrate}$ = 0.78 T_g to 1.02 T_g. For $T_{substrate}$ near and below T_g, glasses with layered smectic-like structures could be prepared with smectic-like order, and layer spacing could be tuned by 16% through choice of $T_{substrate}$ as probed by GIXS. Films prepared at the lowest $T_{substrate}$ consisted of molecules trapped exclusively laying in-plane. Two columnar discotic systems (in which molecules self-assemble into columns that further assemble into hexagonal or rectangular superstructures) were also investigated. For both mesogens, phenanthroperylene-ester and triphenylene-ester, highly organized glasses could be prepared with either edge-on ($T_{substrate}$ ~ T_g) or face-on ($T_{substrate}$ ~ 0.75 T_g) packing. This contrasted with the glasses prepared using a non-mesogen, m-MTDATA that showed isotropic ($T_{substrate}$ ~ T_g) or slightly face-on ($T_{substrate}$ ~ 0.75 T_g) packing. The mechanism to explain the origin on anisotropy in vapor-deposited glasses was empirically extended to mesogenic systems based on the results from the smectic and columnar systems investigated.

The empirical extension of the proposed mechanism requires that the mesogenic disc-shaped systems exhibit edge-on molecular orientation at the vacuum interface of the equilibrium liquid while the non-mesogen exhibit a slightly face-on orientation to prepare the bulk structures observed in the previous study. This was experimentally tested using Near-edge X-ray Absorption Fine Structure (NEXAFS) spectroscopy, for phenanthroperylene-ester, one of the columnar discotic systems investigated above, and m-MTDATA, the non-mesogen disc-shaped system. The equilibrium free surface of the mesogen exhibited an average molecular orientation of 64° from the plane of the substrate, while the free surface of a liquid-cooled glass of m-MTDATA exhibited an average orientation of about 38°, consistent with the qualitative predictions made when applying the mechanism to explain the bulk structures the vapor-deposited glasses.

Chapter 1

Anisotropic organic glasses: An introduction

Ankit Gujral

Introduction.

This introductory chapter outlines recent developments in the preparation of organic glasses with anisotropic structure, with an emphasis on preparing materials for organic electronic device applications. Much of the work undertaken during my graduate career has been driven by a growing need to prepare organic solids for organic electronics. In particular, my work has focused on controlling molecular packing in organic glasses by physical vapor deposition. Below, I will discuss the motivation behind doing so, its implications in device performance, and literature precedent to highlight its importance. Content from this chapter will be added to content by co-authors Mark D. Ediger and Lian Yu towards an article to be published in a forthcoming issue of Current Opinion in Solid State and Materials Science (Elsevier) focusing on glassy materials.

Organic glasses are widely used on industrial scales from foods[1] to pharmaceuticals[2] and organic electronic devices.[3] Recently, organic glasses have found a niche in device engineering with their ubiquitous presence in cellphone displays[4] and growing popularity in television displays[5] in the form of organic light emitting diodes (OLEDs). There have also been developments in organic field effect transistors (OFETs)[6–9] and organic photovoltaics (OPVs),[10–17] leading towards flexible and printable electronics. Organic materials are well suited towards these applications as chemistry can be manipulated to prepare n-type and p-type semiconductors.[18] Glassy organics within the active layers in devices have advantages over their crystalline counterparts for a few reasons: including the fact that glassy thin films can be fabricated over large surface areas without grain boundaries that act as charge traps,[19] their composition can be tuned nearly infinitely[20,21] allowing for homogeneous multicomponent films with variable dopant concentration, and their structures can potentially be manipulated to engineer molecular packing motifs for specific applications. It is the last of these, preparing anisotropic molecular packing structures in glasses (i.e., glasses with a biased subset of possible molecular orientations and nearest-neighbor correlations) that this article focusses on.

Anisotropic molecular packing in these devices plays a crucial role in device performance, in both crystalline and glassy systems. A single crystal pentacene-based OFET, for instance, exhibits highly anisotropic charge carrier mobilities, relative to the axis of charge propagation.[22] This was attributed to the efficiency of charge hopping from one molecule to the next being greater along certain axes in the crystal: Charge transport in molecular systems depends on electron orbital overlap between adjacent molecules to facilitate charge hopping.[18] In pentacene it was shown that the charge transport is highest along the herringbone structure in the crystal lattice. Similarly for sexithienyl it was found that a co-facial molecular packing arrangement was most efficient.[23] In a disordered glass, the random nature of nearest-neighbor interactions creates a tumultuous path for charges to be transported through. And while certain crystalline structures do provide excellent charge transport properties,[22–24] the limitations described above, particularly traps in grain boundaries, currently make these materials challenging to produce for mass market adoption. Even for emitters in OLEDs, careful choice of molecular orientation of the dilute emitter molecule in the matrix can increase light outcoupling efficiency by nearly 30% when compared to an isotropic film.[25] More molecules with a preferential in-plane orientation leads to more efficient emission of light out of the device. This enhancement is due only to geometry and not due to a modification in the electronic states of the film.

Glasses are generally thought of as isotropic materials, but structural anisotropy is not incompatible with a lack of crystalline order. When a glass is prepared by cooling a liquid, an isotropic material results. This occurs as the system is cooled to the point of molecular-scale kinetic arrest below the glass transition temperature, T_g (defined in terms of a structural relaxation time, τ_α, of 100 s, or viscosity, η, of ~10^{12} Pa.s);[26] the structure of the kinetically arrested material is inherited from the disordered liquid from which it was formed. However, as non-equilibrium solids, the details in the route to preparation (such as thermal history, or the presence of external forces) are important in determining the properties of the glass. If asymmetric routes of preparation are adopted, the resulting glass structure may be anisotropic. For instance, deforming a polymeric glass,[27] whereby the glassy solid is stretched (sometimes by as much as

twice the original sample length) leads to a molecular scale rearrangement in which polymer chains are stretched along the direction of the strain. Another way to produce anisotropic glasses is to apply an external field to the liquid of a polar molecule, leading to an anisotropic liquid.[28] Upon cooling such a liquid, the anisotropic structure gets trapped into a glassy state (and is maintained even after the external field has been removed). Spin-coating[29] can induce anisotropic structures into polymeric films, as well, due to the centrosymmetric shear present as solvent evaporates and the film is cast while spinning. Many other routes to preparing glasses with anisotropic molecular packing have been explored recently from using polypeptide-assisted self-assembly,[30] to blade-coating.[31]

While many promising strategies are being developed, we are compelled to limit the scope of our exploration in this article. We will explore 4 routes towards preparing films with anisotropic molecular packing: 1) anisotropic polymer films prepared by spin-coating , 2) physical vapor deposition as a route to anisotropic molecular packing in small-molecule glasses, 3) the use of liquid crystalline moieties as a route to glassy self-assembled structures, and finally 4) combining elements of the last two strategies to prepare highly anisotropic out-of-equilibrium (glassy) solids by vapor-depositing low molecular weight liquid-crystalline mesogens. Our discussion will be driven by how these techniques are being exploited to better device performance in various organic electronic applications.

Anisotropic structures in high-molecular weight polymeric systems

Ever since the 1977 discovery by Heeger, MacDiarmid and Shirakawa[32] of conductivity in polyacetylene (for which they were awarded the Nobel Prize in Chemistry in 2000)[33], there has been a spur of research to optimize charge carrier mobility in organic materials. Experimental investigations and theoretical models[34] indicate that there are two processes to charge transport in a polymeric glass: the fast charge transport mechanism along the covalently-bonded chain, and the slower molecular hopping between chains. It is, therefore, important to prepare materials with ordered interchain structures to increase delocalization by π-conjugation between chains. These interchain structures, as we will explore

below, can have very subtle nearest-neighbor correlations. In this section, we will first discuss a recent meta-analysis that shows how anisotropic structures can exhibit better charge carrier mobility than semi-crystalline or completely isotropic amorphous structures primarily due to nearest-neighbor interactions. We will then explore this concept further through two recent studies.

To explore how short-range interactions may lead to long-range charge transport, Noriega et al.[13] compiled metadata from 13 high molecular weight polymeric systems. The systems were categorized by the researchers into three broad classifications: 1) "semi-crystalline," 2) "poorly ordered" or anisotropic, and 3) "amorphous" or isotropic. Roughly speaking, anisotropic structures have at least enough short-range order to exhibit anisotropic scattering in grazing-incidence X-ray scattering experiments; they lie somewhere between semi-crystalline systems and isotropic systems in the order-disorder continuum of structures. Prior to this study, and similar ones, the prevailing wisdom indicated that semi-crystalline systems exhibited highest carrier mobility due to highly ordered domains of materials. This is reflected in the low activation energy (72 meV) for transport in the films (derived from temperature-dependent FET measurements). But according to this analysis, the boundaries between the highly crystalline structures act as traps, causing a worsening of performance. Anisotropic systems, on the other hand, exhibited similar activation energies to semi-crystalline systems (76 meV) and due to the lack of grain boundaries, did not exhibit any low energy traps that would impede charge transport. Isotropic films had a much higher activation energy (~230 meV) of transport, ruling them out as efficient charge transport materials. To illustrate the principles laid out by Noriega et al. in their large meta-analysis, we will explore two examples of poorly ordered systems below. The first study will let us compare the performance of a poorly ordered film and a semi-crystalline film of the same system, a naphthalene-thiophene copolymer. The second will let us compare the poorly ordered material compared with the disordered material of the same system, a carbazole.

Rivnay et al.[12] recently showed that poorly ordered films outperform highly crystalline films of a high molecular weight polymeric system. They showed that texture and order could be drastically

controlled in an n-type polymeric semiconductor, poly{[*N*,*N*-9-bis(2-octyldodecyl)naphthalene-1,4,5,8-bis(dicarboximide)-2,6-diyl]-alt-5,59-(2,29-bithiophene)}, abbreviated to P(NDI2OD-T2). A spin-coated film exhibited 77.5% face-on packing and very low crystallinity, as determined by X-ray scattering. Upon annealing these films, the morphology changed drastically to 94.6% edge-on lamellar structure accompanied with twice as much crystallinity, as well as a 40% decrease of disorder within crystallites. Figure 1 shows scattering patterns obtained from the as-cast film and the annealed film. Despite the increase in overall order in the films, a significant drop in current density in the bulk is observed; there is little modification to the FET transport along the bottom interface even after the increase in order. According to the researchers, this indicates that the enhanced crystallite order and texture play a secondary role in transport phenomena in this system. The researchers were careful to point out that it is possible the structure at the interface isn't modified in the same way as the bulk material, perhaps complicating interpretation of the OFET transport. While there is ambiguity in the interpretation of the interface charge transport, the bulk findings here are in line with the observations of Noriega et al.

Figure 1.

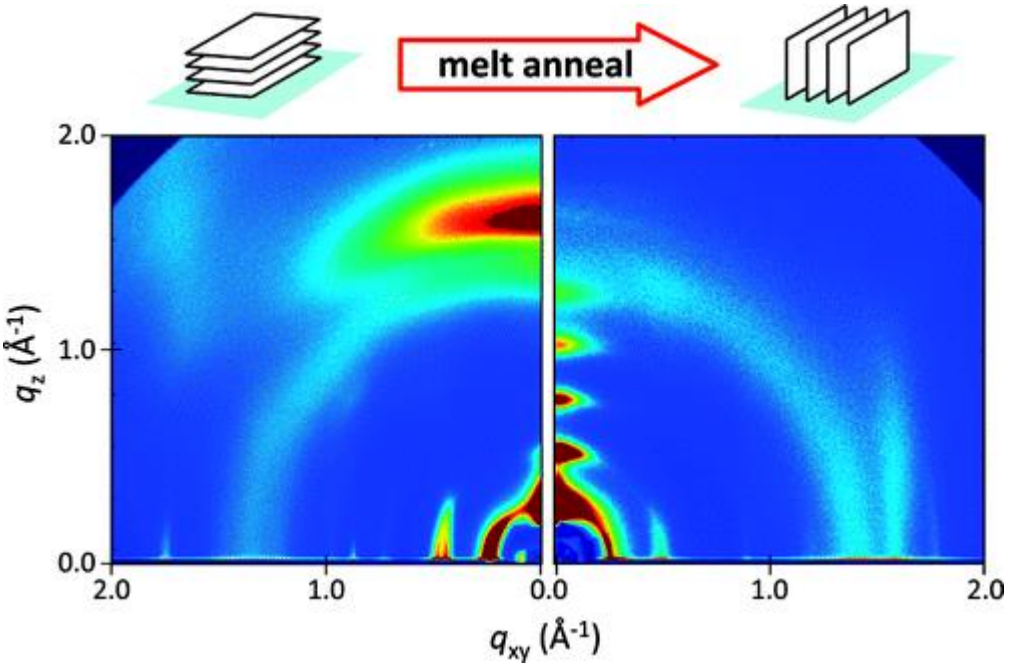

Figure 1. Scattering obtained from an as-cast (left) and annealed (right) film of P(NDI2OD-T2). The vector q_z represents scattering out-of-plane while q_{xy} represents scattering in-plane. The high intensity peak at q_z~1.6 Å^{-1} is indicative of out-of-plane pi-pi stacking in the as-case film that is no longer as prominent upon annealing. This is discussed further in the text. Reproduced from Rivnay et al. 2011.[12]

Beiley et al.[35] showed that the weak short-range interactions of a poorly ordered film outperform an amorphous film of poly[N-9″-hepta-decanyl-2,7-carbazole-alt-5,5-(4′,7′-di-2-thienyl-2′,1′,3′-benzothiadiazole)], abbreviated to PCDTBT. The as-cast film exhibits a prominent out-of-plane peak corresponding to a space of d = 4.0 Å, and is inferred as an out-of-plane pi-pi stacking motif. By contrast, upon annealing that same feature suggests a broadening of nearest-neighbor correlations, indicative of a decrease in coherence length of pi-pi stacking. The observed decrease in structural order coincides with worsening hole transport, perhaps due to the introduction of deeper hole-traps between conjugated domains. This study, too, is consistent with Noriega et al,'s interpretation of structure-mobility relationships in polymeric films.

Similarly, Zhang et al.[36] investigated a rigid copolymer based on indacenodithiophene-benzothiadiazole backbone, with a reported mobility of up to 3.6 $cm^2V^{-1}s^{-1}$. The researchers argue that the rigid backbone leads to two molecular-scale packing motifs that lead to high charge transport: 1) most transport occurs along the rigid backbone with high delocalization and 2) the interchain interactions are highly lamellar, leading to short range π-stacking which is enough to effectively bridge the gap between the chains. This molecular packing motif was observed even in non-crystalline films by X-ray scattering and X-ray spectroscopy.

Physical vapor deposition as a route to anisotropic glasses

Without the advantage of polymeric chains, low molecular weight glasses rely solely on charge hopping between molecules. Increasing the charge transfer integral between neighboring molecules can be achieved by increasing electron orbital overlap. π-conjugated systems, with highly delocalized electrons, have been employed to this end. Remarkably, however, a very low degree of anisotropy in the molecular packing motifs is required to increase electron delocalization, just as in the case of anisotropic polymeric systems discussed in Section 1. The general advantages of disordered glassy materials (like lack of grain

boundaries) can therefore be exploited while simultaneously increasing mobility. Long range order, like in a three-dimensional (3D) crystal, is not required but rather just require a preferential molecular stacking direction. In this section, we will discuss physical vapor deposition as a route to such structurally anisotropic glasses by providing an illustrative example, discussing a proposed mechanism for the origin of anisotropy, and providing examples of enhanced device performance in both single- and two-component systems.

Physical vapor deposition has been shown to prepare organic glasses with structural anisotropy as well as remarkable kinetic stability. These properties can be controlled as a function of the substrate temperature during deposition ($T_{substrate}$). Ediger and coworkers have shown this dependence for a number of systems with varying molecular shapes and chemistries.[37–44] For instance, Gujral et al.[39] prepared vapor deposited glasses of TPD, *N,N′*-bis(3-methylphenyl)-*N,N′*-diphenylbenzidine, a common rod-shaped p-type (hole) transport material, with good glass-forming ability (T_g = 330 K). The TPD glasses prepared ranged from molecular packing arrangements that were highly face-on when $T_{substrate}$ is maintained at ~0.7 T_g during deposition, to slightly edge-on when $T_{substrate}$ = 0.95 T_g, as probed by X-ray scattering (and average molecular orientation determined by spectroscopic ellipsometry). A grazing incidence X-ray scattering pattern and corresponding structure schematic of a glass deposited at $T_{substrate}$ = 0.79 T_g is reproduced in Figure 2. These glasses also exhibited remarkable kinetic stability when compared to a liquid-cooled glass of TPD, potentially increasing the lifetime of the devices in which they are used.

Figure 2

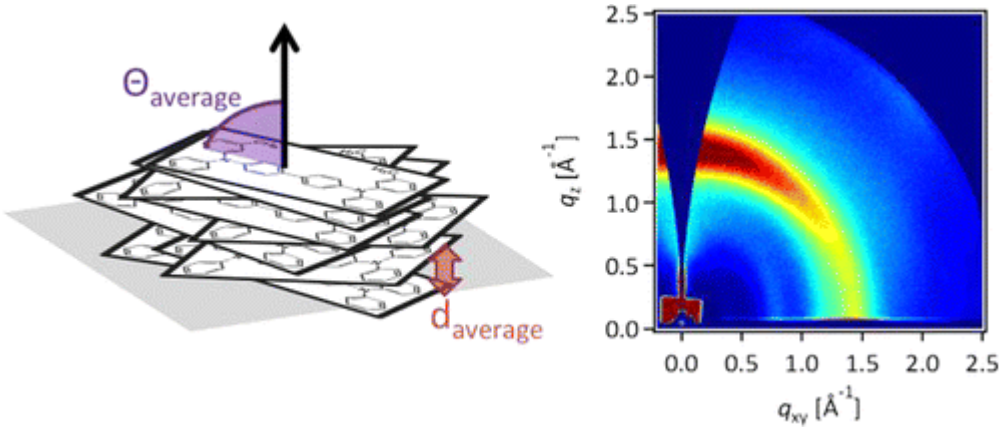

Figure 2. A glass of TPD prepared by physical vapor deposition at $T_{substrate}$ = 0.79 T_g, exhibiting face-on molecular packing. $d_{average}$ = 4.5 Å and $\theta_{average}$ = 69° from substrate normal for the schematic shown. The scattering pattern was obtained by grazing incidence X-ray scattering, with vector q_z corresponding to out-of-plane scattering and q_{xy} corresponding to in-plane scattering. Reproduced from Gujral et al. 2015.[39]

A mechanism[42] has been proposed to determine the origin of the structural anisotropy and kinetic stability of vapor-deposited glasses. The mechanism relies on the system exhibiting two properties: 1) enhanced molecular mobility on the free surface of the glass and 2) an anisotropic structure on the free surface of the equilibrium supercooled liquid of the system. When depositing onto a substrate maintained at $T_{substrate} < T_g$, every molecule that is deposited is, for a brief residence time, at the free surface of the glass before getting buried by further deposition. During this residence time, the molecule, due to the enhanced mobility at the free surface, can partially equilibrate to a lower energy configuration before being buried by the oncoming set of molecules. This leads to a bulk glass with every molecule having partially equilibrated during the deposition process, resulting in glasses with enhanced kinetic stability (and lower enthalpy). To explain the anisotropy, one must consider the preferred orientation of the molecules at the free surface as it is partially equilibrating. To gain insight into the sort of orientations TPD would adopt near the free surface of its liquid, coarse-grained and atomistic molecular dynamics (MD) simulations[42,45] were performed. It was found from the MD simulations that at the very top monolayer of the liquid, the molecules adopted a face-on orientation, while in the next layer down a slight edge-on orientation was preferred. Below this layer, the molecules exhibited an isotropic distribution of orientations, as expected in a bulk liquid of TPD. Returning back to our description of the deposition, at very low $T_{substrate}$, only the very top monolayer has the mobility to rearrange and partially equilibrate, leading to a preferred face-on orientation being trapped into the bulk of the film upon further deposition. And, at intermediate $T_{substrate}$, the mobility extends to the second monolayer, allowing every molecule deposited to equilibrate to the edge-on orientation found in the second monolayer. This is consistent with the experimental findings reproduced here in Figure 2, with $T_{substrate} = 0.7\ T_g$ exhibiting face-on packing.

To show that the anisotropy exhibited in vapor-deposited films leads to enhanced device performance we turn to a study by Yokoyama et al.[46] Using a similar physical vapor deposition preparation technique as described above, the researchers explored the relationship between bulk molecular orientation and charge carrier mobility. Films of BSB-Cz, 4,4’-bis[(N-carbazole)styryl]biphenyl, a rod-shaped

molecular semiconductor, were prepared by vapor deposition on indium tin oxide (ITO) substrates. The films were found to be either optically isotropic or anisotropic depending on $T_{substrate}$, as probed by spectroscopic ellipsometry. The anisotropic glass was inferred to have a highly directional average molecular orientation with molecules laying "flat" in the plane of the device. (This result is consistent with the proposed mechanism, since at room temperature $T_{substrate} = 0.77\ T_g$, leading to preferred face-on packing arrangement that is observed with the optical technique as a "lying flat" in-plane orientation). The researchers found that the charge carrier mobility increased roughly threefold in Time-of-Flight (TOF) measurements in the highly anisotropic material when compared with the isotropic film, to about 10^{-3} $cm^2V^{-1}s^{-1}$. For comparison, single-crystalline pentacene[22] has been reported at roughly 0.5-2.0 $cm^2V^{-1}s^{-1}$. This enhancement was attributed to an overall increase in the overlap between the HOMOs and LUMOs of adjacent molecules in the anisotropic film, based on Marcus theory[47] (i.e., a formalism of thermally activated hopping between molecules).

Similarly, Xing et al.[48] compared vapor-deposited and solution-processed films of TCTA, tris(4-carbazoyl-9-ylphenyl)amine, a p-type (hole) organic semiconductor. Preferential face-on packing, with a nearest-neighbor distance corresponding to a π-π stacking motif, was observed in the vapor-deposited film, as probed by X-ray scattering. This contrasted with the solution processed film that exhibited disordered, isotropic packing. Between the two, the vapor-deposited film consistently outperformed the solution-processed film, with higher current density across the entire range of voltages measured by the authors. The rationale for higher current density was the increased delocalization of electrons along the π-π stacking direction. It should be noted that the temperature of the substrate during deposition ($T_{substrate}$) was maintained at ambient conditions in this study. Relative to T_g (424 K), room temperature would indicate $T_{substrate} \sim 0.7\ T_g$. Applying the proposed mechanism to explain the anisotropy observed in the TCTA films, one would expect[45] highly face-on packing, as observed, when deposited at low $T_{substrate}$.

Another factor that may play a role in the enhancement of performance in vapor-deposited glasses is the increased densities of deposited glasses (by up to ~1.5%[38,42] when compared with liquid-cooled

glasses of the same systems). While it is ambiguous, molecular orientation alone may not be enough to increase carrier mobility, and an increase in density may also play a role in the increased charge transfer integrals between neighboring molecules that lead to more efficient transport.[49] This is a subject worthy of further investigation.

Dilute two-component systems play a key role in OLED design. In certain types of OLED devices, the light emitting molecule is a dilute component within a charge carrier matrix.[50] Light outcoupling efficiency can be increased by controlling the molecular orientation of the emitter molecules in active layers of devices. Molecules emit light perpendicular to their transition dipole moments, so having control of average molecular orientation allows for more efficient emission when compared with a random distribution of molecular dipoles. The usefulness of this type of anisotropy in two-component systems can be illustrated by turning again to an investigation by Yokoyama.[25] As shown in Figure 3, a preferred horizontal orientation of molecular dipoles can be beneficial to light outcoupling for the geometry of most OLED devices. This can be achieved by vapor deposition and solution processing, and is expected to increase light outcoupling efficiency by 30%. This enhancement is remarkable as it requires no modification of the chemistry or geometry of the device, especially as the external quantum efficiency (EQE) of OLEDs approaches its theoretical limit.

Jiang et al.[20] recently studied two-component glasses of Alq_3, aluminum-tris(8-hydroxyquinoline, and DSA-Ph, 1,4-di-[4-(N,N-diphenyl)amino]styryl-benzene. Alq_3 is a roughly spherical molecule, while DSA-Ph is a rod-shaped molecule that has previously been reported to exhibit highly anisotropic structures in single-component glasses[42] prepared by vapor deposition. The researchers showed that, regardless of the relative composition of the two components, glasses prepared by vapor deposition could be prepared with an anisotropic average molecular orientation of DSA-Ph molecules from 47° to 75° from the substrate normal. (Owing to the symmetry of the Alq_3 molecule, it has an isotropic response in the experiments conducted). The molecular orientation of DSA-Ph in the mixture was controlled, as with the single-

component systems explored previously, by the substrate temperature during deposition relative to the glass transition temperature *of the mixture*. It is important to note here that a nearly infinite variation in composition can be accessed between DSA-Ph and Alq_3 (or, more generally, between any emitter and host). This variability is unique to non-equilibrium solids that, unlike their crystalline counterparts, are not limited to a set number of available polymorphs or co-crystals.

Figure 3.

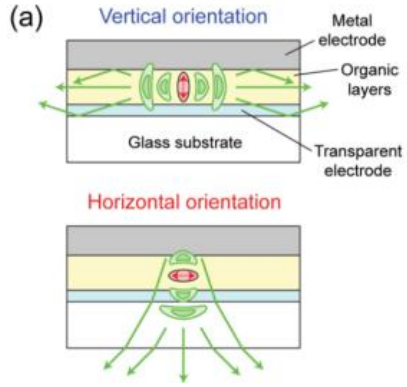

Figure 3. Schematic showing the difference between an emitting molecule with a vertical or horizontal orientation within the emitting layer of an OLED device. Reproduced from Yokoyama 2011.[25]

Glasses of liquid crystals

Liquid crystalline systems, with their tendency to self-assemble, make for very promising candidates to prepare organic solids with anisotropic molecular packing. For high charge mobility applications, columnar discotic mesogens, which form columnar superstructures along π electron-rich aromatic cores, have been exploited.[51] Similarly, for tunable optical properties, chiral mesogens have been exploited.[52] Liquid crystals, however, tend to crystallize upon undercooling, leading to polycrystalline solids. Polycrystallinity, as discussed in the introduction, leads to poor charge transport, as well as light scattering in the case of optical materials. To counter this, rational molecular design principles have been established to prepare films that avoid crystallization while still forming ordered mesophases. Moreover, these mesophases can be trapped into a kinetically arrested (glassy) solid in ambient conditions. Liquid crystals that could be trapped into glassy solids were observed as far back as the early 1970s.[53,54] These systems undergo a glass transition upon cooling from an equilibrium liquid crystalline phase, leading to a solid with liquid crystal-like structure. Since those initial observations, molecular design rules have been used to prepare useful mesophases that can be kinetically arrested into glassy films that are stable at room temperature.

In this section, first we will explore how these systems have been used to develop a fundamental understanding of the relationship between molecular packing and charge transfer. We will then provide examples of efficiency-driven engineering of out-of-equilibrium films with high carrier mobility for organic electronic applications and optimized optical properties for photonic devices.

Molecular design principles were used in one recent study of discotic molecular systems by Feng et al. to achieve a mobility of 0.2 $cm^2V^{-1}s^{-1}$ [55] (similar to reported mobilities of single crystalline pentacene[22] at 0.5 - 2 $cm^2V^{-1}s^{-1}$), with a claim that mobilities in excess of 10 $cm^2V^{-1}s^{-1}$ were achievable if defect-free films could be prepared. To highlight the importance of nearest-neighbor packing arrangements, the authors synthesized a number of discotic systems with peripheral functional groups of a

coronene-derivative core. The peripheral functional groups were either hydrophobic or hydrophilic positioned so as to control the azimuthal rotation angle between nearest neighbors and, on a larger scale, the helical pitch along the columnar superstructure. The overlap integral was found to be very sensitive to the azimuthal angle, even though the nearest-neighbor distances were found to be similar across all the systems investigated. This study highlights the importance of carefully controlling molecular packing anisotropy to optimize device performance.

Kelber et al.[56] have recently designed a hexagonal discotic mesophase that is trapped in a glassy state at room temperature. The aim of the investigation was to prepare a molecular system that struck a balance between avoiding crystallization while exhibiting highly ordered liquid crystalline mesophases frozen into a glassy state at room temperature, all without increasing the molecular weight of the system. Molecular weight is an important parameter as this would allow for the system to be vapor-deposited, a common route to preparing thin films for organic electronic devices. The researchers achieved this by preparing a molecule with two aromatic cores that were slightly distorted due to steric hindrance between the functional groups of the cores. This was realized in a [4]-helicene with a perylene extension carbonyl substituents. The material would form large domains (roughly 0.1 mm across) when cooled through the liquid-to-LC phase transition. The researchers also note the ability to tune the electronic properties of the product, by synthetically replacing a subset of the electron-withdrawing carbonyl groups with electron-donating amines, for instance.

Cholesteric liquid crystals form handed chiral domains potentially useful for polarizers, optical notch filters and reflectors.[57,58] To illustrate the importance of the glassy nature of these materials, we will discuss an optical reflector developed by Chen.[59] The system investigated was a chiral molecule with a 1,3,5-benzenetricarboxylic acid core. The chirality controls the handedness of the helical domains prepared in equilibrium (and trapped into the glass upon cooling). The pitch of the helices controls the wavelength of light preferentially reflected. By varying the relative composition of the two chiralities, **I**-*S* and **I**-*R*, it was found that the wavelengths of light preferentially reflected could be tuned, as shown in Figure 4.

Owing to the solid's glassy state, the composition could be varied nearly infinitely, allowing for careful choice of macroscopic reflector properties.

Figure 4.

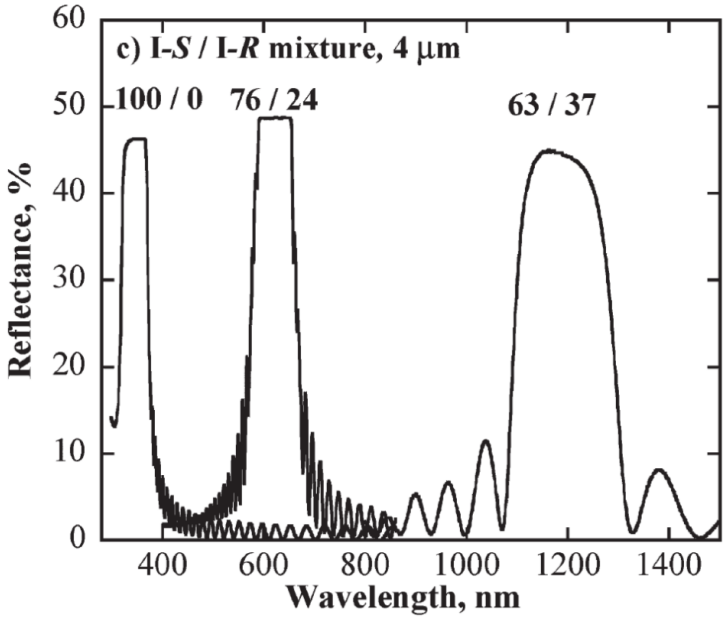

Figure 4. The reflectance spectra of the same molecules with different compositions of the two chiralities in a 4-micron glassy film. Reproduced from Shaw 2004.[59]

Vapor-deposited liquid crystalline films

In Sections 2 and 3, we discussed two different strategies to prepare glasses of small organic molecules with anisotropic molecular packing. The first, physical vapor deposition, relied on rearrangement of molecules at the free surface of the film during deposition; this led to anisotropic but disordered structures that could vary from face-on to slightly edge-on, depending on deposition conditions. The second relied on self-assembly of liquid crystalline moieties in the bulk material; this led to structures that were very similar to equilibrium structures quenched into a kinetically arrested glassy solid. In this section, we will discuss a strategy combining elements from both: vapor-depositing liquid crystal-forming molecules. Phenomenology from both will be applied to explain the wide variety of highly ordered structures accessible, from face-on to highly edge-on columnar packing motifs.

Recently, Gujral et al.[60] showed range of packing motifs accessible by vapor deposition of three disc-shaped molecules. Two of the three systems were mesogens that formed columnar discotic mesophases, phenanthroperylene-ester (T_g = 392 K) and triphenylene-ester (T_g ~ 310 K); those will be the focus of this discussion. The researchers found that when depositing at $T_{substrate}$ near the glass transition temperature, the glasses prepared for both systems exhibited highly ordered columnar packing, with columns propagating in-plane (i.e., parallel to the free surface). Deposited at $T_{substrate} \sim 0.75\ T_g$, the glasses of both systems showed a preferred face-on packing. Schematics of these have been reproduced in Figure 5, for clarity. The researchers also showed that highly ordered vapor-deposited films of phenanthroperylene-ester exhibited the same electron delocalization, at least on a local level, as observed in a glass of the system cooled from the equilibrium mesophase. This was inferred from the observation that the red-shift associated with an annealed film and a highly ordered vapor-deposited film were the same, when compared with a disordered film of phenanthroperylene-ester. The highly ordered domains were hundreds of nm large, based on the topology of the films. The researchers also confirmed that the vapor-deposited films were glassy (out-of-equilibrium) solids by observing that the structures of the films evolved just above the glass transition temperature (and over 100 K below the crystalline melting point). In

addition, the lack of mixed-index peaks in the X-ray scattering of the films, and the comparison with powder diffraction collected from the equilibrium crystalline solids indicates that these films are structurally dissimilar to the crystalline material.

Figure 5.

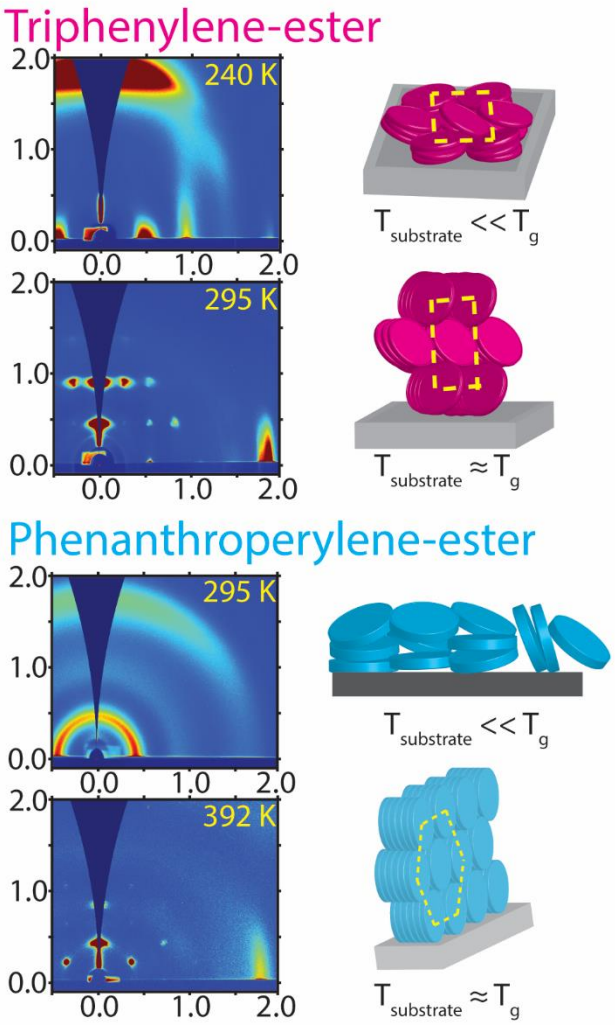

Figure 5. Two-dimensional X-ray scattering patterns alongside schematics of glasses of triphenylene-ester and phenanthroperylene-ester as a function of $T_{substrate}$. The top panels in each correspond to $T_{substrate}$ ~ 0.75 T_g, while the bottom corresponds to $T_{subsrate}$ ~ 0.75 T_g. Reproduced from Gujral et al. 2017 (submitted).[60]

The structures observed in the study above can be explained in terms of the mechanism put forth in Section 2 to explain the origin of structural anisotropy in vapor-deposited glasses, along with additional features of liquid crystal phenomenology. In liquid crystals, it has been observed for a variety of discotic mesogens that the free surface of the equilibrium liquid induces edge-on molecular orientation. In addition to this, the molecules also rearrange to highly ordered columns; since the molecules are preferentially edge-on, the columns that are formed propagate in-plane (parallel to the free surface). Returning to the vapor deposition process, based on the mechanism put forth, explaining the origin of structural anisotropy, the free surface must exhibit 1) molecular mobility and 2) anisotropic molecular packing/orientation. The anisotropic molecular structures at the free surface can be trapped into the bulk of the film by vapor deposition. For low $T_{substrate}$ depositions, molecules land on the free surface and do not have the mobility to rearrange before being trapped into the bulk by further deposition. One can infer from this that when the molecules initially land on the free surface, they adopt a face-on orientation (perhaps to reduce the surface energy of the interface) which is trapped into the bulk upon further deposition. At high $T_{substrate}$, the molecules have enough mobility to rearrange at the free surface before the next set of deposited molecules buried it into the bulk. As indicated for other liquid crystal discotic systems, the preferred orientation is edge-on, so these molecules strive towards an edge-on orientation at high $T_{substrate}$. This is consistent with the results from Gujral et al. where, for both mesogenic systems, edge-on molecular packing is observed throughout the bulk of the systems.

Eccher et al.[61] prepared discotic liquid crystalline films by vapor deposition and spin-coating that were incorporated into devices. Using the devices, the researchers extracted a charge carrier mobility for the films. The substrate temperature during deposition was not actively controlled; depositing the material, a diimidodiester derivative of benzo[*ghi*]perylene, at room temperature led to a slightly disordered edge-on packing. Even though the deposition conditions were not optimized for a specific packing motif, the vapor-deposited films outperformed the highly disordered spin-coated films, but fared worse than spin-coated films that had been annealed for an extended period.

A structural investigation on a smectic mesogen, itraconazole,[40,62] was conducted vapor-deposited films were characterized as a function of $T_{substrate}$ during deposition. It was found that glasses of itraconazole with smectic-like layering could be attained by deposited at $T_{substrate} > T_g$. Interestingly, just below T_g, for intermediate $T_{substrate}$ values, the smectic-like layer spacing decreased monotonically as a function of $T_{substrate}$ (and these smectic-like structures were trapped into glassy solids that were stable in ambient conditions). At the lowest $T_{substrate}$ investigated, the molecules preferentially lie face-on, in the plane of the substrate. This, too, can phenomenologically be explained in terms of the proposed mechanism for the origin of anisotropy in vapor-deposited films. The preferred packing for the material at a vacuum interface is edge-on (smectic layers are parallel to the free surface). Upon depositing, molecules are initially face-on (to reduce surface energy, it is conjectured). For the very lowest $T_{substrate}$ glasses that the researchers prepared, the molecules do not have the mobility required to rearrange to the preferred edge-on packing before further deposition buries them into the bulk. At intermediate $T_{substrate}$, the molecules partially equilibrate and self-assemble towards a smectic-like layering, but do not quite achieve the equilibrium structure before getting buried by oncoming molecules. For the highest $T_{substrate}$ glasses prepared by the researchers, the molecules have the mobility after being deposited to completely equilibrate; the glass prepared under these conditions has the same layer spacing as an annealed film of itraconazole cooled into a glass.

The above studies suggest the proposed mechanism to explain the origin of structural anisotropy in vapor-deposited glasses may be generally applied to other liquid crystal systems that undergo a glass transition. This phenomenon may be used by researchers to engineer films with molecular packing motifs tailored for specific applications.

Concluding remarks

Through this article, we hope we have illustrated not only the technological importance of anisotropic organic glasses but the wide variety of techniques being developed to optimize anisotropic molecular packing. We would like to reiterate that the scope of this article was focused on a small subsection of the work currently underway. The recent uptick in interest in this problem has been very enriching for the entire community, not only from the perspective of fundamental glass science, but also an engineering one, as organic electronic devices penetrate further into mass market use. Vapor deposition, already used in large-scale manufacture of organic devices, has played a central role in this development. There is more to be exploited by combining vapor deposition with other self-assembly techniques, perhaps through the use of external fields during deposition, or modified substrate interactions, among others.

References

(1) Hartel, R. W.; Ergun, R.; Vogel, S. Phase/State Transitions of Confectionery Sweeteners: Thermodynamic and Kinetic Aspects. *Compr. Rev. Food Sci. Food Saf.* **2011**, *10* (1), 17–32.

(2) Grohganz, H.; Löbmann, K.; Priemel, P.; Tarp Jensen, K.; Graeser, K.; Strachan, C.; Rades, T. Amorphous Drugs and Dosage Forms. *J. Drug Deliv. Sci. Technol.* **2013**, *23* (4), 403–408.

(3) Facchetti, A. Made to Order: Organic Semiconductors. *Nat. Mater.* **2013**, *12* (July), 598–600.

(4) Chansin, G.; Ghaffarzadeh, K.; Zervox, H. *OLED Display Forecasts 2016-2026: The Rise of Plastic and Flexible Displays: IDTechEx*; 2016.

(5) Wilcox, J. K. Trends to Watch for in 2017 - Consumer Reports https://www.consumerreports.org/lcd-led-oled-tvs/5-tv-trends-to-follow-in-2017/ (accessed Aug 2, 2017).

(6) Van Breemen, A. J. J. M.; Herwig, P. T.; Chlon, C. H. T.; Sweelssen, J.; Schoo, H. F. M.; Setayesh, S.; Hardeman, W. M.; Martin, C. a.; De Leeuw, D. M.; Valeton, J. J. P.; Bastiaansen, C. W. M.; Broer, D. J.; Popa-Merticaru, A. R.; Meskers, S. C. J. Large Area Liquid Crystal Monodomain Field-Effect Transistors. *J. Am. Chem. Soc.* **2006**, *128* (7), 2336–2345.

(7) Tsao, H. N.; Cho, D.; Andreasen, J. W.; Rouhanipour, A.; Breiby, D. W.; Pisula, W.; Müllen, K. The Influence of Morphology on High-Performance Polymer Field-Effect Transistors. *Adv. Mater.* **2009**, *21*, 209–212.

(8) Honsho, Y.; Miyakai, T.; Sakurai, T.; Saeki, A.; Seki, S. Evaluation of Intrinsic Charge Carrier Transport at Insulator-Semiconductor Interfaces Probed by a Non-Contact Microwave-Based Technique. *Sci. Rep.* **2013**, *3*, 3182.

(9) Horowitz, B. G. Organic Field-Effect Transistors. **1998**, No. 5, 365–377.

(10) Park, H. K.; Schriver, K. E.; Haglund, R. F. Resonant Infrared Laser Deposition of Polymer-Nanocomposite Materials for Optoelectronic Applications. *Appl. Phys. A Mater. Sci. Process.* **2011**, *105*, 583–592.

(11) Embracing the Organics World. *Nat. Mater.* **2013**, *12* (July), 591.

(12) Rivnay, J.; Steyrleuthner, R.; Jimison, L. H.; Casadei, A.; Chen, Z.; Toney, M. F.; Facchetti, A.; Neher, D.; Salleo, A. Drastic Control of Texture in a High Performance N-Type Polymeric Semiconductor and Implications for Charge Transport. *Macromolecules* **2011**, *44* (13), 5246–5255.

(13) Noriega, R.; Rivnay, J.; Vandewal, K.; Koch, F. P. V; Stingelin, N.; Smith, P.; Toney, M. F.; Salleo, A. A General Relationship between Disorder, Aggregation and Charge Transport in Conjugated Polymers. **2013**.

(14) Kim, J. W.; Kim, H. J.; Kim, T.-M.; Kim, T. G.; Lee, J.-H.; Kim, J. W.; Kim, J.-J. High Performance Organic Planar Heterojunction Solar Cells by Controlling the Molecular Orientation. *Curr. Appl. Phys.* **2013**, *13*, 7–11.

(15) Lu, C.; Chen, H.-C.; Chuang, W.-T.; Hsu, Y.-H.; Chen, W.-C.; Chou, P.-T. Interplay of Molecular Orientation, Film Formation, and Optoelectronic Properties on Isoindigo- and Thienoisoindigo-Based Copolymers for Organic Field Effect Transistor and Organic Photovoltaic Applications. *Chem. Mater.* **2015**, *27* (19), 6837–6847.

(16) Schmidt-Mende, L.; Fechtenkötter, A.; Müllen, K.; Moons, E.; Friend, R. H.; MacKenzie, J. D.

Self-Organized Discotic Liquid Crystals for High-Efficiency Organic Photovoltaics. *Science* **2001**, *293* (5532), 1119–1122.

(17) Walba, D. M.; Clark, N. A.; Korblova, E.; Callahan, R. A.; Richardson, J. M.; Moran, M.; Rochelle, T. M.; Shoemaker, R. K.; Yoon, D. K.; Maclennan, J.; Glaser, M.; Zhu, C.; Chen, D.; Shao, R.; Coffin, D.; Rumbles, G. THE B4 BANANA PHASE FOR ORGANIC PHOTOVOLTAICS. **2010**, *2099* (2005), 11704.

(18) Ando, S.; Nishida, J.; Fujiwara, E.; Tada, H.; Inoue, Y.; Tokito, S.; Yamashita, Y. Novel P- and N-Type Organic Semiconductors with an Anthracene Unit. *Chem. Mater.* **2005**, *17* (6), 1261–1264.

(19) Bolognesi, A.; Berliocchi, M.; Manenti, M.; DiCarlo, A.; Lugli, P.; Lmimouni, K.; Dufour, C. Effects of Grain Boundaries, Field-Dependent Mobility, and Interface Trap States on the Electrical Characteristics of Pentacene TFT. *IEEE Trans. Electron Devices* **2004**, *51* (12), 1997–2003.

(20) Jiang, J.; Walters, D. M.; Zhou, D.; Ediger, M. D. Substrate Temperature Controls Molecular Orientation in Two-Component Vapor-Deposited Glasses. *Soft Matter* **2016**, *12* (13), 3265–3270.

(21) Whitaker, K. R.; Scifo, D. J.; Ediger, M. D.; Ahrenberg, M.; Schick, C. Highly Stable Glasses of *Cis* -Decalin and *Cis* / *Trans* -Decalin Mixtures. *J. Phys. Chem. B* **2013**, *117* (42), 12724–12733.

(22) Lee, J. Y.; Roth, S.; Park, Y. W. Anisotropic Field Effect Mobility in Single Crystal Pentacene. *Appl. Phys. Lett.* **2006**, *88* (25), 252106.

(23) Brédas, J. L.; Calbert, J. P.; da Silva Filho, D. a; Cornil, J. Organic Semiconductors: A Theoretical Characterization of the Basic Parameters Governing Charge Transport. *Proc. Natl. Acad. Sci. U. S. A.* **2002**, *99* (9), 5804–5809.

(24) Takeya, J.; Goldmann, C.; Haas, S.; Pernstich, K. P.; Ketterer, B.; Batlogg, B. Field-Induced Charge Transport at the Surface of Pentacene Single Crystals: A Method to Study Charge Dynamics of 2D Electron Systems in Organic Crystals. **2003**.

(25) Yokoyama, D. Molecular Orientation in Small-Molecule Organic Light-Emitting Diodes. *J. Mater. Chem.* **2011**, *21* (48), 19187–19202.

(26) Angell, C. A.; Ngai, K. L.; McKenna, G. B.; McMillan, P. F.; Martin, S. W. Relaxation in Glassforming Liquids and Amorphous Solids. *J. Appl. Phys.* **2000**, *88* (6), 3113.

(27) Choy, C. L. Thermal Conductivity of Polymers. *Polymer (Guildf).* **1977**, *18* (April 1976), 984–1004.

(28) Karbovnyk, I. D.; Olenych, I.; Kukhta, I. N.; Lugovskii, A.; Sasnouski, G.; Chutora, T.; Luchechko, A. P.; Khalakhan, I.; Kukhta, A. Electric Field Oriented Nanostructured Organic Thin Films with Polarized Luminescence. *J. Fluoresc.* **2009**, *19* (6), 989–996.

(29) Nardes, A. M.; Kemerink, M.; Janssen, R. A. J.; Bastiaansen, J. A. M.; Kiggen, N. M. M.; Langeveld, B. M. W.; van Breemen, A. J. J. M.; de Kok, M. M. Microscopic Understanding of the Anisotropic Conductivity of PEDOT:PSS Thin Films. *Adv. Mater.* **2007**, *19* (9), 1196–1200.

(30) Rosu, C.; Tassone, C. J.; Chu, P.-H.; Balding, P. L.; Gorman, A.; Hernandez, J. L.; Hawkridge, M.; Roy, A.; Negulescu, I. I.; Russo, P. S.; Reichmanis, E. Polypeptide-Assisted Organization of π-Conjugated Polymers into Responsive, Soft 3D Networks. *Chem. Mater.* **2017**, *29* (12), 5058–5062.

(31) Diao, Y.; Tee, B. C.-K.; Giri, G.; Xu, J.; Kim, D. H.; Becerril, H. a; Stoltenberg, R. M.; Lee, T. H.; Xue, G.; Mannsfeld, S. C. B.; Bao, Z. Solution Coating of Large-Area Organic Semiconductor Thin Films with Aligned Single-Crystalline Domains. *Nat. Mater.* **2013**, *12* (7), 665–671.

(32) Chiang, C. K.; Fincher, C. R.; Park, Y. W.; Heeger, A. J.; Shirakawa, H.; Louis, E. J.; Gau, S. C.; MacDiarmid, A. G. Electrical Conductivity in Doped Polyacetylene. *Phys. Rev. Lett.* **1977**, *39* (17), 1098–1101.

(33) The Nobel Prize in Chemistry 2000 https://www.nobelprize.org/nobel_prizes/chemistry/laureates/2000/ (accessed Jul 26, 2017).

(34) Coropceanu, V.; Cornil, J.; Da, D. A.; Filho, S.; Olivier, Y.; Silbey, R.; Brédas, J.-L. Charge Transport in Organic Semiconductors. *Chem. Rev.* **2007**, *107*, 926–952.

(35) Beiley, Z. M.; Hoke, E. T.; Noriega, R.; Dacuña, J.; Burkhard, G. F.; Bartelt, J. A.; Salleo, A.; Toney, M. F.; McGehee, M. D. Morphology-Dependent Trap Formation in High Performance Polymer Bulk Heterojunction Solar Cells. *Adv. Energy Mater.* **2011**, *1* (5), 954–962.

(36) Zhang, X.; Bronstein, H.; Kronemeijer, A. J.; Smith, J.; Kim, Y.; Kline, R. J.; Richter, L. J.; Anthopoulos, T. D.; Sirringhaus, H.; Song, K.; Heeney, M.; Zhang, W.; Mcculloch, I.; Delongchamp, D. M. Molecular Origin of High Field-Effect Mobility in an Indacenodithiophene–benzothiadiazole Copolymer. *Nat. Commun.* **2013**, *4*.

(37) Dawson, K. J.; Zhu, L.; Yu, L.; Ediger, M. D. Anisotropic Structure and Transformation Kinetics of Vapor-Deposited Indomethacin Glasses. *J. Phys. Chem. B* **2011**, *115* (3), 455–463.

(38) Dalal, S. S.; Fakhraai, Z.; Ediger, M. D. High-Throughput Ellipsometric Characterization of Vapor-Deposited Indomethacin Glasses. *J. Phys. Chem. B* **2013**, *117* (49), 15415–15425.

(39) Gujral, A.; O'Hara, K. A.; Toney, M. F.; Chabinyc, M. L.; Ediger, M. D. Structural Characterization of Vapor-Deposited Glasses of an Organic Hole Transport Material with X-Ray Scattering. *Chem. Mater.* **2015**, *27* (9), 3341–3348.

(40) Gujral, A.; Gómez, J.; Jiang, J.; Huang, C.; O'Hara, K. A.; Toney, M. F.; Chabinyc, M. L.; Yu, L.; Ediger, M. D. Highly Organized Smectic-like Packing in Vapor-Deposited Glasses of a Liquid Crystal. *Chem. Mater.* **2017**, *29*, 849–858.

(41) Laventure, A.; Gujral, A.; Lebel, O.; Pellerin, C.; Ediger, M. D. Influence of Hydrogen Bonding on the Kinetic Stability of Vapor-Deposited Glasses of Triazine Derivatives. *J. Phys. Chem. B* **2017**, *121* (10), 2350–2358.

(42) Dalal, S. S.; Walters, D. M.; Lyubimov, I.; de Pablo, J. J.; Ediger, M. D. Tunable Molecular Orientation and Elevated Thermal Stability of Vapor-Deposited Organic Semiconductors. *Proc. Natl. Acad. Sci. U. S. A.* **2015**, *112* (14), 4227–4232.

(43) Gomez, J.; Gujral, A.; Huang, C.; Bishop, C.; Yu, L.; Ediger, M. D. Non-Liquid Crystal Former Can Form Nematic-like Stable Glasses by PVD. *To be Submitt.* **2016**.

(44) Dawson, K.; Kopff, L. A.; Zhu, L.; McMahon, R. J.; Yu, L.; Richert, R.; Ediger, M. D. Molecular Packing in Highly Stable Glasses of Vapor-Deposited Tris-Naphthylbenzene Isomers. *J. Chem. Phys.* **2012**, *136* (9), 94505.

(45) Walters, D. M.; Antony, L.; de Pablo, J. J.; Ediger, M. D. Influence of Molecular Shape on the Thermal Stability and Molecular Orientation of Vapor-Deposited Organic Semiconductors. *J. Phys. Chem. Lett.* **2017**, *Accepted*.

(46) Yokohama, D.; Setoguchi, Y.; Sakaguchi, A.; Suzuki, M.; Adachi, C. Orientation Control of Linear-Shaped Molecules in Vacuum-Deposited Organic Amorphous Films and Its Effect on Carrier Mobilities. *Adv. Funct. Mater.* **2010**, *20*, 386–391.

(47) Marcus, R. A. On the Theory of Oxidation-Reduction Reactions Involving Electron Transfer. I. *J. Chem. Phys.* **1956**, *24* (5), 966–978.

(48) Xing, X.; Zhong, L.; Zhang, L.; Chen, Z.; Qu, B.; Chen, E.; Xiao, L. Essential Differences of Organic Films at the Molecular Level via Vacuum Deposition and Solution Processes for Organic Light- Emitting Diodes. *J. Phys. Chem. C* **2013**, *117*, 25405–25408.

(49) Antony, L. W.; Jackson, N. E.; Lyubimov, I.; Vishwanath, V.; Ediger, M. D.; de Pablo, J. J. Influence of Vapor Deposition on Structural and Charge Transport Properties of Ethylbenzene Films. *ACS Cent. Sci.* **2017**, *3* (5), 415–424.

(50) Yersin, H. Triplet Emitters for OLED Applications. Mechanisms of Exciton Trapping and Control of Emission Properties; Springer, Berlin, Heidelberg; pp 1–26.

(51) Sergeyev, S.; Pisula, W.; Geerts, Y. H. Discotic Liquid Crystals: A New Generation of Organic Semiconductors. *Chem. Soc. Rev.* **2007**, *36* (12), 1902–1929.

(52) Chen, H. P.; Ou, J. J.; Chen, S. H. Glassy Liquid Crystals as Self-Organized Films for Robust Optoelectronic Devices. In *Nanoscience with Liquid Crystals*; Li, Q., Ed.; Springer International Publishing, 2014; pp 179–208.

(53) Suga, H.; Seki, S. Thermodynamic Investigation on Glassy States of Pure Simple Compounds. *J. Non. Cryst. Solids* **1974**, *16* (2), 171–194.

(54) Sorai, M.; Seki, S. Heat Capacity of N-(*O* -Hydroxy- *P* -Methoxybenzylidene)- *P* -Butylaniline: A Glassy Nematic Liquid Crystal. *Mol. Cryst. Liq. Cryst.* **1973**, *23* (3–4), 299–327.

(55) Feng, X.; Marcon, V.; Pisula, W.; Hansen, M. R.; Kirkpatrick, J.; Grozema, F.; Andrienko, D.; Kremer, K.; Müllen, K. Towards High Charge-Carrier Mobilities by Rational Design of the Shape and Periphery of Discotics. *Nat. Mater.* **2009**, *8* (5), 421–426.

(56) Kelber, J.; Achard, M.-F.; Durola, F.; Bock, H. Distorted Arene Core Allows Room-Temperature Columnar Liquid-Crystal Glass with Minimal Side Chains. *Angew. Chemie Int. Ed.* **2012**, *51* (21), 5200–5203.

(57) Kim, C.; Marshall, K. L.; Wallace, J. U.; Chen, S. H. Photochromic Glassy Liquid Crystals Comprising Mesogenic Pendants to Dithienylethene Cores. *J. Mater. Chem.* **2008**, *18* (46), 5592.

(58) Wei, S. K. H.; Chen, S. H. Spatially Resolved Lasers Using a Glassy Cholesteric Liquid Crystal Film with Lateral Pitch Gradient. *Appl. Phys. Lett.* **2011**, *98* (11), 111112.

(59) Chen, S. H. Multifunctional Glassy Liquid Crystals for Photonics. *J. Soc. Inf. Disp.* **2004**, *12* (3), 205.

(60) Gujral, A.; Gomez, J.; Ruan, S.; Toney, M. F.; Bock, H.; Yu, L.; Ediger, M. D. Preparing Highly Organized Glasses of Discotic Liquid Crystalline Systems by Vapor Deposition. *Chem. Mater. submitted*.

(61) Eccher, J.; Zajaczkowski, W.; Faria, G. C.; Bock, H.; von Seggern, H.; Pisula, W.; Bechtold, I. H. Thermal Evaporation versus Spin-Coating: Electrical Performance in Columnar Liquid Crystal OLEDs. *ACS Appl. Mater. Interfaces* **2015**, *7* (30), 16374–16381.

(62) Gómez, J.; Jiang, J.; Gujral, A.; Huang, C.; Yu, L.; Ediger, M. D. Vapor Deposition of a Smectic Liquid Crystal: Highly Anisotropic, Homogeneous Glasses with Tunable Molecular Orientation. *Soft Matter* **2016**, *12* (11), 2942–2947.

Chapter 2

Structural characterization of vapor-deposited glasses of an organic hole transport material with X-ray scattering

Ankit Gujral, Kathryn A. O'Hara, Michael F. Toney,

Michael L. Chabinyc, M. D. Ediger

Published in *Chemistry of Materials*, 27 (9), 3341-3348, **2015**.

Abstract

Vapor-deposited organic glasses can be produced with enhanced thermal stability and tunable molecular orientation by controlling the substrate temperature during deposition. Recent work has also shown improved charge carrier mobility associated with anisotropic molecular packing in organic electronics. Here grazing-incidence wide angle x-ray scattering (GIWAXS) is used to characterize the structural anisotropy in glasses of a hole transport material, N, N'-bis (3-methylphenyl)-N, N'-diphenylbenzidine, commonly known as TPD, prepared by physical vapor deposition at substrate temperatures between 0.79 T_g and 0.98 T_g, where T_g is the glass transition temperature. A GIWAXS-derived orientation order parameter is used to quantify the anisotropy observed in the scattering patterns of the glasses. The GIWAXS-order parameter exhibits both positive and negative values as a function of substrate temperature, indicating face-on and edge-on packing, and correlates well with a spectroscopic ellipsometry-derived order parameter that is sensitive to molecular orientation. We propose molecular packing arrangements based on the combination of the two order parameters and explore the relationship between kinetic stability and glass structure.

Introduction

Amorphous materials are extensively utilized as active layers in organic electronic devices. Both low molecular weight and polymeric glasses are used as semiconducting materials in a range of devices including organic photovoltaics, thin film transistors, and organic light emitting diodes (OLEDs).[1–4] In OLEDs, for example, glasses are used both as transport layers for electrons and holes, and as hosts for emitters;[5] in this last application, the compositional flexibility of glasses plays a critical role. One of the advantages that a glass has over its crystalline counterpart is the lack of grain boundaries that can act as traps for charges in polycrystalline films, and thus reduce the efficiency of a device. Glasses are also macroscopically homogeneous, making them ideal for devices requiring smooth films covering large areas. On a local scale, the disordered structure of glasses is not ideal as local variations in packing lead to non-uniform electronic coupling between neighboring molecules that create a distribution of electronic states that limit charge transport.[6] However, because glasses are non-equilibrium materials and can be prepared in a wide range of different structures, it may be possible to identify preparation routes that make glasses which are better suited for charge transport.

Recently, considerable work has been focused on achieving improved charge mobility for both low molecular weight and polymeric glasses through the use of anisotropic structures. [7–15] A desirable packing for improved charge carrier efficiency involves π orbital overlaps, which can lead to a large charge transfer integral, in the direction of transport.[6] For molecules with extended conjugation, this intermolecular overlap can generally be improved through locally anisotropic packing. In semiconducting polymers this is well known; for example the use of thermal annealing of a polymer into a liquid-crystalline phase to increase anisotropic order can lead to significant increase in charge carrier mobility upon subsequent crystallization.[9] In other examples, crystalline order is not essential for enhancement in charge carrier mobility. For instance, a recent study shows that an indacenodithiophene–benzothiadiazole copolymer can achieve very high charge mobility due to locally anisotropic structures even in the absence of high crystallinity.[10] For low molecular weight systems, several groups have developed methods to

induce anisotropic order into semiconducting thin films using external fields,[16] zone casting,[12] solution shearing[13] and solvent vapor annealing.[14] A liquid-crystalline hexabenzocoronene derivative, for instance, has been magnetically aligned creating a highly anisotropic structure with increased charge carrier mobility.[16] In a related example, mobility was observed to increase by five orders of magnitude along columns of a discotic liquid crystal system after homeotropic columnar alignment created a highly anisotropic microstructure.[15]

Physical vapor deposition, a technique widely used in the commercial fabrication of amorphous active layers for OLEDs, has been shown to produce anisotropic glasses in which molecular orientation is not random. By controlling the temperature of the substrate ($T_{substrate}$) during the deposition process, molecular orientation can be controlled in the deposited film.[17,18,19,20] For molecules of roughly linear shape, the long molecular axis tends to lie in the plane of the device for low substrate temperatures while at higher substrate temperatures the long axis has a tendency to be perpendicular to the substrate plane.[19] Yokoyama et al.[20] measured charge mobility in glasses of BSB-Cz, a light emitting molecule used in OLEDs. They reported that deposition conditions that led to planar orientations of the molecular long axis increased electron mobility by nearly an order of magnitude relative to a glass with nearly isotropic orientation. While this work certainly supports the general idea that anisotropic packing can increase charge mobility, molecular orientation is an incomplete measure of structure and tells us little about how neighboring molecules interact with each other in the film. To gain a better understanding of molecular packing and electronic coupling, a structural probe is required. X-ray scattering techniques have been widely implemented as a structural tool for organic thin films,[21,22,23,24,25] including the aforementioned study on BSB-Cz,[20] as well as a GIWAXS study on vapor-deposited DBP:C60 films utilized in organic solar cells.[26]

Here we use grazing incidence wide-angle x-ray scattering (GIWAXS) to study the structural anisotropy in vapor-deposited glasses of TPD, a hole transport material commonly used in OLEDs. We investigate glasses deposited at six substrate temperatures between 0.79 T_g and 0.98 T_g, and compare these results

with experiments on a liquid-cooled glass of TPD. A GIWAXS-derived orientation order parameter[27] is used to quantify the anisotropy observed in the scattering patterns of the glasses for wavevectors corresponding to nearest-neighbor packing ($q \approx 1.4$ Å $^{-1}$). To our knowledge, this is the first use of GIWAXS to systematically study the structure of vapor-deposited organic glass thin films as a function of substrate temperature during deposition. We complement the GIWAXS measurements with conventional wide angle x-ray scattering (WAXS) experiments in order to more fully characterize an unusual scattering feature at low wavevector. Vapor deposition of TPD films has previously been shown to produce glasses with remarkably enhanced thermal stability[28] and the present experiments provide an opportunity to explore the structural basis for this stability.

We find that the GIWAXS-derived order parameter for TPD glasses depends significantly upon the substrate temperature during deposition, exhibiting both positive and negative values. The order parameter from GIWAXS is highly correlated with a previously-reported order parameter[19] characterizing molecular orientation, derived from spectroscopic ellipsometry. Based on both order parameters, we suggest a qualitative model of molecular packing in TPD glasses. In particular, deposition near 0.72 T_g produces glasses in which the molecules have a tendency to exhibit "face on" stacking. None of the vapor-deposited glasses show sharp diffraction peaks and it is clear that the remarkable kinetic stability exhibited by some of these TPD glasses is not a result of crystallinity. TPD glasses deposited onto substrates near 0.91 T_g show anisotropic scattering at $q \approx 0.4$ Å $^{-1}$ and we characterize the range of substrate temperatures for which this scattering is significant.

Experimental Methods

Sample Preparation: Glasses of TPD (Sigma-Aldrich, 99% purity, used without further purification) were prepared by physical vapor deposition at a deposition rate of 0.2 ± 0.02 nm/s in a high vacuum environment (base pressure ~10^{-7} torr) at UW-Madison.

For the GIWAXS samples, TPD was deposited onto the substrate, a <100> cut silicon wafer, which was maintained at the desired temperature throughout the deposition process. A liquid-cooled sample was prepared by transforming a vapor-deposited film to the metastable supercooled liquid state by ramping the sample to 350 K (T_g+20 K) and cooling at a controlled rate of 1 K/min under flowing nitrogen. All the GIWAXS samples were 100 – 130 nm thick.

Samples for wide angle x-ray scattering (WAXS) were prepared with a previously described[18] temperature gradient stage that utilizes two independently controlled thermal stages, held at different temperatures. A rectangular <100> cut silicon substrate bridges the two stages, thereby setting up a temperature gradient across the substrate, with the maximum and minimum temperatures set by the temperatures at the stages. Deposition occurs while the temperature gradient is maintained across the substrate, yielding a library of glasses deposited at different substrate temperatures. The precise substrate temperature corresponding to each position on a temperature gradient sample was calibrated by comparing optical properties of the glasses on the gradient sample with the optical properties of isothermally prepared glasses;[18] the optical properties were measured by spectroscopic ellipsometry. The absolute error in substrate temperature is estimated to be less than 2 K. The WAXS samples were 1.5 to 2.5 microns thick.

GIWAXS Measurements: GIWAXS measurements were conducted on vapor-deposited glasses of TPD at the Stanford Synchrotron Radiation Lightsource (SSRL) at beam line 11-3 in grazing incidence geometry. The beam has a wavelength (λ) of 0.973 Å, and the beam line is equipped with a MAR345 area detector. For the data presented here, the incidence angle was varied from 0.12°-0.20°. The samples were kept under He atmosphere during x-ray exposure to reduce scatter from atmospheric gases. Typical exposure times for these samples ranged from 50-200 s. The samples were shipped from UW-Madison, and the optical properties of the samples were measured before and after the GIWAXS experiments using spectroscopic ellipsometry to ensure the samples had not degraded in transit or due to exposure to the x-ray beam.

The data was extracted using the WxDiff Integration Tool software package (SSRL, 2010) using established data processing techniques.[29] The diffraction pattern from polycrystalline LaB_6 was used to calibrate the sample-to-detector distance and beam center. Due to the nearly completely horizontal polarization of the x-ray beam from the synchrotron source, a polarization correction (98%) was applied to the data. A χ correction was applied to the data to get an accurate reciprocal space map from the MAR345 flat area detector.[21] Below we compare scattering along q_{xy} and q_z for vapor-deposited TPD glasses (see Figure 4). For this purpose, we integrate the corrected scattering data in a χ slice between 71°-85° to obtain q_{xy} and between 11°-25° to obtain q_z. (χ = 0° along q_z).

High-throughput WAXS Measurements: WAXS measurements were conducted on vapor-deposited glasses of TPD on a Bruker D8 Discover diffraction instrument, with an Inconel 625 alloy knife-edge installed to block air scatter. The instrument is equipped with a Cu K-alpha x-ray source (λ= 1.54 Å) and a VANTEC500 area detector. The incident angle was fixed at 2° and the exposure time for each measurement was 1800 s. The WAXS measurements were performed on the temperature gradient samples (described above) that contain glasses deposited across a ~ 40 K range of substrate temperatures. Every point along the length of the sample corresponds to a glass deposited at a different substrate temperature and 9 or 10 spots were measured per sample. Three samples with overlapping temperature ranges were studied. With a temperature gradient that spans a 40 K range across a 3.2 cm substrate, a WAXS measurement performed with a 2 mm collimator produces data that averages results from glasses with a 2.5 K range of substrate temperatures.

To compare results from the two scattering experiments, data are expressed as a function of the scattering vector, $q = (4\pi/\lambda)\sin\theta$, where θ is half the scattering angle and λ is the wavelength of the incident x-ray beam. q is related to a real-space periodicity by $d = 2\pi/q$.

Results and Discussion

GIWAXS Measurements

Figure 1 shows GIWAXS diffraction patterns obtained from TPD glasses vapor-deposited at several characteristic substrate temperatures. Particular substrate temperatures were chosen based upon published ellipsometry experiments, which characterized these glasses in terms of kinetic stability and average molecular orientation.[19] A coordinate system is defined for the scattering vector q associated with the GIWAXS patterns, with q_z defined as the component of q in the specular direction (perpendicular to the substrate) and q_{xy} defined as the q component parallel to the substrate. q_x and q_y are treated as equivalent because the samples are isotropic in the xy-plane. The isotropic order in-plane was confirmed by the observation that rotating vapor-deposited samples in the xy-plane caused no change in the GIWAXS or WAXS measurements; a similar result has been obtained using variable angle spectroscopic ellipsometry (VASE).[19]

Glasses of TPD prepared by vapor deposition exhibit different local packing structures depending on the substrate temperature during deposition. Interpreting the GIWAXS patterns in Figure 1 allows for a qualitative picture of the structure of these glasses. A point of reference when studying the structural anisotropy of amorphous materials is the structure associated with the liquid-cooled glass [bottom-right panel in Figure 1]. The diffraction pattern of the liquid-cooled glass is isotropic as the sample scatters equally in all directions. (The intense feature in the upper right of this panel is an artifact due to substrate diffuse scattering.) Because of the disordered local packing characteristic of molecular glasses, the scattering shows a broad amorphous halo with no sharp rings or peaks. For the TPD glass deposited at a substrate temperature ($T_{substrate}$) of 300 K, the scattering pattern is qualitatively very similar to the liquid-cooled isotropic glass, even though TPD glasses deposited at $T_{substrate}$ = 300 K are known to be 1.1% more dense and to exhibit remarkably enhanced thermal stability. For the sample deposited at $T_{substrate}$ = 260 K, there is a strong concentration of scattering intensity near q_z at $q \approx 1.4$ Å^{-1}. This broad feature along q_z could be interpreted as an imperfect lamellar-like structure with a real-space periodicity of approximately

4.5 Å ($d = 2\pi/q$). This spacing is consistent with a physical picture of adjacent molecules stacking flat with an intermolecular distance of around 4.5 Å. In contrast, the sample deposited at $T_{substrate}$ = 315 K shows a slight concentration of scattering intensity along q_{xy}.

Figure 1.

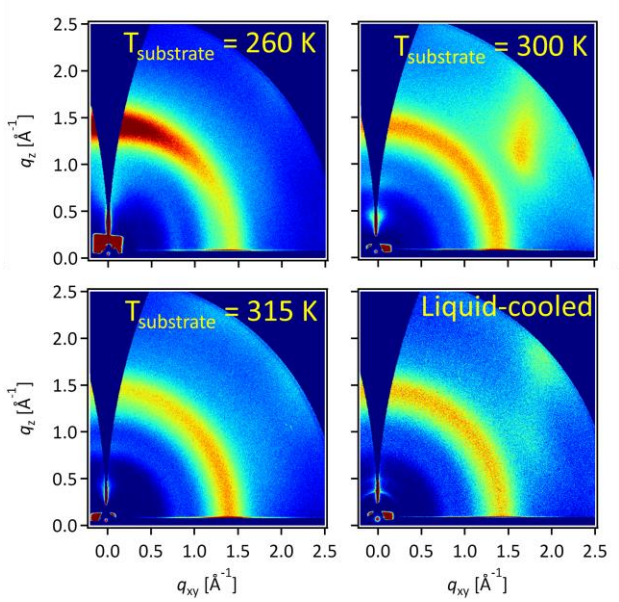

Figure 1. GIWAXS scattering patterns obtained from TPD glasses vapor-deposited at three substrate temperatures and from the liquid-cooled glass. The concentration of intensity observed along q_z and q_{xy} indicates anisotropic packing in $T_{substrate}$ = 260 K and $T_{substrate}$ = 315 K samples, respectively. The liquid-cooled glass and the $T_{substrate}$ = 300 K vapor-deposited glass exhibit very similar isotropic scattering, despite having quite different thermal stabilities. The features in the upper right of the images in the right column are an artifact due to Si substrate diffuse scattering.

Quantifying anisotropic scattering in TPD glasses

To quantify the anisotropic scattering observed in Figure 1, an order parameter can be calculated based on the scattering near q ≈ 1.4 Å^{-1}. The GIWAXS-derived order parameter (S_{GIWAXS}) is defined as follows:

$$S_{GIWAXS} = \frac{1}{2}(3 < cos^2\chi > -1) \qquad (1)$$

To calculate S_{GIWAXS}, we utilize a $<cos^2 \chi>$ average[27] of the scattering intensity between q values of 1.1 and 1.7 Å^{-1} along χ, as defined in equation 1, where χ is the azimuthal angle in reciprocal space, with χ = 0° defined along q_z:

$$< cos^2\chi >= \frac{\int_0^{90} I(\chi)\,(cos^2\chi)(\sin\chi)d\chi}{\int_0^{90} I(\chi)(\sin\chi)d\chi} \qquad (2)$$

S_{GIWAXS} can be viewed as quantifying the position of highest scattering intensity as well as the sharpness of the scattering intensity, and varies between limits of +1 and -0.5. Values of S_{GIWAXS} near +1 would indicate a relatively sharp peak in intensity along q_z, and no scattering intensity elsewhere with q ≈ 1.4 Å^{-1}. Because the scattering at this value of q is attributable to the nearest neighbor distance, S_{GIWAXS} = +1 would be consistent with a strong tendency for the molecules to stack in an orientation that is parallel to the substrate or "face-on". An order parameter of S_{GIWAXS} = -0.5 would indicate a sharp peak in intensity along q_{xy} at q ≈ 1.4 Å^{-1}, corresponding to molecules oriented edge-on. Possible packing arrangements consistent with these extreme values of S_{GIWAXS} are represented in the schematic in Figure 2c. The TPD glasses studied here show only a slight tendency towards such extreme molecular packing arrangements and show no evidence of crystalline planes.

Figure 2.

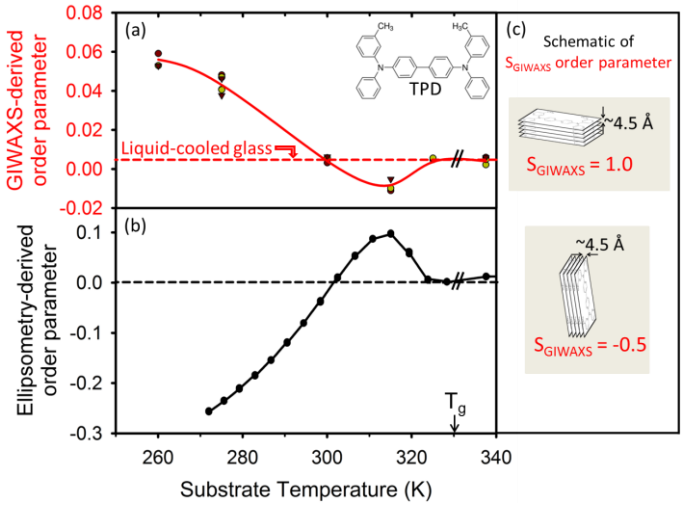

Figure 2. (a) The GIWAXS-derived order parameter, S_{GIWAXS}, plotted as a function of substrate temperature during deposition. S_{GIWAXS} exhibits positive and negative values, depending on substrate temperature, implying a slight tendency towards vertical and horizontal packing, respectively. Individual data points represent S_{GIWAXS} calculated at specific incidence angles between 0.14° and 0.20°. (b) The ellipsometry-derived order parameter, S_{VASE}, as a function of substrate temperature; S_{VASE} characterizes molecular orientation. (c) Schematic showing one possible interpretation of the two extreme S_{GIWAXS} values. The magnitudes of observed S_{GIWAXS} values are much smaller than these extreme values, indicating only a slight tendency towards these packing arrangements.

The GIWAXS-derived order parameter is plotted as a function of $T_{substrate}$ for vapor-deposited TPD glasses in Figure 2a, and shows both positive and negative values for substrate temperatures below the glass transition temperature (T_g) of the material at 330 K. The isotropic liquid-cooled glass, as a point of reference plotted at the right edge of the figure, exhibits an order parameter of nearly zero (S_{GIWAXS} = +0.004±0.001). The glasses deposited at $T_{substrate}$ = 260 K and $T_{substrate}$ = 315 K show significantly different order parameters than the liquid-cooled glass. Consistent with Figure 2c, we interpret the 260 K sample to indicate a weak tendency for molecules to lay face-on and parallel to the substrate. We interpret the 315 K sample to indicate an even weaker tendency to stand edge-on with a planar stacking. The glass deposited at $T_{substrate}$ = 325 K exhibits the same S_{GIWAXS} value as the liquid-cooled glass, indicating an isotropic sample. At $T_{substrate}$ = 300 K, there is a turnover point, where $S_{GIWAXS} \approx 0$ as the order parameter switches between positive and negative values.

In Figure 2, it can be seen that S_{GIWAXS} for the liquid-cooled glass is slightly offset from zero, implying that the scattering from this sample is not truly isotropic. On the other hand, we expect a bulk sample of a liquid-cooled glass to have an isotropic structure and thus exhibit isotropic scattering. The reasons for this discrepancy may be twofold. It is possible that weak (anisotropic) background scattering accounts for the offset from $S_{GIWAXS} = 0$. Our efforts to account for the background scattering did not significantly change the value of S_{GIWAXS} but these corrections are difficult for samples with broadly distributed scattering. It is also possible that molecular packing in the film is not uniform throughout its depth. The portions of the film near the free surface and the substrate might have a unique structure, with molecules having a greater tendency to exhibit face-on stacking than the bulk of the film. The effect of these near-surface layers might not be negligible for a 100 nm film. For the purposes of further discussion, the nearly zero order parameter value of S_{GIWAXS} = +0.004 obtained for the liquid-cooled glass will be taken to correspond to an isotropic sample.

It is instructive to compare S_{GIWAXS} with an analogous order parameter derived from VASE: S_{VASE}. VASE can be used to measure average molecular orientation in vapor-deposited glasses[17–19,30] and has previously

been used to characterize vapor-deposited TPD. Figure 2b shows a subset of previously published[19] VASE-derived order parameter values for TPD as a function of substrate temperature which, along with Figure 2a, gives an important comparison of the two independently measured order parameters. The derivation of S_{VASE} is shown elsewhere,[19] and is based on the dichroism of the glass. S_{VASE} is a measure of the average orientation of the transition dipoles for the molecules that make up a glass. In the case of TPD, the transition dipole lines up with the long axis of the molecule, so the order parameter determines the average orientation of the long molecular axis in the glass. S_{VASE} also varies from +1 to -0.5, where S_{VASE} = +1 corresponds to all transition dipole orientations being perpendicular to the substrate (all molecules standing up), while S_{VASE} = -0.5 corresponds to all transition dipoles lying in the plane of the substrate. Figure 2 shows that the two order parameters are well correlated and they will be used together to suggest molecular models for the TPD glasses below.

Comparing in-plane and out-of-plane structure

In Figure 3 we show a direct comparison of the line-cut diffraction patterns along q_{xy} and q_z as probes of the in-plane and out-of-plane structure for TPD glasses deposited at different substrate temperatures. This complements the analysis discussed above based upon the S_{GIWAXS} order; S_{GIWAXS} accounts for the anisotropy in nearest neighbor packing but averages over all the structural information in the scattering pattern. The most anisotropic glass that we studied ($T_{substrate}$ = 260 K) shows a significantly different scattering pattern along q_z and q_{xy} in Figure 3. Scattering for this sample shows the sharpest scattering features observed for any of the vapor-deposited TPD glasses, indicating more ordered packing. The peak at q = 1.4 $Å^{-1}$, corresponding to a 4.5 Å real-space molecular packing sharpens along q_z. Along q_{xy}, a shoulder grows at 1.2 $Å^{-1}$, while the shoulder at 0.75 $Å^{-1}$ grows into a peak, when compared with the isotropic liquid-cooled glass. The liquid-cooled and $T_{substrate}$ = 325 K glasses look very similar to each other and are both essentially isotropic, with nearly identical scattering patterns along q_z and q_{xy}.

The comparison in Figure 3 between the glass deposited at 300 K and the liquid-cooled glass is particularly interesting as these two samples have very similar scattering patterns and very different

kinetic stabilities. It has been reported that the $T_{substrate}$ = 300 K glass exhibits enhanced thermal stability with an onset transition temperature to the equilibrium supercooled liquid 16 K above that of the liquid-cooled glass. The 300 K glass also has 1.1% higher density than the liquid-cooled glass.[19] Nevertheless, the two glasses are remarkably similar in structure. The two glasses share nearly identical scattering patterns from q = 0.55 to 2.2 $Å^{-1}$ in both q_{xy} and q_z, suggesting similar overall intramolecular and intermolecular packing. However, the $T_{substrate}$ = 300 K glass does show a small anisotropic peak near 0.4 $Å^{-1}$ that is absent in the liquid-cooled glass. This low q anisotropic peak is investigated further in Figure 4.

In Figure 3, it is worth noting that none of the vapor-deposited glasses, regardless of their degree of anisotropic scattering, show any crystalline diffraction. For comparison, the bottom panel in Figure 3 shows the powder pattern that we obtained for crystalline TPD (as received from the manufacturer). The vapor-deposited glasses do not resemble this powder pattern, previous single crystal scattering results, [31] or DFT calculations of the scattering of an alternate polymorph of TPD[32]. The enhanced kinetic stability exhibited by the glasses prepared at 260 K and 300 K is a feature related to subtle changes in amorphous packing and not a result of crystalline order.

Figure 3.

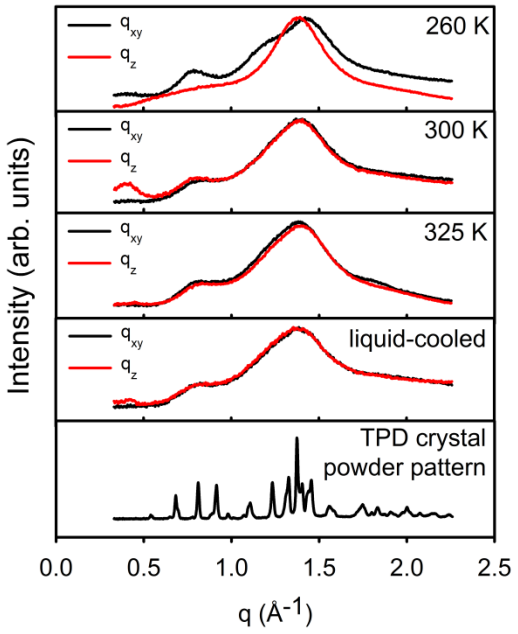

Figure 3. 1D diffraction curves along q_{xy} (black) and along q_z (red) for glasses of TPD deposited at 260 K, 300 K, and 325 K, as well as a liquid-cooled glass of TPD and powdered TPD crystals. The $T_{substrate}$ = 260 K sample shows the most variation between q_{xy} and q_z, along with a sharpening of features. The other three glasses show remarkably similar structural signatures in spite of their different thermal stability. None of the glasses show any crystalline structure.

Anisotropic scattering near q = 0.4 Å^{-1}

To investigate the anisotropic scattering peak near q = 0.4 Å^{-1} shown in Figure 3 for the sample deposited at 300 K, we employed a high-throughput WAXS characterization technique. We vapor-deposited TPD onto substrates with a temperature gradient imposed (and fixed) during deposition.[18,19] This creates a library of glasses fabricated at different substrate temperatures along the length of the substrate (as described in *Experimental Methods*); a related approach using a gradient of annealing temperatures has recently been described.[33] WAXS measurements were performed on these samples one spot at a time across the length of the sample, with every spot corresponding to a glass deposited at a different temperature. We investigated substrate temperatures in a 60 K range around 300 K to track the dependence of the anisotropic peak near 0.4 Å^{-1}. Figure 4a shows the intensity of the peak along q_z as a function of substrate temperature. Figure 4b shows a detailed view of this scattering feature in the 2D WAXS diffraction pattern; the box depicts the approximate integration limits used to calculate the intensity plotted in Figure 4a. Figure 4c shows that a similar scattering feature occurs in the same region of the 2D diffraction pattern from the GIWAXS measurements. The 2nd order diffraction peak of the feature can be seen at 0.8 Å^{-1} in both the WAXS and GIWAXS, indicating a high degree of order. The WAXS samples were 1.5-2.5 microns thick in comparison to the 100-130 nm samples utilized for the GIWAXS measurements. Since similar scattering features are observed for films of very different thicknesses, we infer that this peak is related to molecular order in the vapor-deposited glass.

The physical origin of the anisotropic peak shown in Figure 4 is unclear. Its position might suggest layering with a periodicity related to the long dimension of the TPD molecule. The length of TPD[31] is about 17 Å and a layer of this thickness would give rise to a peak at q = 0.37 Å^{-1}. We note that the shape of this scattering feature with the central node is reminiscent of scattering from SmC_R liquid crystals which exhibit a hollow cone distribution of tilt angles and some SmC liquid crystal phases.[34–36] If this interpretation is accurate, it would be an interesting result as TPD has no reported liquid crystal phases.

An anisotropic scattering peak in a similar q-range has previously been observed in vapor-deposited glasses of indomethacin[37] ($q = 0.6$ Å^{-1}; $d = 1.04$ nm). As in the case of TPD, the peak arose along q_z only, but unlike TPD it was a single broad peak which persisted through a larger range of substrate temperatures. The anisotropic scattering peak for indomethacin was attributed to a tendency towards molecular layering with a real-space periodicity corresponding to a single molecular diameter. Similar layering behavior corresponding to about a molecular diameter has been observed in vapor-deposited glasses of three other molecular systems. The intensity of the anisotropic scattering varied significantly among these four systems.[38]

Figure 4.

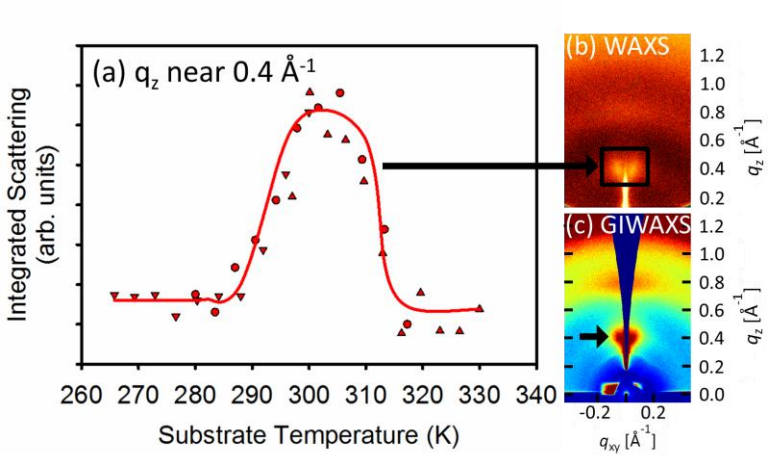

Figure 4. (a) Integrated scattering intensity of the anisotropic peak near q ≈ 0.4 Å^{-1} as a function of substrate temperature. (b) 2D WAXS diffraction pattern from a TPD glass deposited at $T_{substrate}$ = 301 K with area of integration indicated. The data in panel (a) is collected from many such 2D WAXS diffraction patterns obtained from glasses deposited at different substrate temperatures. (c) GIWAXS diffraction pattern obtained from $T_{substrate}$ = 300 K sample, indicating the feature observed in WAXS can also be observed in GIWAXS experiments.

A molecular model for anisotropic TPD glasses

The combination of VASE and GIWAXS has previously proved useful for understanding the microstructure of amorphous materials[27] and here we use these techniques to give us a more complete understanding of the molecular packing in TPD glasses. As shown in Figure 2, there is a strong correlation between the two order parameters. Both follow the same trends, with crossover and maximum magnitude order parameters occurring at the same substrate temperatures. $S_{VASE}<0$ in the low temperature regime implies that molecules preferentially have their long axes parallel to the substrate, but it cannot be determined from VASE if the molecules lie face-on or edge-on. The anisotropy of the scattering peak at q $\approx$ 1.4 $Å^{-1}$ suggests that the molecules lay face-on at low substrate temperatures. This inference is made based on the 4.5 Å real-space periodicity (= $d_{average}$) from q = 1.4 $Å^{-1}$, which is geometrically consistent only with the molecules lying face-on on the substrate. The upper panel in Figure 5 shows a crude representation of what we infer to be a possible face-on structure and also a smaller cartoon showing a structure that would be inconsistent with GIWAXS (but still consistent with VASE). From S_{VASE}, the average molecular orientation angle ($\theta_{average}$) relative to the surface normal can be determined[19,30] ($\theta_{average}$ = arccos[(2/3 S_{VASE} +1/3)$^{1/2}$]). As a point of reference, an isotropic distribution of molecular orientations has S_{VASE} = 0 and $\theta_{average}$ = 54.7°. For the $T_{substrate}$ = 260 K sample, $\theta_{average}$ = 69°. The $T_{substrate}$ = 315 K sample has $\theta_{average}$ = 51° and also has $d_{average}$ = 4.5 Å; a crude image is shown in Figure 5. For illustrative purposes, we approximate the TPD molecules as flat, and we amplify the order in the films to elucidate the structure differences between glasses prepared at the two substrate temperatures shown. The actual structures must be much more disordered than those illustrated; one source of disorder may be a range of local directors for face-on packing. It should be possible to use computer simulations to generate more realistic structures that are quantitatively consistent with the VASE and GIWAXS data.

Figure 5.

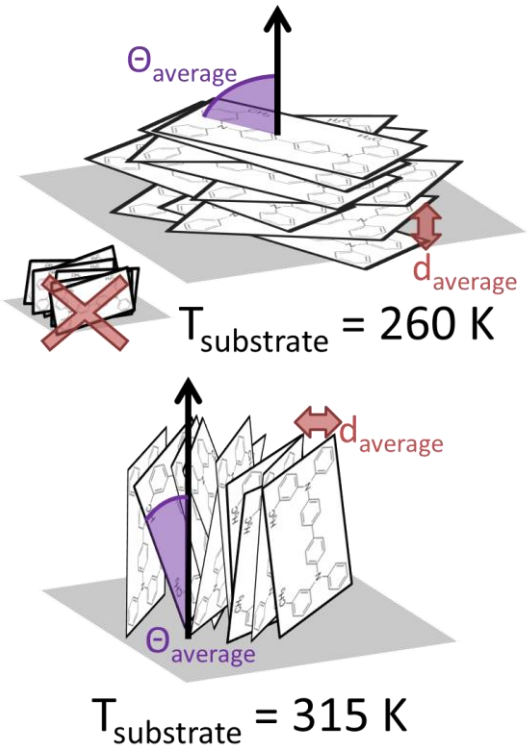

Figure 5. A schematic representing the microstructures of TPD glasses with the highest magnitude positive and negative order parameters in this study. $d_{average}$ and the orientation of nearest-neighbor stacking is obtained from GIWAXS measurements, while $\theta_{average}$ is obtained from VASE and measured from the substrate normal. $d_{average}$ for both glasses is ~4.5 $Å^{-1}$, while $\theta_{average,260\ K} = 69^{\circ}$ and $\theta_{average,315K} = 50^{\circ}$. For illustrative purposes, the degree of order has been enhanced in the schematics.

Yokoyama et al.[20] measured charge mobility in vapor-deposited glasses of BSB-Cz. They reported that low temperature deposition led to a planar orientation of the molecular long axis; relative to a glass with nearly isotropic orientation, the electron mobility increased by nearly an order of magnitude. These authors interpreted the BSB-Cz results to indicate increased stacking along the surface normal. If the packing observed in low substrate temperature vapor-deposited TPD and BSB-Cz glasses are similar, the results presented here may provide further insight into the microstructure associated with enhanced charge carrier mobility.

On the origin of structural anisotropy in vapor-deposited stable glasses

The anisotropy in the structure and in the molecular orientation that is quantified in Figure 2 must ultimately be traced back to the vapor deposition process. We first review the mechanism by which glasses of high kinetic stability are formed. Molecules near the free surface of a glass can be highly mobile if the temperature is not too low.[39,40,41] During deposition, this mobility gives molecules near the surface an opportunity to sample various configurations and partially equilibrate before being buried and fixed in position by subsequent deposition. Since this partial equilibration can occur well below Tg, highly stable glasses can be formed.[28,42] The mobility associated with the free, growing surface depends strongly on the temperature of the substrate ($T_{substrate}$) during the deposition, which leads to glass properties that depend upon $T_{substrate}$. For many systems, including TPD, deposition near 0.87 T_g produces the glass with the greatest kinetic stability.[18,19]

Recent computer simulations of coarse-grained TPD molecules[19] extend this picture further by indicating that the molecular orientation in the glass is inherited from the molecular orientation near the surface of the equilibrium liquid. In the simulations, the top layer of the equilibrium liquid consists of molecules with a tendency to lie in the plane of the free surface while molecules just below the surface exhibit a tendency to orient perpendicular to the substrate. Even deeper in the equilibrium liquid, the structure is isotropic. During deposition, the substrate temperature controls the depth to which equilibration takes

place near the surface. At a given deposition rate, there is a low substrate temperature regime that traps the molecules in the horizontal alignment since only the very top layer of molecules can equilibrate during deposition. At an intermediate substrate temperature, there is just enough mobility to equilibrate the surface to the depth associated with vertical alignment, and this alignment is then trapped in the glass. The computer simulations and this explanation are consistent with S_{VASE} data in Figure 2. This picture can be extended to the GIWAXS results. From this perspective, we would explain the face-on packing at low substrate temperatures inferred by GIWAXS as resulting from each layer of incoming molecules being frozen into a planar orientation during deposition. Glasses prepared on substrates near 315 K, on the other hand, capture not only the slightly vertical orientation of the molecules as described by S_{VASE} in the second layer from the free surface, but also the parallel packing of these molecules, thus explaining the negative value of S_{GIWAXS}. This view accounts for the strong correlation between S_{VASE} and S_{GIWAXS}, and could be tested by computer simulation.

Concluding Remarks

Grazing incidence wide-angle x-ray scattering was utilized to characterize the structure of vapor-deposited glasses of TPD, a hole transport material used in organic electronic devices. The TPD glasses were deposited at various substrate temperatures and exhibited a range of anisotropic structures. The x-ray scattering results indicate only subtle structural differences between a liquid-cooled glass and a vapor-deposited glass with high kinetic stability. None of the vapor-deposited TPD glasses, including those with high kinetic stability, showed any indications of crystallinity.

An order parameter, S_{GIWAXS}, was derived to describe the structural anisotropy of the most prominent feature in the diffraction patterns ($q \approx 1.4$ Å^{-1}), which we interpret in terms of nearest-neighbor packing. S_{GIWAXS} exhibited a strong correlation with a previously published order parameter for molecular orientation, S_{VASE}, based on measurements on the same system from variable angle spectroscopic ellipsometry. By combining the GIWAXS results with previously published VASE results, we have inferred a possible microstructure for the glassy films. We expect that these two observables might be

used in conjunction with molecular dynamics simulations to further our understanding of the molecular packing in these films, with the ultimate goal to better understand charge carrier mobility in vapor-deposited glasses.

Acknowledgements. The WAXS experiments were supported by the U.S. Department of Energy, Office of Basic Energy Sciences, Division of Materials Sciences and Engineering, award DE-SC0002161. The GIWAXS experiments were supported by NSF through the University of Wisconsin Materials Research Science and Engineering Center (DMR-1121288), which also provided instrumentation support. KO and MLC were partially supported by NSF DMR award 1410438. Use of the Stanford Synchrotron Radiation Lightsource, SLAC National Accelerator Laboratory, is supported by the U.S. Department of Energy, Office of Science, Office of Basic Energy Sciences under Contract No. DE-AC02-76SF00515.

References

1. Sirringhaus, H. 25th anniversary article: organic field-effect transistors: the path beyond amorphous silicon. *Adv. Mater.* **26,** 1319–35 (2014).

2. Dou, L. *et al.* 25th anniversary article: a decade of organic/polymeric photovoltaic research. *Adv. Mater.* **25,** 6642–71 (2013).

3. Huang, Y., Kramer, E. J., Heeger, A. J. & Bazan, G. C. Bulk heterojunction solar cells: morphology and performance relationships. *Chem. Rev.* **114,** 7006–43 (2014).

4. Reineke, S. *et al.* White organic light-emitting diodes with fluorescent tube efficiency. *Nature* **459,** 234–8 (2009).

5. Kulkarni, A. P., Tonzola, C. J., Babel, A. & Jenekhe, S. A. Electron Transport Materials for Organic Light-Emitting Diodes. *Chem. Mater.* **16,** 4556–4573 (2004).

6. Coropceanu, V. *et al.* Charge transport in organic semiconductors. *Chem. Rev.* **107,** 926–52 (2007).

7. Noriega, R. *et al.* A general relationship between disorder, aggregation and charge transport in conjugated polymers. *Nat. Mater.* **12,** 1038–44 (2013).

8. Wakamiya, A. *et al.* On-top π-stacking of quasiplanar molecules in hole-transporting materials: inducing anisotropic carrier mobility in amorphous films. *Angew. Chem. Int. Ed. Engl.* **53,** 5800–4 (2014).

9. McCulloch, I. *et al.* Liquid-crystalline semiconducting polymers with high charge-carrier mobility. *Nature* **5,** 328–333 (2006).

10. Zhang, X. *et al.* Molecular origin of high field-effect mobility in an indacenodithiophene-benzothiadiazole copolymer. *Nat. Commun.* **4,** 2238 (2013).

11. Shklyarevskly, I. O. *et al.* High anisotropy of the field-effect transistor mobility in magnetically aligned discotic liquid-crystalline semiconductors. *J. Am. Chem. Soc.* **127,** 16233–7 (2005).

12. Tracz, A. *et al.* Uniaxial alignment of the columnar super-structure of a hexa (alkyl) hexa-peri-hexabenzocoronene on untreated glass by simple solution processing. *J. Am. Chem. Soc.* **125,** 1682–3 (2003).

13. Giri, G. *et al.* Tuning charge transport in solution-sheared organic semiconductors using lattice strain. *Nature* **480,** 504–8 (2011).

14. Yip, H.-L. *et al.* Solvent-vapor annealing-induced growth, alignment, and patterning of π-conjugated supramolecular nanowires. *J. Mater. Res.* **26,** 311–321 (2011).

15. Eccher, J., Faria, G. C., Bock, H., von Seggern, H. & Bechtold, I. H. Order induced charge carrier mobility enhancement in columnar liquid crystal diodes. *ACS Appl. Mater. Interfaces* **5,** 11935–43 (2013).

16. Shklyarevskly, I. O. *et al.* High anisotrophy of the field-effect transistor mobility in magnetically aligned disotic liquid-crystalline semiconductors. *J. Am. Chem. Soc.* **127,** 16233–16237 (2005).

17. Dalal, S. S. & Ediger, M. D. Molecular Orientation in Stable Glasses of Indomethacin. *J. Phys. Chem. Lett.* **3,** 1229–1233 (2012).

18. Dalal, S. S., Fakhraai, Z. & Ediger, M. D. High-throughput ellipsometric characterization of vapor-deposited indomethacin glasses. *J. Phys. Chem. B* **117,** 15415–25 (2013).

19. Dalal, S. S., Walters, D. M., Lyubimov, I., de Pablo, J. J. & Ediger, M. D. Tunable Molecular Orientation and Elevated Thermal Stability of Vapor-Deposited Organic Semiconductors. *PNAS* (to be submitted) (2015).

20. Yokoyama, D., Setoguchi, Y., Sakaguchi, A., Suzuki, M. & Adachi, C. Orientation control of linear-shaped molecules in vacuum-deposited organic amorphous films and its effect on carrier mobilities. *Adv. Funct. Mater.* **20,** 386–391 (2010).

21. Rivnay, J., Mannsfeld, S. C. B., Miller, C. E., Salleo, A. & Toney, M. F. Quantitative determination of organic semiconductor microstructure from the molecular to device scale. *Chem. Rev.* **112,** 5488–519 (2012).

22. Tsao, H. N. *et al.* The influence of morphology on high-performance polymer field-effect transistors. *Adv. Mater.* **21,** 209–212 (2009).

23. Kim, B.-G. *et al.* A molecular design principle of lyotropic liquid-crystalline conjugated polymers with directed alignment capability for plastic electronics. *Nat. Mater.* **12,** 659–64 (2013).

24. Feng, X. *et al.* Towards high charge-carrier mobilities by rational design of the shape and periphery of discotics. *Nat. Mater.* **8,** 421–426 (2009).

25. Chabinyc, M. L. X-ray Scattering from Films of Semiconducting Polymers. *Polym. Rev.* **48,** 463–492 (2008).

26. Chen, C.-W. *et al.* Morphology, molecular stacking, dynamics and device performance correlations of vacuum-deposited small-molecule organic solar cells. *Phys. Chem. Chem. Phys.* **16,** 8852–64 (2014).

27. Hammond, M. R. *et al.* Molecular order in high-efficiency polymer/fullerene bulk heterojunction solar cells. *ACS Nano* **5,** 8248–57 (2011).

28. Swallen, S. F. *et al.* Organic glasses with exceptional thermodynamic and kinetic stability. *Science* **315,** 353–6 (2007).

29. Baker, J. L. *et al.* Quantification of thin film crystallographic orientation using X-ray diffraction with an area detector. *Langmuir* **26,** 9146–51 (2010).

30. Yokoyama, D., Sakaguchi, A., Suzuki, M. & Adachi, C. Horizontal orientation of linear-shaped organic molecules having bulky substituents in neat and doped vacuum-deposited amorphous films. *Org. Electron.* **10,** 127–137 (2009).

31. Kennedy, A. R. *et al.* Tetraaryl biphenyl diamine hole transport materials: a structural study utilizing both single crystal and high resolution powder diffraction. *J. Mater. Chem.* **12,** 168–172 (2002).

32. Malagoli, M. & Brédas, J. L. Density functional theory study of the geometric structure and energetics of triphenylamine-based hole-transporting molecules. *Chem. Phys. Lett.* **327,** 13–17 (2000).

33. Verploegen, E. *et al.* Effects of Thermal Annealing Upon the Morphology of Polymer-Fullerene Blends. *Adv. Funct. Mater.* **20,** 3519–3529 (2010).

34. Kumar, S. *Liquid Crystals: Experimental Study of Physical Properties and Phase Transitions*. 79 (Cambridge University Press, 2001).

35. Keith, C., Lehmann, A., Baumeister, U., Prehm, M. & Tschierske, C. Nematic phases of bent-core mesogens. *Soft Matter* **6,** 1704 (2010).

36. Lagerwall, J. P. F. & Giesselmann, F. Current topics in smectic liquid crystal research. *Chemphyschem* **7,** 20–45 (2006).

37. Dawson, K. J., Zhu, L., Yu, L. & Ediger, M. D. Anisotropic structure and transformation kinetics of vapor-deposited indomethacin glasses. *J. Phys. Chem. B* **115,** 455–63 (2011).

38. Dawson, K. *et al.* Molecular packing in highly stable glasses of vapor-deposited tris-naphthylbenzene isomers. *J. Chem. Phys.* **136,** 094505 (2012).

39. Brian, C. W. & Yu, L. Surface self-diffusion of organic glasses. *J. Phys. Chem. A* **117,** 13303–9 (2013).

40. Fakhraai, Z. & Forrest, J. A. Measuring the surface dynamics of glassy polymers. *Science* **319,** 600–4 (2008).

41. Zhu, L. *et al.* Surface Self-Diffusion of an Organic Glass. *Phys. Rev. Lett.* **106,** 256103 (2011).

42. Kearns, K. L. *et al.* Hiking down the energy landscape: progress toward the Kauzmann temperature via vapor deposition. *J. Phys. Chem. B* **112,** 4934–42 (2008).

Chapter 3

Highly Organized Smectic-like packing in vapor-deposited glasses of a liquid crystal

Ankit Gujral, Jaritza Gomez, Jing Jiang, Chengbin Huang, Kathryn A. O'Hara, Michael F. Toney, Michael L. Chabinyc, Lian Yu, M. D. Ediger

Published in *Chemistry of Materials*, 29 (2), 849-858, **2017**.

Abstract

Glasses of a model smectic liquid crystal-forming molecule, itraconazole, were prepared by vapor deposition onto substrates with temperatures ranging from $T_{substrate} = 0.78\ T_g$ to $1.02\ T_g$, where $T_g = 330$ K is the glass transition temperature. The films were characterized using x-ray scattering techniques. For $T_{substrate}$ near and below T_g, glasses with layered smectic-like structures can be prepared and the layer spacing can be tuned by 16% through choice of $T_{substrate}$. Remarkably, glasses prepared with $T_{substrate}$ above T_g exhibit much higher structural organization than a thermally annealed film. These results are explained by a mechanism based upon preferred molecular orientation and enhanced molecular motion at the free surface, indicating that molecular organization in the glass is independent of the anchoring preferred at the substrate. These results suggest new strategies of optimizing molecular packing within active layers of organic electronic and optoelectronic devices.

Introduction

Control of molecular organization in solids, a long-standing goal in the chemical and materials sciences, is needed to advance many different areas of science and technology. This issue is at the heart of crystal engineering[1,2] and is essential for many types of organic electronic devices. For example, in organic field effect transistors the selection of crystal polymorph and orientation serves to optimize charge transport.[3] The emitting molecules can be oriented in a glassy host to maximize light output in organic light emitting diodes.[4] For organic photovoltaics, anisotropic amorphous packing can help to maximize □-stacking and charge transport.[5] While some approaches in these fields utilize equilibrium states of matter, metastable states are often successfully employed to expand the set of attainable structures. Here we show that physical vapor deposition of liquid crystalline materials is a particularly promising route to highly organized nonequilibrium molecular solids.

Liquid crystalline (LC) states have often been utilized to produce molecular organization in solids.[1,6–8] For these systems, there are well-developed methods to control structure in the fluid state and molecular alignment can then be transferred into the solid state. Typically, thermal annealing and specially prepared substrates[9–13] are used to prepare large LC domains in equilibrium and subsequent cooling yields a solid, either crystalline or glassy, that inherits structural organization from the LC phase. In optoelectronics, for example, solid-state lasers with multiple lasing wavelengths in the same device are made by tuning the LC order (via composition) and then quenching into a glassy solid.[1] For organic electronics, both smectic (forming two dimensional molecular sheets) and discotic phases (forming one dimensional molecular columns), have been shown to promote anisotropic charge carrier mobility.[6,8,14] Enhancements in mobility have been observed in a number of highly aligned liquid-crystalline systems.[15,16] In one case, a discotic phase of a perylenediimide derivative[17] was reported to exhibit a 5 orders of magnitude enhancement in charge mobility along the direction of π-stacking upon alignment and similar performance improvements have been reported for other systems. [6] [18]

Physical vapor deposition, a technique used commercially in the fabrication of organic light emitting diodes (OLEDs),[19] can also be used to control molecular organization in solids. Glass films produced by this method are molecularly smooth, macroscopically homogenous and grain boundary-free, making them particularly useful in OLEDs and other multilayer device architectures.[20] Depending on deposition parameters, these glassy materials can be anisotropic, with tunable molecular orientation,[21,22] polar order,[23] and anisotropic molecular packing.[24,25] The structural order produced by vapor deposition, albeit small compared with that found in equilibrium LC systems, has been shown in one case to enhance charge carrier mobility by nearly an order of magnitude.[26] In contrast to the LC work described above, vapor deposition directly produces anisotropic order, without thermal annealing steps.

Can the ability of physical vapor deposition to prepare mildly anisotropic solids from non-LC systems be combined with the structure-forming tendency of LC molecules to directly produce ordered molecular solids? There is precedent for using physical vapor deposition to create thin films of LC systems[27–29]. Particularly relevant is the work of Echher et al., which compared the electrical performance of vapor-deposited films with spin-coated and annealed films of a columnar LC system.[29] They reported that the columnar order was higher for vapor-deposited films than spin-coated films, leading to improved charge transport characteristics similar to those obtained by thermal annealing. In another recent study, it was shown that controlling the substrate temperature ($T_{substrate}$) during physical vapor deposition produced a remarkable control over molecular orientation in glassy films of itraconazole, a rod-like molecule that can form isotropic, nematic and smectic phases;[30] the average tilt angle in the as-deposited solids varied from 27˚ to 76˚ relative to the film normal as a function of $T_{substrate}$. These films were found to be macroscopically homogeneous and molecularly smooth, making the process potentially useful in device fabrication. In contrast to the behavior of equilibrium LC systems, molecular orientation in vapor-deposited films of itraconazole did not depend upon the identity of the underlying substrate.

Here we use wide angle x-ray scattering (WAXS) and grazing incidence wide angle x-ray scattering (GIWAXS) to characterize the molecular packing of itraconazole glasses prepared by vapor deposition at

various substrate temperatures. For $T_{substrate}$ near and below T_g, the glasses were found to have highly aligned smectic-like layering propagating through the film along the surface normal, independent of the total thickness of the film (in the range 100 – 1800 nm). Remarkably, glasses prepared by vapor deposition above T_g exhibit much more organized smectic layering than could be produced by extended thermal annealing in the equilibrium smectic phase. The layer spacing could be controlled through $T_{substrate}$ and ranged from 30 Å to 25 Å. Combining this x-ray data with previous measurements of average molecular orientation,[30] we describe the microstructures of the various glasses produced. Our results are consistent with the mechanism advanced in ref [21], where preferred molecular orientation in a deposited glass is a combined result of the high molecular mobility observed on free surfaces of glasses[31,32] and the tendency for molecules to self-assemble into anisotropic structures at the free surface of a liquid[21]. This mechanism and our experimental results indicate that molecular organization in the deposited glass is independent of the anchoring preferred at the substrate.

These results suggest that vapor deposition of LC systems can be a general route for the production of highly organized organic solids. Although our test system is a smectic LC, the proposed mechanism indicates that highly organized columnar and nematic phases should also be produced by vapor deposition, because these systems are also known to self-organize at the free surface.[33–35] Vapor deposition might be a particularly useful approach for columnar systems such as those currently being explored for use in organic electronics. In comparison to methods based upon thermal annealing, vapor deposition offers two key advantages: 1) as-deposited samples can be more ordered than those produced by thermal equilibration, and 2) multi-layer devices can be prepared without concern that thermal annealing of one layer will disrupt the packing of an underlying layer.

Experimental Methods

Sample preparation. The structure of itraconazole is shown in Figure 1c; the name “itraconazole” has been used in the literature to refer to any subset of the 8 stereoisomers of this structure.[36] The material utilized in our experiments was purchased from Sigma Aldrich (>98% purity) as a 1:1:1:1 racemic mix-

ture of the 4 cis- stereoisomers[36,37] and was used as-received; in this paper, "itraconazole" always refers this mixture. The systematic name for this group of stereoisomers is cis-2-sec-butyl-4-[4-(4-{4-[2-(2,4-dichlorophenyl)-2-(1H-1,2,4-triazol-1-ylmethyl)-1,3-dioxolan-4-ylmethoxy]phenyl}-piperazin-1-yl)phenyl]-2,4-dihydro-1,2,4-triazol-3-one[38]. Itraconazole is an isotropic liquid above 363 K. As the temperature is lowered, it exhibits a nematic phase down to 346 K and then exhibits a smectic phase which undergoes a transition to a smectic glass at T_g = 330 K cooling at 1 K/min.[39] (See Supplementary Information Figure SI1 for DSC thermograph). Itraconazole is a good glass-former and can be maintained below its melting point (439 K) for extended periods of time without nucleation.

Glasses of itraconazole were prepared by physical vapor deposition onto silicon <100> substrates with a native oxide. The deposition rate was 0.2 ± 0.02 nm/s in a vacuum environment (10^{-7} torr). The deposition rate was monitored using a quartz crystal microbalance. All the vapor-deposited glasses of itraconazole, for all $T_{substrate}$ values, were macroscopically homogeneous and pin-hole free.[30]

For the samples investigated by asymmetric wide-angle x-ray scattering (WAXS), a temperature gradient setup was used, as previously described,[22] to create a library of glasses prepared at different substrate temperatures. This is achieved by having two independently controlled temperature stages bridged by a rectangular substrate. The temperature differential between the two stages creates a temperature gradient along the silicon substrate that is maintained throughout the deposition process. The precise substrate temperature associated with various locations on the substrate was established by comparison with samples prepared at a single temperature; we find no discernable difference between the properties of a film prepared isothermally and a sample prepared at the same temperature on a temperature-gradient substrate. After deposition, the higher temperature stage was cooled to room temperature at 1 K/min. The absolute error in substrate temperature is estimated to be less than 2 K. The samples used for WAXS measurements were 1.8 microns thick.

For the samples investigated by grazing-incidence wide-angle x-ray scattering (GIWAXS), itraconazole was deposited onto isothermal substrates. For $T_{substrate}$ above room temperature, the temperature stage was

cooled to room temperature at 1 K/min after deposition. Both 100 nm and 300 nm thick samples were prepared for GIWAXS.

To compare the structure of a vapor deposited film with a thermally annealed film, a 1.8-micron thick vapor-deposited glass film was heated into the isotropic liquid, quenched to room temperature, and then annealed for 7 days at 337 K (where the equilibrium state is the smectic phase). This sample was then cooled to room temperature for characterization by WAXS.

High-throughput WAXS measurements. Asymmetric WAXS measurements were conducted on a Bruker D8 Discover diffraction instrument equipped with a Cu K-α x-ray source (λ= 1.54 Å), a beam spot size of 2 mm and a VANTEC500 area detector. A knife-edge made of Inconel 625 was installed to block air scatter. For the 2D WAXS patterns and the q scans in Figure 2, the incident angle was fixed at θ= 2.5˚ for all measurements. For each measurement, the sample was exposed to x-rays for 240 s (with a 50 W power output of x-ray source). The exposures were done at various points along the length of the high-throughput temperature gradient sample, with every point corresponding to a unique $T_{substrate}$. A similar procedure was used for the χ scans in Figure 4 and the 2D patterns in Figure 6 except that the incident angle was adjusted for every pattern by matching the Bragg condition associated with the 2nd order reflection along q_z to within 0.01 degrees. The 2nd order reflection was used rather than the primary peak at q_z~0.2 Å^{-1} so as to avoid the influence of background scattering. For a list of angles and corresponding $T_{substrate}$, please see SI Table 1. The integration limits used to construct Figure 4 can be found in SI Table 2.

GIWAXS measurements. GIWAXS measurements were conducted on beamline 11-3 at the Stanford Synchrotron Radiation Lightsource (SSRL) with a wavelength of 0.973 Å. The incident angle was fixed to 0.14˚ such that the scattering occurred from the bulk of the film and samples were typically exposed for 200 seconds. The data was processed using the SSRL-developed WxDiff Integration Tool software. The diffraction patterns were corrected for polarization of the beam and χ-corrected to obtain an accurate reciprocal space map, as described by Baker et al.[40]

Results

2D scattering patterns from vapor deposited glasses of itraconazole. Figure 1a shows a subset of the x-ray scattering patterns obtained from glasses of itraconazole vapor-deposited at different $T_{substrate}$ values. The panels in Figure 1a were obtained from grazing incidence wide angle x-rays scattering (GIWAXS) from 300 nm thick films. The itraconazole glasses produced by vapor deposition exhibit remarkably diverse local packing structures as a function of $T_{substrate}$, as indicated in the schematics of Figure 1b. As described in more detail below, these range from highly ordered structures similar to smectic A packing, to a smectic C-like packing, and finally to a more disordered but highly anisotropic structure. Of these, only the smectic A structure is a known equilibrium state of itraconazole.

To aid in our analysis, a coordinate system associated with the scattering vector, q, is defined in $Å^{-1}$ for the 2D GIWAXS patterns, with q_z corresponding to out-of-plane scattering plotted along the vertical axis and q_{xy} corresponding to in-plane scattering plotted along the horizontal axis.[40] The scattering vector is defined by $q = 4\pi \sin(\theta)/\lambda$, where θ is half the scattering angle and λ is the x-ray wavelength. q_x and q_y are equivalent since rotating the sample in the xy-plane led to no significant change in the scattering pattern. The in-plane isotropy of these glasses has also been confirmed using optical microscopy and atomic force microscopy, neither of which show domain structure on the observable length scales.[30]

Glasses deposited at $T_{substrate} = 335$ K $= T_g + 5$ K (top row of Figure 1) show the scattering features expected for a highly aligned smectic A liquid crystal. Sharp diffraction peaks are seen in the grazing incidence wide-angle x-ray scattering (GIWAXS) pattern at around $q_z \sim 0.2$ $Å^{-1}$, with higher order peaks appearing at $q_z \sim 0.4$ $Å^{-1}$, and faintly at $q_z \sim 0.6$ $Å^{-1}$. (There is a weak feature at $q_z \sim 0.3$ $Å^{-1}$ due to sample reflectivity.) This sequence of peaks indicates a periodic structure with long-range order and a large correlation length out of the plane of the substrate, with a periodicity of about $d = 30$ Å ($d = 2\pi/q$). This length-scale is similar to that observed in the equilibrium smectic liquid structure and to the molecular length (33 Å by DFT[39] and 30 Å from single crystal x-ray studies[38]). It is consistent with end-to-end stacking of the molecules in a smectic microstructure. The GIWAXS measurements also show a large in-plane scattering

peak at q_{xy}~1.4 $Å^{-1}$. This indicates the lateral (side-by-side) packing expected for rod-like molecules in smectic layers, with a nearest-neighbor spacing d ~ 4.5 Å. The GIWAXS results (and the asymmetric WAXS results discussed below) are consistent with the view that for $T_{substrate}>T_g$, the films are in the equilibrium smectic phase during deposition. Upon cooling to room temperature, this smectic structure gets trapped in the glassy state, i.e., the glass structure is inherited from the equilibrium smectic liquid. The most remarkable feature of glasses deposited near 335 K is the strong alignment of the smectic layers parallel with the substrate, as we discuss below.

Figure 1.

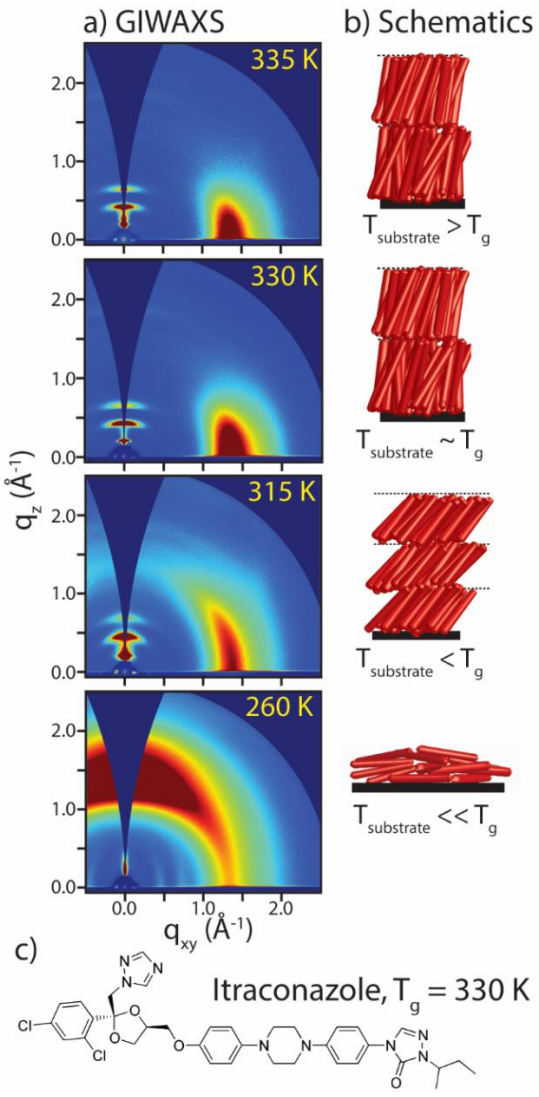

Figure 1. X-ray scattering patterns for glasses of itraconazole prepared by vapor deposition onto substrates with temperatures indicated. a) 2D GIWAXS scattering from 300 nm films. b) Schematics of proposed microstructures, with each red cylinder representing an itraconazole molecule, showing smectic-like layering for glasses prepared at high substrate temperatures. c) Molecular structure of itraconazole.

Glasses deposited at $T_{substrate}$ = 330 K = T_g (second row of Figure 1) are similar to the those formed above T_g. The out-of-plane peaks observed in the GIWAXS pattern are in the same position along q_z. However, these peaks are broader in q_{xy} than in the glass described above. Qualitatively, this kind of peak broadening is consistent with some small lateral disorder, such as modulations in the layering.[41,42]

Glasses deposited at $T_{substrate}$ = 315 K = T_g – 15 K (third row in Figure 1) show qualitatively similar out-of-plane diffraction peaks as described above but they are shifted to higher values along q_z, indicating smaller layer spacings in these glasses (due to an increase in the average tilt of the molecules). The out-of-plane peaks also broaden azimuthally (along χ, see Figure 4 inset for schematic definition of χ), indicative of a textured structure within the film, i.e., a distribution of molecular layer orientations. The azimuthal peak broadening described here is likely convolved with lateral (along q_{xy}) broadening as we discuss below. The in-plane diffraction peak seen in the GIWAXS at q~1.4 A^{-1} along q_{xy} also broadens azimuthally, consistent with a slightly more orientationally disordered (textured) in-plane structure than for the glasses prepared at $T_{substrate} \sim T_g$. This structure is similar to some equilibrium smectic C systems.[43]

A much different diffraction pattern is seen for itraconazole glasses formed with $T_{substrate}$ = 260 K (fourth row in Figure 1) as compared to the higher $T_{substrate}$ films. The out-of-plane peaks at q_z~0.2, 0.4 and 0.6 $Å^{-1}$ are no longer present and a broad peak is seen at q_z~1.4 $Å^{-1}$, indicating that the molecules in the film are predominantly lying in the plane of the substrate. Broad low-intensity peaks are observed in the GIWAXS at low q_{xy} values, consistent with a nematic or weakly smectic-like packing in-plane. (A line cut along q_{xy} is provided in Supplementary Information Figure SI2). Based on the x-ray and optical evidence for in-plane isotropy for all the PVD glasses, any in-plane smectic layer propagation must be randomly distributed in-plane.

The thermodynamic state of the as-deposited films. The films of itraconazole prepared by vapor deposition are out-of-equilibrium (glassy) solids at room temperature (where all the x-ray measurements are performed). They are non-crystalline as evidenced by the observation that not all the x-ray diffraction peaks are sharp. The as-deposited glasses are solids that can be temperature-cycled below T_g with no

change in structure. The films prepared by depositing at and above T_g, upon cooling to room temperature, are similar to glassy liquid crystals obtained by cooling the equilibrium smectic liquid,[44] as studied previously.[1,45] (Although not all glassy smectic liquid crystals will exhibit the high level of alignment observed in these samples as we discuss below.) The microstructures of the films prepared by depositing at $T_{substrate}<T_g$, however, are quite different than a glass prepared by cooling the equilibrium smectic liquid. When these samples are heated to about T_g + 15 K the as-deposited structure is lost, and the equilibrium smectic liquid state is formed. Upon cooling to room temperature, a glassy smectic is formed, with its structure inherited from the equilibrium smectic state. The observation that the as-deposited structure is irreversibly lost upon thermally cycling just above T_g further indicates the films are not crystalline as itraconazole does not melt until a much higher temperature (439 K).

Tuning smectic-like layer spacing by choice of $T_{substrate}$. As introduced in Figure 1, the choice of $T_{substrate}$ in a range just below T_g allows the preparation of itraconazole glasses in which the spacing of the smectic-like layered structures is controlled. This is investigated more closely in Figure 2 using the asymmetric WAXS data. Representative 2D patterns are shown at the top of the figure. In these panels, one can observe the first and second order reflections corresponding to the smectic layers (and sometimes also the third order reflection). (The WAXS patterns also show a faint reflectivity peak at q_z~0.3 Å^{-1}, and background intensity below 0.2 Å^{-1} caused by the low incident angle geometry of these measurements.)

Figure 2.

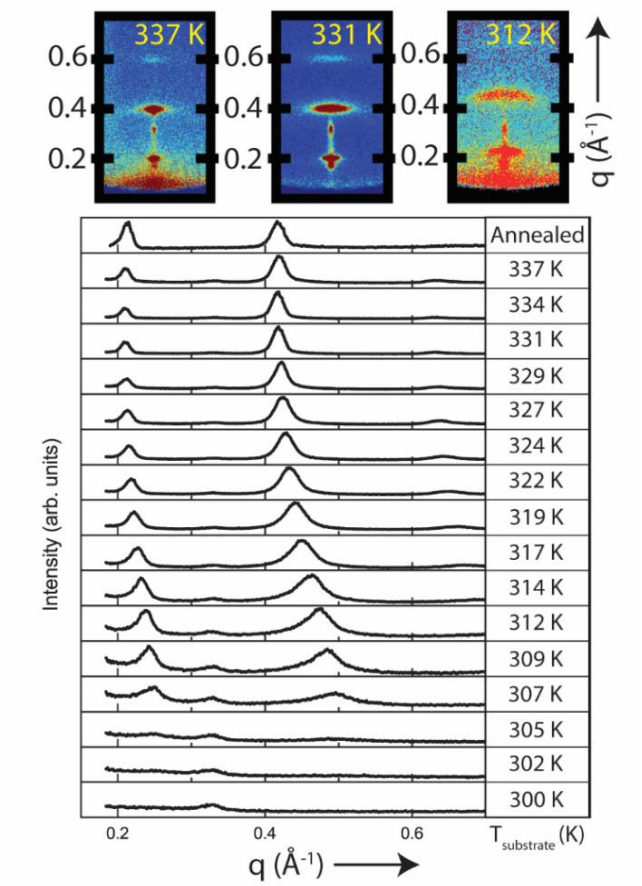

Figure 2. WAXS scattering intensities along vector q, as defined in top panel, for an annealed glass and various vapor-deposited glasses of itraconazole. Top: Representative 2D asymmetric WAXS patterns from itraconazole glasses deposited at $T_{substrate}$ indicated inset. The width of the pattern is approximately the integration area used to obtain the 1D diffractograms shown below. Bottom: Scattering intensity along q from WAXS for glasses of itraconazole deposited at the indicated substrate temperatures ($T_{substrate}$). The first panel shows data for a thermally annealed film. The shift of the scattering peaks to higher q at lower deposition temperatures indicates a decrease in the thickness of the smectic-like layers. All curves for vapor-deposited glasses have been normalized to the data presented for $T_{substrate}$ = 337 K.

The main panel of Figure 2 illustrates the spacing of the smectic-like layers by showing a line cut from the WAXS data along q for various glasses of itraconazole deposited between 337 K and 300 K. These data were obtained by integrating over an azimuthal angle approximately the width of the WAXS patterns at the top of the figure. For comparison, data is also presented for as a vapor-deposited sample that was heated into the isotropic liquid state and then annealed at 337 K for one week. All the x-ray scattering measurements shown in Figure 2 were conducted at room temperature.

The diffraction peaks shown in Figure 2 for the samples vapor-deposited at $T_{substrate} \geq 307$ K indicate smectic-like layering the samples. Each of these samples shows the fundamental peak (~0.23 $Å^{-1}$) and higher order reflections (~0.45 $Å^{-1}$ and sometimes 0.7 $Å^{-1}$). These peaks shift to higher q values and broaden systematically as $T_{substrate}$ is reduced. Higher q values indicate smaller layer spacing, while the broadening is a sign of shorter coherence lengths and more disorder in the layered structure.

Figure 3.

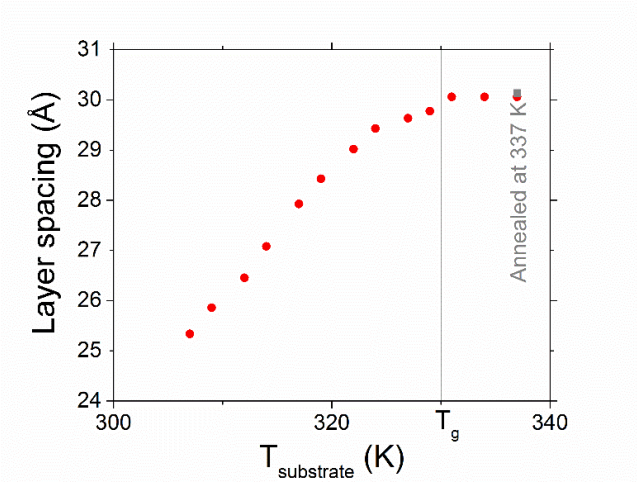

Figure 3. Thickness of smectic-like layers for vapor-deposited itraconazole glasses, as a function of substrate temperature during deposition ($T_{substrate}$), as derived from the position of scattering peaks along q_z. $T_{substrate} = T_g$ is demarcated with a vertical line. The layer spacing for a sample thermally annealed at 337 K is indicated by the gray square.

The spacing associated with the smectic-like layers is shown as a function of the substrate temperature during deposition in Figure 3, with the glass transition temperature marked with a vertical black line at 330 K. Above T_g, the layer spacing remains nearly constant, consistent with the view that the film being deposited is in the equilibrium smectic phase before being cooled into a glassy solid. For samples directly deposited into a glassy state below T_g, however, the layer spacing is systematically and monotonically reduced by up to 16%, from ~30 to ~25 Å. A broadening of the diffraction peaks along q is also observed at lower substrate temperature during deposition, suggestive of less long-range order in films and perhaps less layer spacing uniformity. This is quantified by the peak width along q and is shown in supplementary information Figure SI3.

Alignment of smectic-like layers in vapor-deposited glasses of itraconazole. Figure 4 shows azimuthal line cuts across the second order diffraction peak at q~0.4 $Å^{-1}$ for vapor-deposited and thermally annealed glasses of itraconazole, and allows a quantitative comparison of the degree of alignment of the smectic-like layers in the different samples. The scattering intensity was collected at the Bragg condition for the peaks and is plotted against χ, the azimuthal angle (defined such that $\chi = 0^\circ$ is along q_z and $\chi = 90^\circ$ is along q_{xy}). Higher intensity and sharper peaks correspond to well-ordered structures with large coherence lengths and a narrow distribution of directors. Figures 4b shows the same data as Figure 4a but with an expanded vertical axis.

The most striking feature of Figure 4 is that several vapor-deposited itraconazole glasses show more highly aligned smectic layers than the thermally annealed sample, indicating that these vapor deposited films are more highly ordered. In particular, the scattering intensity for the sample directly deposited at 337 K is more than one order of magnitude larger than for the thermally annealed sample. The annealed sample was obtained by heating a highly ordered vapor-deposited glass into the isotropic liquid, quenching rapidly, annealing for 7 days at 337 K (where the equilibrium phase is smectic), and finally cooling at 1 K/min to ambient conditions. In contrast, the highly aligned sample vapor-deposited at 337 K required only 2.5

hours to prepare at the 2 Å/s deposition rate. We further discuss the comparison between vapor-deposited and annealed samples below.

For the vapor-deposited glasses shown in Figure 4, the degree of smectic order is much lower when the substrate temperature during deposition is lower. Figure 4b shows, in addition, that the peaks arising from glasses deposited at $T_{substrate} < T_g$ broaden significantly. These features indicate that depositions at lower $T_{substrate}$ lead to layered structures with smaller coherence lengths. Qualitatively, the peak broadening observed in the second order peak may arise from at least two types of imperfections. 1) Peak broadening along the azimuthal angle (χ) indicates that the layers are not entirely parallel to the substrate but rather exhibit a textured structure. 2) Lateral peak broadening (along q_{xy}) is indicative of in-plane defects. We have not attempted to distinguish between these two explanations and we note that Figure 4 would appear very similar if the linecut had been taken along q_{xy} rather than along χ.

Probing lateral molecular packing. The GIWAXS scattering data near q =1.4 $Å^{-1}$, as discussed in the description of Figure 1, contains information about nearest-neighbor packing in vapor-deposited itraconazole glasses. For example, the very strong feature along q_{xy} in Figure 1a is expected from the scattering of closely-packed, nearly vertical rod-like molecules. Figure 5 plots an orientation order parameter $S_{N\text{-}N}$ based upon this feature in red; $S_{N\text{-}N}$ was measured from the GIWAXS patterns as described previously.[25] A value of $S_{N\text{-}N} = +1$ would indicate molecules packing parallel to each other in the plane of the substrate, while $S_{N\text{-}N} = -0.5$ would indicate molecules parallel to each other and normal to the substrate. For films deposited at $T_{substrate} \geq T_g$, there is a strong tendency for the molecules to pack normal to the substrate, consistent with smectic-like layers parallel to the substrate. For films deposited a little below T_g, the observed packing becomes more isotropic. For glasses grown at $T_{substrate} << T_g$, $S_{N\text{-}N}$ is positive, indicating a tendency for the molecules to pack with their long axes laying in the plane of the substrate and parallel to each other. Although the maximum value of $S_{N\text{-}N} = +0.12$ is quite small, it is twice the value reported for glasses of TPD vapor-deposited at low substrate temperatures.[25]

Figure 4.

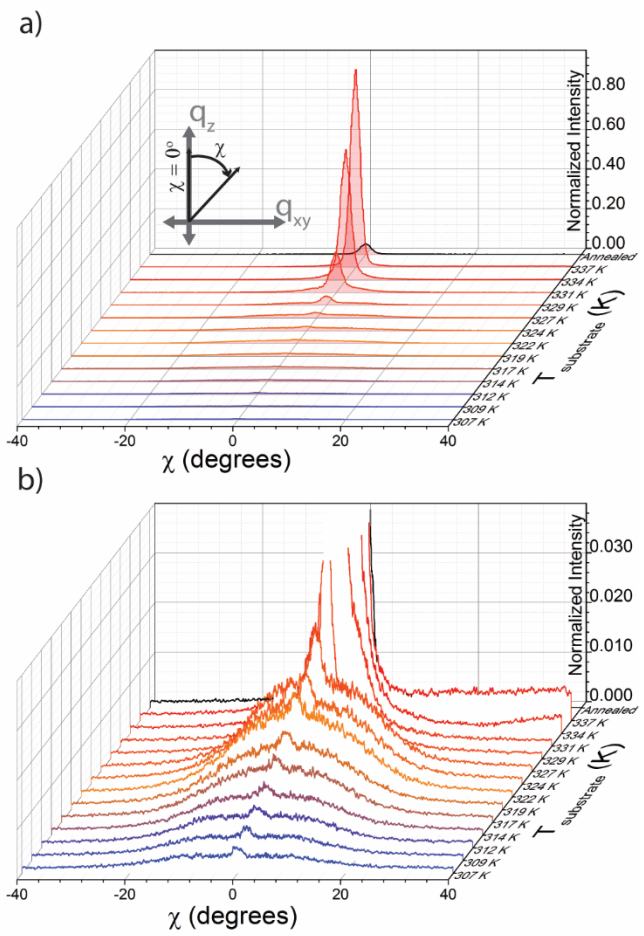

Figure 4. WAXS scattering data showing the 2nd order out-of-plane diffraction peak (q_z~0.4 Å^{-1}) along the azimuthal angle χ for itraconazole glasses deposited at various substrate temperatures ($T_{substrate}$), with χ defined in the inset. The intensity and width of this scattering feature characterize the quality of smectic organization and alignment. Multiple line cuts are shown offset in the z-axis, corresponding to different values of $T_{substrate}$. Panel b is a vertically expanded version of panel a. The black curve shows data for a sample annealed at 337 K. For both panels, intensities are normalized to the peak intensity observed for the film deposited at $T_{substrate}$ = 337 K.

Figure 5 also plots an FTIR-based orientation order parameter S_{FTIR} as described in detail elsewhere.[30,39] Based on IR dichroism, S_{FTIR} is a measure of the average molecular orientation of an axis very nearly parallel to the long axis of itraconazole molecules in the glass. $S_{FTIR} = +1$ would indicate molecules standing vertically while $S_{FTIR} = -0.5$ would indicate that all the molecules are lying in the plane of the substrate. Figure 5 shows a strong anti-correlation between $S_{N\text{-}N}$ and S_{FTIR}. For $T_{substrate} \geq T_g$, S_{FTIR} indicates that the molecules have a strong tendency to stand upright, consistent with the negative $S_{N\text{-}N}$ value and a smectic structure with planes parallel to the substrate. For $T_{substrate}$ near 260 K, S_{FTIR} indicates a tendency for the molecules to lay nearly flat in the plane, in agreement with the positive $S_{N\text{-}N}$ value. An interesting point of comparison is the S_{FTIR} value measured by Tarnacka and coworkers[39] for itraconazole in a homeotropically aligned smectic phase (plotted as the purple star in Figure 5). The good agreement of this value with S_{FTIR} for the vapor-deposited samples is consistent with direct deposition into a highly aligned smectic structure.

Figure 5.

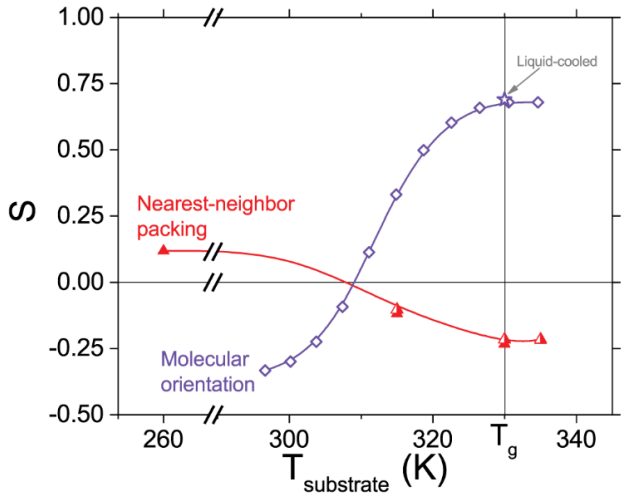

Figure 5. Orientation order parameters for nearest-neighbor packing ($S_{N\text{-}N}$) obtained from the GIWAXS data and for molecular orientation obtained from FTIR (S_{FTIR}), as a function of substrate temperature during deposition ($T_{substrate}$). $S_{N\text{-}N}$ quantifies the anisotropy in lateral nearest-neighbor molecular packing, varying from face-on at S = +1 to edge-on at S = -0.5; full triangles are 300 nm films and half-filled triangles are 120 nm films. S_{FTIR} is a measure of the average orientation of the long molecular axis, varying from vertical at S = 1 to horizontal at S = -0.5; open diamonds are vapor-deposited glasses[30] and the purple star is for the equilibrium liquid[36]). The solid lines are guides to the eye.

Comparison of thermally annealed and vapor-deposited itraconazole films. Figure 6 shows the intriguing result that the itraconazole sample vapor-deposited at 337 K has more highly organized smectic layers than a sample thermally annealed at 337 K for one week. Initially, we were surprised that a non-equilibrium assembly process would be more effective in producing smectic alignment than extensive thermal equilibration. Figure 6 shows a comparison of WAXS data for these two samples that allows further insight into this issue. The scattering at q~1.4 $Å^{-1}$ along a wide range of χ in the thermally annealed sample would not be present in a smectic phase with planes propagating exclusively along the surface normal and this feature is indeed absent from the vapor-deposited sample. For the thermally annealed sample, the slightly larger scattering at q=1.4 $Å^{-1}$ around χ=0˚ is consistent with a smectic population with planar anchoring (i.e., the molecular long axis lies along the interface). The differences in the orientation of smectic packing are schematically illustrated in Figure 6. We expect that the silicon substrate with the native oxide promotes planar anchoring[46] and, for the thermally annealed sample, this competes with the homeotropic anchoring (i.e., the molecular long axis lies nearly normal to the interface) preferred at the free surface. With this interpretation in mind, we can understand that the peak at q ~ 0.4 $Å^{-1}$ along χ=0˚ is weaker in the thermally annealed sample because it represents only the fraction of the smectic layers that propagate only the surface normal.

Figure 6.

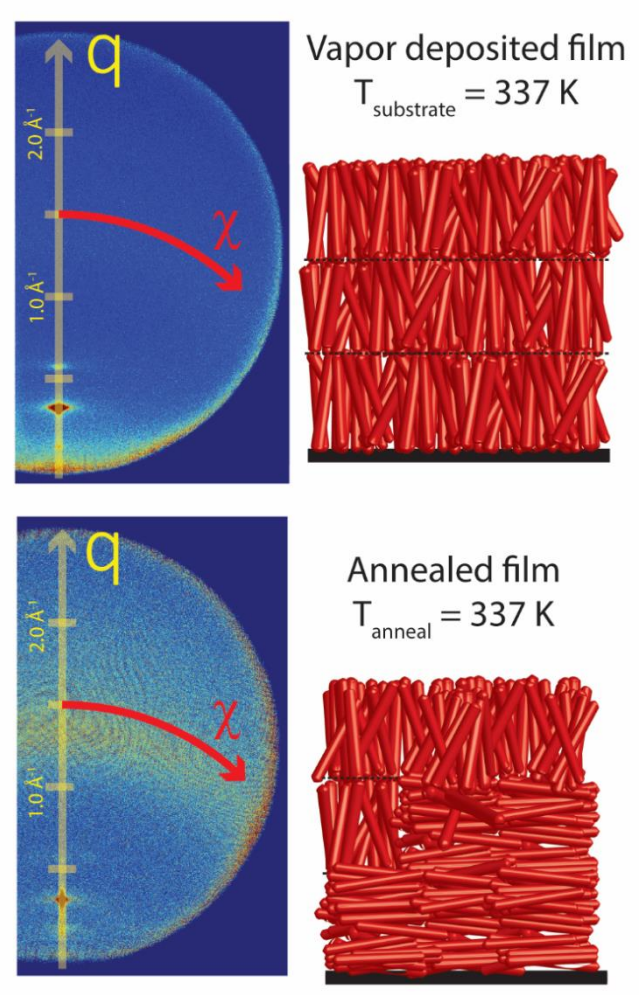

Figure 6. WAXS scattering patterns and possible structures for vapor-deposited and annealed films of itraconazole (1.8 microns thick). Top panel: 2D scattering pattern of film vapor-deposited at $T_{substrate}$ = 337 K with schematic structure. Bottom panel: 2D scattering pattern of film annealed for one week at T_{anneal} = 337 K with schematic structure. The presence of the broad peak at q~1.4 $Å^{-1}$ in the annealed film indicates some population of molecules with planar alignment. In contrast, the vapor-deposited film shows no evidence of planar alignment.

Structure. We present schematic structures for vapor-deposited itraconazole glasses in Figure 7 for three representative substrate temperatures, based upon the x-ray measurements presented here and results previously reported in ref [30]. The spacing of the smectic-like structures shown in the top two panels comes from the values reported in Figure 3. An average molecular orientation at each substrate temperature can be determined from S_{FTIR}, as plotted in figure 5:[30]

$\theta_{avg} = \arccos[(2/3S_{FTIR}+1/3)^{1/2}]$

Here θ_{avg} is measured from the substrate normal. It is important to note that, for the smectic-like structures prepared by vapor deposition, a collection of the structures shown in Figure 7 with a narrow distribution of molecular layer orientations is likely present across the film; the wider the distribution of layer orientations, the broader the azimuthal spread in the out-of-plane x-ray diffraction peaks. While the layers on average always propagate perpendicular to the substrate leading to out-of-plane diffraction peaks, structures like those shown in Figures 7 a and b likely have random in-plane orientation, leading to in-plane isotropy on the length-scales probed here and in microscopy[30] studies. At the lowest values of $T_{substrate}$, layers are not formed, and instead, the molecules lie nearly flat in the plane of the substrate. To the best of our knowledge, the tunable layer spacing and highly variable molecular orientation exhibited by vapor-deposited itraconazole glasses is unprecedented.

The microstructures shown in Figure 7 persist throughout the thickness of the vapor-deposited itraconazole glasses. The peak positions in the x-ray scattering patterns are consistent for films ranging from around 100 nm to 1.8 microns, indicating that the spacing of the smectic-like layers is independent of thickness. The orientation order parameter for nearest-neighbor packing S_{N-N} is the same for 100 nm and 300 nm films. Furthermore, ref. [30] shows that the optical birefringence of the vapor-deposited glasses is the same for films between 180 nm and 650 nm, while S_{FTIR} is independent in the range of 330 nm to 1800 nm.

Figure 7.

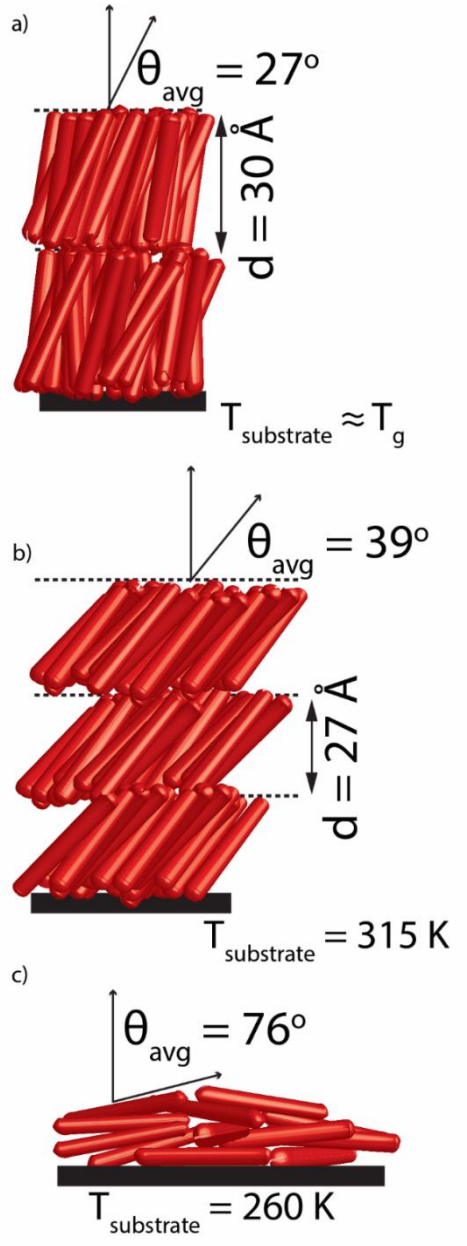

Figure 7. Schematics of a representative subset of microstructures for itraconazole glasses deposited at different substrate temperatures: a) $T_{substrate}$ ~ Tg; b) $T_{substrate}$ = 315 K; c) $T_{substrate}$ = 260 K. While the structure in panel a is very similar to a highly aligned equilibrium smectic liquid, the structures shown in panels b and c have no equilibrium analogues for itraconazole. The values of the average tilt angle and the average layer spacing are derived from FTIR and WAXS as described in the text.

Discussion

In this section, we address a number of questions about the mechanism by which vapor deposition produces ordered glasses of itraconazole and, in particular, how to understand the strong influence of substrate temperature on the type of order trapped in the glass (Figure 7). We also discuss how non-equilibrium deposition can lead to more highly ordered solids than thermal equilibration (Figure 6). Finally, we describe how the unique structures that can be prepared by vapor deposition might be utilized.

Mechanism of layer formation in itraconazole glasses. We begin by briefly reviewing what is known about vapor deposition of molecules that do not form liquid-crystals. Vapor deposition onto substrates near 0.85 T_g produces high density, low enthalpy glasses of many organic molecules.[22,47] High mobility near the free surface during deposition allows nearly complete equilibration of just-deposited molecules into tightly packed configurations; further deposition traps these molecules into place. Clearly surface equilibration will also occur for deposition with $T_{substrate} = T_g$, but under these conditions there is no thermodynamic driving force to form a high-density material. At low substrate temperatures ($T_{substrate} << 0.85T_g$), surface mobility will be insufficient to reach high density states even though they are thermodynamically favored.

The above mechanism for the formation of well-packed glasses is sufficient to explain the structures shown in Figure 7 if we add one new element, as discussed previously.[30] At the equilibrium free-surface of smectic and nematic forming liquids, molecules favor a smectic-like structure, homeotropically anchored at the vacuum interface.[33,48,49] With this mechanism, deposition onto substrates at T_g will lead to a smectic structure with a single director normal to the substrate (Figure 7a); every new layer of molecules wants to form a smectic structure anchored to the free surface and each layer can fit coherently on top of the previous one. Deposition at T_g + 7 K leads to structures with even higher perfection because the bulk material further equilibrates during the deposition process. At T_g + 7 K, structural rearrangements in the bulk take place on the time scale of 1 second while the deposition requires 500-10000 seconds, depending upon film thickness; for comparison, molecular motions are nearly 100 times slower at T_g.[39,50] When

deposition occurs onto substrates just below T_g (middle panel in Figure 7), molecules near the free surface of the film still have a driving force to achieve the equilibrium smectic layer but not quite enough time to do so. An incompletely organized smectic layer with the "wrong" layer spacing gets trapped into place by further deposition since at these temperatures reorganization in the bulk material is negligible. Since mobility at the surface depends strongly on temperature, the system more closely attains its equilibrium structure at higher values of $T_{substrate}$, as shown in Figure 3.

At $T_{substrate}$ near 0.8 T_g, surface mobility is so low that just-deposited molecules make no progress in their attempt to create homeotropically-anchored smectic layers. In this regime, molecules tend to lie parallel to the substrate; we expect that this minimizes the energy for an incoming molecule landing on a relatively flat surface.[21] Interestingly, the molecules in these glasses have a slight tendency to form smectic-like or nematic-like structures with directors in the plane of the substrate. This can be seen in Figure 1a in the 2D GIWAXS scattering pattern of $T_{substrate}$ = 260 K. Along q_{xy}, small diffuse peaks appear at around 0.24, 0.48 and 0.72 $Å^{-1}$, indicating a periodic structure in the plane of the substrate; see supplementary figure SI2. This feature is isotropic in the plane, indicating the presence of weakly-organized domains of randomly oriented in-plane layers.

The above mechanism allows an understanding of the surprising result that vapor-deposited glasses can be more ordered than thermally equilibrated samples, as shown in Figure 6. A key feature of the proposed mechanism is that molecular organization in the as-deposited glass is being completely controlled by the free surface; $T_{substrate}$ determines the mobility near the free surface and this determines the extent to which the equilibrium surface structure is attained. In contrast, during thermal equilibration in the smectic regime, molecular organization of a thin film depends upon the preferred structure at both the free surface and the substrate. For the substrates used in these experiments, we expect that planar anchoring is preferred. Thus the bulk sample equilibrates as best it can with incompatible boundary conditions at the two interfaces and achieves a somewhat disordered compromise as represented by the schematic in Figure 6.

The proposal that smectic alignment for vapor-deposited itraconazole is completely controlled by the free surface is supported by preliminary deposition experiments on various substrates. We have observed that deposition onto silicon substrates treated to promote homoetropic anchoring has no effect on the structure of the vapor-deposited glasses. In addition, deposition of itraconazole at 325 K onto an already-deposited layer prepared at 270 K results in strong smectic layering with the director along the surface normal, even though molecules in the underlying layer are nearly planar. This conclusion expands upon birefringence results reported in reference [30] indicating that the structures of the vapor-deposited itraconazole glasses prepared here do not depend on the identity of the underlying substrate. Our assumption of high mobility at the surface of itraconazole glasses is consistent with previous work on organic glass formers indicating up to 8 orders of magnitude enhancement of surface diffusion relative to the bulk;[31,32] this assumption could be tested experimentally.

While not investigated here, it is likely that the vapor-deposited glasses of itraconazole exhibit polar order, as observed previously for deposition of polar molecules.[23,51] The mechanism described above implies that glasses deposited at different substrate temperatures could exhibit different levels of polar order and this warrants further investigation.

In comparison with previous literature on vapor-deposited LC systems, the current results provide evidence of both more highly ordered samples and tunable smectic spacing. In earlier studies of vapor-deposited thiophene, the microstructures achieved in the prepared films were similar to those of the known equilibrium smectic state; since only out-of-plane x-ray scattering was reported, it is not possible to characterize the extent to which the smectic layers were oriented along the surface normal. Variable layer spacing at equilibrium has been reported for some systems that exhibit a regular smectic A-to-smectic C transition.[43] In this case, the equilibrium layer spacing is reduced with temperature over a range of about 10%. While solids with variable smectic spacing might be formed by quenching these materials, we are unaware of such reports.

Potential applications. As discussed in the introduction, organized solids prepared via LC states are being widely explored for use in organic electronics and optoelectronics. Glassy liquid crystals have already been used as thin film transistors, solid-state lasers, optical memory, phosphorescent organic light emitting diodes (PhOLEDs) and, optical devices such as polarizers and notch filters.[1] For these applications, active layers are prepared by thermal annealing to attain an equilibrium LC state followed by cooling to form the liquid crystal glass.

Relative to processes that rely on thermal annealing, vapor-deposition expands the range of molecular packing arrangements and orientations available for organic electronic and optoelectronic applications. Deposition allows preparation of non-equilibrium microstructures such as smectic layers with tunable layer spacings, as shown in Figure 3. In addition, deposition can directly prepare highly oriented smectic structures that are functionally monodomains, even on substrates which would not support such high levels of organization via thermal annealing, as shown in Figure 6. Previous work has established that vapor-deposited glasses of itraconazole are macroscopically homogeneous and molecularly smooth, as required for many applications.[30] Vapor deposition is already used on a massive scale to produce organic light emitting diodes for cellphone displays and this illustrates the compatibility of deposition with high throughput manufacturing. In contrast, the preparation of multilayer devices by thermal annealing may be time-consuming and could be complicated both by the influence of underlying layers on molecular anchoring and the possibility that annealing one layer might degrade the structure of an underlying layer.

Concluding Remarks

Glasses of itraconazole, a model LC system, were formed by physical vapor deposition. Glasses with a range of interesting microstructures can be prepared by controlling the substrate temperature during the deposition process. Deposition onto substrates above T_g yielded highly aligned smectic layers with the director normal to the substrate; these samples were better aligned than a thermally annealed sample. Deposition just below T_g allowed the spacing of the smectic-like layers to be controlled over a range of 16%. At the lowest substrate temperatures investigated, molecules preferentially lay nearly flat in the

plane of the substrate. These microstructures are formed throughout the thickness of the film and are stable at temperatures below T_g.

The mechanism proposed here to explain the observed microstructures suggests that similarly interesting structures will be formed by vapor deposition of other LC systems such as those used in organic electronics. Key elements of the mechanism are the smectic organization preferred by molecules at the free surface of the glass and enhanced molecular mobility near the free surface. An important consequence of this mechanism is that the anchoring preferred at the substrate is irrelevant. Vapor deposition is thus a tool for the preparation of structures in LC glasses that cannot be obtained by thermal annealing. An important next step is to extend this work to other types of liquid crystals in order explore what novel structures can be attained in these systems through the control of substrate temperature. Columnar systems are a particularly interesting target as they have often been utilized for organic electronics because of the efficient charge transport that is possible along the columns.

ACKNOWLEDGMENT

WAXS experiments were supported by the National Science Foundation (DMR-1234320). GIWAXS experiments were supported by NSF through the University of Wisconsin Materials Research Science and Engineering Center (DMR-1121288), which also provided instrumentation support. K.O. and M.L.C. were partially supported by NSF DMR award 1410438. Use of the Stanford Synchrotron Radiation Lightsource, SLAC National Accelerator Laboratory, is supported by the U.S. Department of Energy, Office of Science, Office of Basic Energy Sciences under Contract No. DE-AC02-76SF00515.

ABBREVIATIONS

GIWAXS – Grazing incidence wide angle x-ray scattering, **WAXS** – Wide angle x-ray scattering, $\mathbf{T_{substrate}}$ – Substrate temperature during deposition, LC – liquid crystal

References

(1) Chen, H. P.; Ou, J. J.; Chen, S. H. Glassy Liquid Crystals as Self-Organized Films for Robust Optoelectronic Devices. In *Nanoscience with Liquid Crystals*; Li, Q., Ed.; Springer International Publishing, 2014; pp 179–208.

(2) Desiraju, G. R. Crystal Engineering: From Molecule to Crystal. *J. Am. Chem. Soc.* **2013**, *135* (27), 9952–9967.

(3) Lu, C.; Chen, H.-C.; Chuang, W.-T.; Hsu, Y.-H.; Chen, W.-C.; Chou, P.-T. Interplay of Molecular Orientation, Film Formation, and Optoelectronic Properties on Isoindigo- and Thienoisoindigo-Based Copolymers for Organic Field Effect Transistor and Organic Photovoltaic Applications. *Chem. Mater.* **2015**, *27* (19), 6837–6847.

(4) Yokoyama, D. Molecular Orientation in Small-Molecule Organic Light-Emitting Diodes. *J. Mater. Chem.* **2011**, *21* (48), 19187–19202.

(5) Menke, S. M.; Holmes, R. J. Exciton Diffusion in Organic Photovoltaic Cells. *Energy Environ. Sci.* **2014**, *7* (2), 499–512.

(6) O'Neill, M.; Kelly, S. M. Liquid Crystals for Charge Transport, Luminescence, and Photonics. *Adv. Mater.* **2003**, *15* (14), 1135–1146.

(7) Pisula, W.; Zorn, M.; Chang, J. Y.; Müllen, K.; Zentel, R. Liquid Crystalline Ordering and Charge Transport in Semiconducting Materials. *Macromol. Rapid Commun.* **2009**, *30* (14), 1179–1202.

(8) Kline, R. J.; DeLongchamp, D. M.; Fischer, D. A.; Lin, E. K.; Heeney, M.; McCulloch, I.; Toney, M. F. Significant Dependence of Morphology and Charge Carrier Mobility on Substrate Surface Chemistry in High Performance Polythiophene Semiconductor Films. *Appl. Phys. Lett.* **2007**, *90* (6), 2005–2008.

(9) Stöhr, J.; Samant, M. . Liquid Crystal Alignment by Rubbed Polymer Surfaces: A Microscopic Bond Orientation Model. *J. Electron Spectros. Relat. Phenomena* **1999**, *98–99*, 189–207.

(10) Yeung, F. S.; Ho, J. Y.; Li, Y. W.; Xie, F. C.; Tsui, O. K.; Sheng, P.; Kwok, H. S. Variable Liquid Crystal Pretilt Angles by Nanostructured Surfaces. *Appl. Phys. Lett.* **2006**, *88* (5), 51910.

(11) Janning, J. L. Thin Film Surface Orientation for Liquid Crystals. *Appl. Phys. Lett.* **1972**, *21* (4), 173.

(12) Castellano, J. A. Surface Anchoring of Liquid Crystal Molecules on Various Substrates. *Mol. Cryst. Liq. Cryst.* **1983**, *94*, 33–41.

(13) Stöhr, J. Liquid Crystal Alignment on Carbonaceous Surfaces with Orientational Order. *Science (80-.).* **2001**, *292* (5525), 2299–2302.

(14) McCulloch, I.; Heeney, M.; Bailey, C.; Genevicius, K.; Macdonald, I.; Shkunov, M.; Sparrowe, D.; Tierney, S.; Wagner, R.; Zhang, W.; Chabinyc, M. L.; Kline, R. J.; McGehee, M. D.; Toney, M. F. Liquid-Crystalline Semiconducting Polymers with High Charge-Carrier Mobility. *Nat. Mater.* **2006**, *5* (4), 328–333.

(15) Van Breemen, A. J. J. M.; Herwig, P. T.; Chlon, C. H. T.; Sweelssen, J.; Schoo, H. F. M.; Setayesh, S.; Hardeman, W. M.; Martin, C. a.; De Leeuw, D. M.; Valeton, J. J. P.; Bastiaansen, C. W. M.; Broer, D. J.; Popa-Merticaru, A. R.; Meskers, S. C. J. Large Area Liquid Crystal Monodomain Field-Effect Transistors. *J. Am. Chem. Soc.* **2006**, *128* (7), 2336–2345.

(16) Shklyarevskly, I. O.; Jonkheijm, P.; Stutzmann, N.; Wasserberg, D.; Wondergem, H. J.; Christianen, P. C. M.; Schenning, A. P. H. J.; Leeuw, D. M. D.; Tomovic, Z.; Müllen, K.; Wu, J.; Maan, C. J. High Anisotrophy of the Field-Effect Transistor Mobility in Magnetically Aligned Disotic Liquid-Crystalline Semiconductors. *J. Am. Chem. Soc.* **2005**, *127* (8), 16233–16237.

(17) Eccher, J.; Faria, G. C.; Bock, H.; von Seggern, H.; Bechtold, I. H. Order Induced Charge Carrier Mobility Enhancement in Columnar Liquid Crystal Diodes. *ACS Appl. Mater. Interfaces* **2013**, *5* (22), 11935–11943.

(18) Liu, C.; Fechtenkötter, A.; Watson, M. D.; Müllen, K.; Bard, A. J. Room Temperature Discotic Liquid Crystalline Thin Films of Hexa- P Eri -Hexabenzocoronene: Synthesis and Optoelectronic Properties. *Chem. Mater.* **2003**, *15* (1), 124–130.

(19) Li, Z.; Li, Z. R.; Meng, H. *Organic Light-Emitting Materials and Devices*; CRC Press, 2006.

(20) Baldo, M.; Deutsch, M.; Burrows, P.; Gossenberger, H.; Gerstenberg, M.; Ban, V.; Forrest, S. Organic Vapor Phase Deposition. *Adv. Mater.* **1998**, *10* (18), 1505–1514.

(21) Dalal, S. S.; Walters, D. M.; Lyubimov, I.; de Pablo, J. J.; Ediger, M. D. Tunable Molecular Orientation and Elevated Thermal Stability of Vapor-Deposited Organic Semiconductors. *PNAS* **2015**, *112* (14), 4227–4232.

(22) Dalal, S. S.; Fakhraai, Z.; Ediger, M. D. High-Throughput Ellipsometric Characterization of Vapor-Deposited Indomethacin Glasses. *J. Phys. Chem. B* **2013**, *117* (49), 15415–15425.

(23) Noguchi, Y.; Miyazaki, Y.; Tanaka, Y.; Sato, N.; Nakayama, Y.; Schmidt, T. D.; Brütting, W.; Ishii, H. Charge Accumulation at Organic Semiconductor Interfaces due to a Permanent Dipole Moment and Its Orientational Order in Bilayer Devices. *J. Appl. Phys.* **2012**, *111* (11), 114508.

(24) Dawson, K.; Kopff, L. A.; Zhu, L.; McMahon, R. J.; Yu, L.; Richert, R.; Ediger, M. D. Molecular Packing in Highly Stable Glasses of Vapor-Deposited Tris-Naphthylbenzene Isomers. *J. Chem. Phys.* **2012**, *136* (9), 94505.

(25) Gujral, A.; O'Hara, K. A.; Toney, M. F.; Chabinyc, M. L.; Ediger, M. D. Structural Characterization of Vapor-Deposited Glasses of an Organic Hole Transport Material with X-Ray Scattering. *Chem. Mater.* **2015**, *27* (9), 3341–3348.

(26) Yokoyama, D.; Setoguchi, Y.; Sakaguchi, A.; Suzuki, M.; Adachi, C. Orientation Control of Linear-Shaped Molecules in Vacuum-Deposited Organic Amorphous Films and Its Effect on Carrier Mobilities. *Adv. Funct. Mater.* **2010**, *20*, 386–391.

(27) Grelet, E.; Dardel, S.; Bock, H.; Goldmann, M.; Lacaze, E.; Nallet, F. Morphology of Open Films of Discotic Hexagonal Columnar Liquid Crystals as Probed by Grazing Incidence X-Ray Diffraction. *Eur. Phys. J. E. Soft Matter* **2010**, *31* (4), 343–349.

(28) Kramer, M.; Hoffmann, V. Infrared Spectroscopic Characterization of Orientation and Order of Thin Oligothiophene Films. *Opt. Mater. (Amst).* **1998**, *9* (1–4), 65–69.

(29) Eccher, J.; Zajaczkowski, W.; Faria, G. C.; Bock, H.; von Seggern, H.; Pisula, W.; Bechtold, I. H. Thermal Evaporation versus Spin-Coating: Electrical Performance in Columnar Liquid Crystal OLEDs. *ACS Appl. Mater. Interfaces* **2015**, *7* (30), 16374–16381.

(30) Gómez, J.; Jiang, J.; Gujral, A.; Huang, C.; Yu, L.; Ediger, M. D. Vapor Deposition of a Smectic Liquid Crystal: Highly Anisotropic, Homogeneous Glasses with Tunable Molecular Orientation. *Soft Matter* **2016**, *12* (11), 2942–2947.

(31) Brian, C. W.; Yu, L. Surface Self-Diffusion of Organic Glasses. *J. Phys. Chem. A* **2013**, *117* (50), 13303–13309.

(32) Zhu, L.; Brian, C. W.; Swallen, S. F.; Straus, P. T.; Ediger, M. D.; Yu, L. Surface Self-Diffusion of an Organic Glass. *Phys. Rev. Lett.* **2011**, *106* (25), 256103.

(33) Sadati, M.; Ramezani-Dakhel, H.; Bu, W.; Sevgen, E.; Liang, Z.; Erol, C.; Taheri Qazvini, N.; Rahimi, M.; Lin, B.; Roux, B.; Schlossman, M.; de Pablo, J. J. Structural Organization of Liquid Crystals at Liquid Crystal-Air Interface: Synchrotron X-Ray Reflectivity and Computational Simulations. *Bull. Am. Phys. Soc.* **2016**, [Access: aps.org/Meeting/MAR16/Session/S37.9].

(34) Kimura, N.; Hayashi, S.; Takenaka, T. Infrared Studies on Molecular Orientation in Nematic Films of MBBA with Two Free Surfaces. *Bull. Inst. Chem. Res. Kyoto Univ.* **1980**, *58* (5–6), 559–563.

(35) Tarakhan, L. M. Determination of the Surface Tension of 5CB Liquid Crystal by the Pendant Drop Method. *Ukr. J. Phys.* **2006**, *51* (1), 22–26.

(36) Shi, W.; Nacev, B. A.; Bhat, S.; Liu, J. O. Impact of Absolute Stereochemistry on the Antiangiogenic and Antifungal Activities of Itraconazole. *Chem. Lett* **2010**, *1*, 155–159.

(37) Kurka, O.; Kučera, L.; Bednář, P. Analytical and Semipreparative Chiral Separation of *Cis* - Itraconazole on Cellulose Stationary Phases by High-Performance Liquid Chromatography. *J. Sep. Sci.* **2016**, *39* (14), 2736–2745.

(38) Peeters, O. .; Blaton, N. .; De Ranter, C. . Cis-2-Sec-Butyl-4-[4-(4-{4-[2-(2,4-Dichlorophenyl)-2-(1H-1,2,4-Triazol-1-Ylmethyl)-1,3-Dioxolan-4-Ylmethoxy]phenyl}-Piperazin-1-Yl)phenyl]-2,4-Dihydro-1,2,4-Triazol-3-One (Itraconazole). *Acta Crystallogr. Sect. C* **1996**, *52*, 2225–2229.

(39) Tarnacka, M.; Adrjanowicz, K.; Kaminska, E.; Kaminski, K.; Grzybowska, K.; Kolodziejczyk, K.; Wlodarczyk, P.; Hawelek, L.; Garbacz, G.; Kocot, A.; Paluch, M. Molecular Dynamics of Itraconazole at Ambient and High Pressure. *Phys. Chem. Chem. Phys.* **2013**, *15* (47), 20742–20752.

(40) Baker, J. L.; Jimison, L. H.; Mannsfeld, S.; Volkman, S.; Yin, S.; Subramanian, V.; Salleo, A.; Alivisatos, A. P.; Toney, M. F. Quantification of Thin Film Crystallographic Orientation Using X-Ray Diffraction with an Area Detector. *Langmuir* **2010**, *26* (11), 9146–9151.

(41) Fewster, P. F. *X-Ray Scattering from Semiconductors*, 1st ed.; Imperial College Press: London, 2000.

(42) Guinier, A. *X-Ray Diffraction in Crystals, Imperfect Crystals and Amorphous Bodies*; W.H. Freeman: San Francisco, 1963.

(43) Lagerwall, J. P. F.; Giesselmann, F. Current Topics in Smectic Liquid Crystal Research. *Chemphyschem* **2006**, *7* (1), 20–45.

(44) Benmore, C. J.; Mou, Q.; Benmore, K. J.; Robinson, D. S.; Neuefeind, J.; Ilavsky, J.; Byrn, S. R.; Yarger, J. L. A SAXS-WAXS Study of the Endothermic Transitions in Amorphous or Supercooled Liquid Itraconazole. *Thermochim. Acta* **2016**, *644*, 1–5.

(45) *Mechanical and Thermophysical Properties of Polymer Liquid Crystals*; Brostow, W., Ed.; Springer Science & Business Media: Glasgow, 1998.

(46) Perova, T. S.; Vij, J. K.; Kocot, A. Observation of an Anchoring Transition in a Discotic Liquid Crystal. *Europhys. Lett.* **1998**, *44* (2), 198–204.

(47) Dawson, K.; Zhu, L.; Kopff, L. A.; McMahon, R. J.; Yu, L.; Ediger, M. D. Highly Stable Vapor-Deposited Glasses of Four Tris-Naphthylbenzene Isomers. *J. Phys. Chem. Lett.* **2011**, *2* (21), 2683–2687.

(48) Pershan, P. S.; Braslau, a; Weiss, a H.; Als-Nielsen, J. Smectic Layering at the Free Surface of Liquid Crystals in the Nematic Phase: X-Ray Reflectivity. *Phys. Rev. A* **1987**, *35* (11), 4800–4813.

(49) Jerome, B. Surface Effects and Anchoring in Liquid Crystals. *Reports Prog. Phys.* **1999**, *54* (3), 391–451.

(50) Angell, C. A.; Ngai, K. L.; McKenna, G. B.; McMillan, P. F.; Martin, S. W. Relaxation in Glass-forming Liquids and Amorphous Solids. *J. Appl. Phys.* **2000**, *88* (6), 3113.

(51) Plekan, O.; Cassidy, A.; Balog, R.; Jones, N. C.; Field, D. Spontaneous Electric Fields in Films of Cis-Methyl Formate. *Phys. Chem. Chem. Phys.* **2012**, *14* (28), 9972–9976.

Chapter 4

Preparing highly organized glasses of discotic liquid crystalline systems by vapor deposition

Ankit Gujral, Jaritza Gomez, Shigang Ruan, Michael F. Toney, Harald Bock, Lian Yu, M. D. Ediger

Submitted on July 8, 2017 to *Chemistry of Materials,* American Chemical Society.

Abstract

Anisotropic molecular packing, particularly in highly ordered liquid-crystalline arrangements, has the potential for optimizing performance in organic electronic and optoelectronic applications. Here we show that physical vapor deposition can be used to prepare highly organized out-of-equilibrium (glassy) solids of discotic liquid-crystalline systems. Using grazing incidence X-ray scattering, atomic force microscopy and UV/Vis spectroscopy, we compare three systems: a rectangular columnar liquid crystal, a hexagonal columnar liquid crystal and a non-mesogen. The packing motifs accessible by vapor deposition are highly organized for the liquid crystalline systems and vary from face-on to edge-on columnar arrangements depending upon the substrate temperature during deposition. The structures formed at a given substrate temperature can be understood as resulting from partial equilibration toward the structure of the equilibrium liquid crystal surface during the deposition process.

Introduction

One of the central challenges in materials science is the control of molecular organization in solids. The ability to control molecular packing is required for the development of many technologically important fields. Among these fields are organic electronics and optoelectronics where molecular-scale packing modifications are being explored to engineer better devices.[1] Organic light emitting diodes (OLEDs), for instance, exhibit better outcoupling when emitter molecules are oriented in the solid matrix with their transition dipoles lying in-plane such that they emit preferentially perpendicular to the device face.[2] Microstructures with enhanced π-orbital overlap may also exhibit better charge carrier mobility in molecular systems;[3,4] many such structures that have anisotropic molecular packing arrangements. Preparation routes that lead to optimized microstructures have been investigated for small molecule and polymeric organic systems, a few of which are summarized here. Solution-shearing has been used to prepare anisotropic structures that lead to enhanced charge carrier mobility.[5] Lattice strain, in combination with solution shearing, has been used to further increase orbital overlap between component molecules, thereby further enhancing mobility.[6] Films prepared in the presence of external fields can also exhibit anisotropic packing and improved performance.[7,8]

Liquid crystalline systems have been exploited for organic electronic applications as a result of their propensity to self-assemble into highly ordered, anisotropic structures.[9–11] Columnar liquid crystalline systems, in particular, are ideal candidates for organic semiconducting devices as they self-assemble into columnar superstructures governed, in part, by molecular cores rich in π-electrons.[12] The cores can form highly conjugated structures within the columns that exhibit high charge carrier mobility. However, the preparation of highly organized films of columnar liquid crystalline moieties has thus far required a thermal annealing process, sometimes on chemically altered substrates, to achieve the correct molecular packing structures.[13] For instance, a sacrificial layer is required to induce face-on packing in certain discotic systems.[14] While thermal annealing and chemically-tailored substrates may allow a

desired structure to be achieved, these processing steps may also have deleterious effects on the performance of devices.

Physical vapor deposition, a method used in the industrial manufacture of OLEDs,[15] can be used to control molecular organization in glassy solids by controlling deposition conditions, even for molecules without liquid crystalline phases.[16,17] The structures prepared are trapped as non-equilibrium solids that are independent of underlying substrate chemistry; anisotropic structures can be achieved without subsequent annealing. Vapor-deposited glasses of non-liquid crystal systems show subtle structural and optical anisotropy (compared with liquid crystalline structures) but have, nonetheless, exhibited enhanced charge carrier mobility.[3] Tunability of structure of vapor-deposited glasses of non-liquid crystal formers has also been shown for a large number of systems, with structure controlled by the substrate temperature during deposition ($T_{substrate}$).[16,18,19]

Combining vapor deposition as a route to anisotropic structures with the self-assembly of liquid crystals has recently been shown in one case to prepare films with highly organized and widely tunable structures.[20,21] The structural anisotropy accessible by vapor deposition was investigated in itraconazole, a rod-shaped mesogen which enters the smectic phase (forming molecular layers) just above the glass transition temperature, T_g. The vapor-deposited structures varied from molecules laying almost exclusively in-plane (on average, 76º from substrate normal) to molecules "standing up" with the molecular long axes nearly along the substrate normal (27º from the normal). The layer spacing for $T_{substrate} = T_g$ to $T_g - 20$ K tracked the average molecular tilt angle, with higher tilts corresponding to smaller spacing, trapping the film into smectic-like packing arrangements not accessible in equilibrium, while below T_g - 20 K the molecules lie almost entirely in-plane. Some of the structures accessed by vapor deposition were more ordered than those prepared by extended thermal annealing of the same material.[20] Applying this approach to discotic liquid crystalline systems may provide access to highly tunable columnar structures, with columns propagating either in the plane of the substrate (useful, for instance, in field effect transistors) or out-of-plane (useful in photovoltaics). Important precedents exist

for vapor deposition of discotic liquid crystals. Of particular relevance to the current work is a study by Eccher et al.[22] which showed that vapor-deposited films of a discotic liquid crystal exhibited higher columnar order when compared with a spin-coated film of the same material. This led to higher charge carrier mobility in the vapor-deposited film. However, the range of possible structures that can be achieved by vapor deposition has not been investigated for any discotic system.

Here we investigate properties of films prepared by physical vapor deposition of three disc-shaped molecules (as shown in Figure 1): 2,6,10-triethoxycarbonyl-triphenylene (a rectangular columnar mesogen, hereafter called triphenylene-ester), 1,16-di(methoxycarbonyl)-6,7,12,13-tetra(ethoxycarbonyl)phenanthro[ghi-1,2,3,4]perylene (a hexagonal columnar mesogen, hereafter called phenanthroperylene-ester) and m-MTDATA (4,4',4"-tris[phenyl(m-tolyl)amino]triphenylamine, a non-mesogen). The films were deposited over a range of substrate temperatures ranging from ~0.75 T_g to 0.99 T_g. We characterized molecular packing in the films as a function of $T_{substrate}$ by grazing incidence wide angle X-ray scattering (GIWAXS). Films prepared at low $T_{substrate}$ exhibited face-on packing arrangements for all three systems. Films prepared at $T_{substrate} \sim T_g$ exhibited edge-on packing with highly organized columnar structures for the two mesogens, while an isotropic disordered structure was observed for the non-mesogen. Atomic force microscopy (AFM) was used to determine surface morphology of the various films, and domain-like structures were found in the highly-organized films. UV/Visible spectroscopy (UV/Vis) was used to investigate the local electronic properties of the films with results indicating that π-conjugated structures persist in the highly-ordered films even though they were directly prepared as solids by vapor deposition. We investigated the thermodynamic state of the films by conducting temperature annealing experiments; the as-deposited films are shown to be out-of-equilibrium (glassy) materials.

Figure 1.

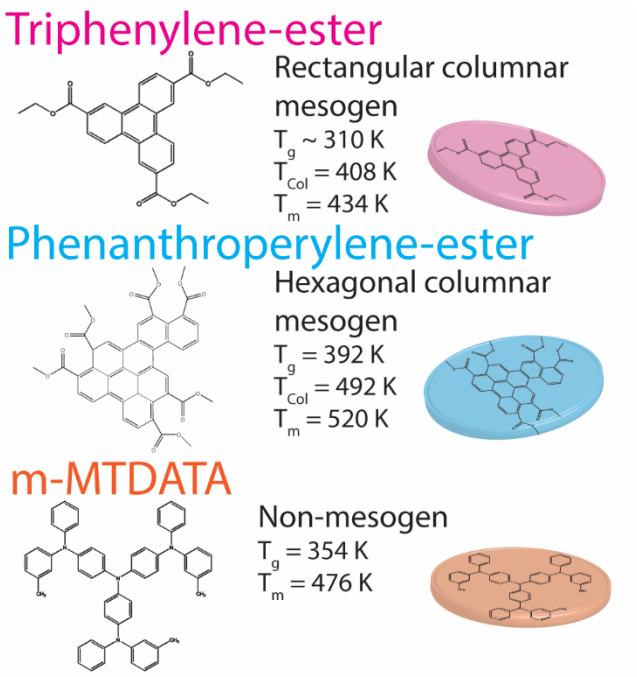

Figure 1. The three systems investigated, with molecular structures and transition temperatures. Also shown is a color-coded schematic that will be used to describe the systems in later figures.

These results suggest that vapor deposition of discotic liquid crystals may be generally useful for preparation of highly organized films and that the substrate temperature during deposition will provide access to a wide range of packing arrangements. The structures observed in this work can be explained by a mechanism invoking a combination of two factors: the tendency to self-assemble at the free surface of the equilibrium liquid[16,23–25], and enhanced mobility at the free-surface of glasses[26,27]. The generality of this mechanism suggests that these results may be extended to other columnar liquid crystal systems, and other classes of liquid crystals, that have a propensity to self-assemble into highly organized structures at vacuum interfaces.

Experimental Methods

Materials. m-MTDATA was purchased from Sigma-Aldrich (>99% pure) and used as-received. m-MTDATA does not exhibit any liquid crystalline phases. It has a melting point of T_m = 476 K and a glass transition temperature of T_g =354 K. The triphenylene-ester was synthesized as described in ref [28]. It exhibits a columnar phase below 408 K and its crystalline solid has a melting temperature T_m = 434 K. We estimate that T_g ~ 310 K based on *in-situ* thin film transformation experiments. The phenanthroperylene-ester was synthesized as described in ref [29]. It exhibits a columnar hexagonal phase below 492 K. Its crystalline solid undergoes a melting transition at T_m = 520 K. It undergoes a glass transition at T_g = 392 K.

Vapor deposition. Glasses of the three systems were prepared by physical vapor deposition onto either a silicon <100> substrate with native oxide or a fused silica substrate. The deposition rate was maintained at 0.2 ± 0.02 nm/s in a vacuum chamber (base pressure ~ 10^{-7} torr), monitored using a Quartz Crystal Microbalance (Sycon). The substrates were held on copper blocks that were maintained at the desired substrate temperature using a LakeShore 336 PID controller (LakeShore Cryotronics, Inc.) paired with resistive cartridge heaters (Southwest Heater Corp.) and platinum resistive temperature detectors (Omega Engineering., Spectris PLC). Thermal paste (Apiezon N or H, for low or high temperatures, respectively) was smeared between the substrates and the copper to maintain thermal contact in the vacuum

environment. Roughly 150 nm films were deposited on silicon substrates for grazing incidence wide-angle X-ray scattering (GIWAXS) and for the Atomic Force Microscopy (AFM) measurements. For UV/Visible absorption spectroscopy (UV/Vis), 90-120 nm films were prepared on fused silica substrates.

GIWAXS. GIWAXS measurements were conducted at beamline 11-3 at the Stanford Synchrotron Radiation Lightsource (SSRL). The wavelength of the incident beam was 0.973 Å, with a detector resolution of 0.002 $Å^{-1}$/pixel (detector distance = 300 mm). The incident angle was set to 0.14° to assure that the scattering occurred in the bulk of the film and exposure was typically less than 120 seconds. The data was processed with the SSRL-developed WxDiff software package. Following the protocol outlined in Baker et al.,[30] the diffraction patterns were corrected for polarization of the beam and χ-corrected to obtain accurate reciprocal space maps. GIWAXS measurements were performed at room temperature except as noted.

AFM. Atomic force microscopy (AFM) measurements were conducted on a Bruker MultiMode 8 AFM using ScanAsyst PeakForce Tapping mode. The measurements were conducted at room temperature.

UV/Vis. UV/Visible absorption spectra were collected on a JA Woollam M-2000 Variable Angle Spectroscopic Ellipsometer with a wavelength range of 245 nm to 1000 nm. The samples were mounted and measured in transmission geometry at normal incidence. A spot size of roughly 2 mm was used. These samples were also analyzed using X-ray diffraction, with the results indicating no significant difference in structure for films prepared on fused silica and on silicon.

Results

Molecular packing. Figure 2 shows two-dimensional (2D) grazing incidence wide angle X-ray scattering (GIWAXS) patterns for vapor-deposited films of the triphenylene-ester, the phenanthroperylene-ester and m-MTDATA; scattering intensity is illustrated in a linear color-scheme from red to blue representing high to low intensity): Also shown are schematic illustrations describing molecular packing motifs that are consistent with the GIWAXS patterns, as we discuss below. For each system, two GIWAXS patterns are

shown, one for a sample deposited at roughly $T_{substrate}$~0.75T_g (top pattern within each panel) and the other for $T_{substrate}$~T_g (bottom pattern within each panel); the absolute $T_{substrate}$ is indicated. The GIWAXS measurements were all made at room temperature for this section of the paper.

As shown in Figure 2, films prepared at low $T_{substrate}$ for all three systems exhibit a roughly face-on molecular packing motif, while at $T_{substrate}$~T_g quite distinct packing structures are attained by the three systems. To facilitate our discussion, we begin with a brief description of the 2D scattering patterns. The axes of the 2D GIWAXS patterns represent components of the scattering wavevector, q (reported in $Å^{-1}$), defined as $q = 4\pi*\sin\theta/\lambda$, where θ is ½ the scattering angle and λ is the wavelength of the X-ray beam. q_{xy} and q_z represent the in-plane and out-of-plane wavevectors, respectively. For our samples, we did not observe a significant change in the scattering pattern upon rotating the films in the xy-plane (substrate plane). Thus, q_x and q_y are equivalent and the films are in-plane isotropic on the length-scale probed by the GIWAXS experiments (roughly 1 mm^2); The scattering position of the bright peaks in the pattern correspond inversely to real-space periodicity of the structures, d, by the relationship $d = 2\pi/q$. Scattering features along q_{xy} (horizontal axis) correspond to ordering in the plane of the substrate while features appearing along q_z (vertical axis) correspond to ordering out-of-plane.

We will begin our analysis with the triphenylene-ester, a columnar rectangular mesogen, focusing on the data in the top panel (pink) in Figure 2. Scattering patterns from two glasses are displayed describing the two representative structures accessible by vapor-depositing at low and high $T_{substrate}$ for the system. Even though some of these scattering patterns indicate high levels of liquid crystal-like order, they are best described as "glasses" as we discuss below. For the pattern obtained from the glass prepared at $T_{substrate}$ = 240 K (~0.77T_g), a broad diffraction peak can be seen at q_z ~1.75 $Å^{-1}$, corresponding to a real-space 3.7 Å periodic structure propagating out-of-plane, that can be inferred to be a π-π stacking structure. A diffraction peak appearing in-plane at q_{xy}~0.5 $Å^{-1}$ indicates in-plane periodicity corresponding to roughly 13 Å, approximately a molecular diameter. These two features combined show a columnar

structure with columns propagating out-of-plane as shown in the schematic alongside the pattern. There is some disorder within the columns reflected in the breadth of the peak at q_z ~1.75 $Å^{-1}$.

By comparison, the film prepared at $T_{substrate}$ = 295 K ($T_{substrate}$ ~ T_g), is highly ordered with columns propagating in-plane. The in-plane columnar structures are evidenced from the sharp in-plane diffraction peak at q_{xy} ~ 1.8 $Å^{-1}$ (notice this peak is not detectable along q_z). This peak corresponds to a real-space periodic structure of 3.5 Å, indicating a more tightly packed π-π interaction between molecules within the same column than in the sample prepared at lower $T_{substrate}$. The sharpness of the peak, azimuthally as well as along q_{xy}, indicate that the columns formed in this film are much more highly ordered and oriented than those in the low deposition temperature film. The columns themselves form a rectangular superstructure, as inferred from the rectangular grid-like pattern, with columns packing farther apart out-of-plane ($d_{out\text{-}of\text{-}plane}$ = 13.6 Å) than in-plane ($d_{in\text{-}plane}$ = 11.5 Å), as shown in the schematic (a = 13.6 Å, b = 11.5 Å, c = 3.5 Å). This structure in the high $T_{substrate}$ film is similar to planar aligned equilibrium liquid films of columnar liquid crystal structures (with columns parallel to substrate).[31] As the GIWAXS experiments indicate that the film is macroscopically isotropic in the plane of the substrate, we infer that there must be an isotropic distribution of in-plane columnar structures in domain-like formations. The peak at q_{xy} ~ 1.8 $Å^{-1}$ results from the subset of structures with columns perpendicular to the beam while the rectangular grid-like pattern results from the subset of columns that propagate along the beam. We discuss the likely size of these domains below. GIWAXS patterns obtained for intermediate values of $T_{substrate}$ for this system show structures similar to the two displayed in Figures 2, with a transition between the two structures occurring over about 10 K in $T_{substrate}$ near 265 K. The observation that this transition occurs about 50 K below T_g (~310 K) is highly relevant for understanding the mechanism by which vapor deposition prepares these ordered structures.

Vapor-deposited films of the phenanthroperylene-ester, a hexagonal columnar mesogen, also exhibit two representative structures, as shown in the second (blue) panel of Figure 2. The film deposited at low $T_{substrate}$ exhibits a preferred face-on packing arrangement with a broad diffraction peak (with

scattering spread radially) centered around q_z~1.75 $Å^{-1}$; this broad orientational pattern indicates a packing arrangement with a wide distribution of out-of-plane periodic structures. This peak corresponds to a 3.6 Å disordered out-of-plane packing structure. There is another highly textured ring diffracting most strongly in-plane at q_{xy} ~ 0.45 $Å^{-1}$ (or, d ~ 13.9 Å), corresponding to a molecular diameter indicating nearest-neighbor order predominantly orthogonal to the π- π interaction direction. Films deposited at high $T_{substrate}$ (near T_g) are highly ordered. There is a sharp feature indicative of π - π stacking in-plane at q_{xy} ~ 1.8 $Å^{-1}$ (d = 3.5 Å), and sharp peaks at q_z ~ 0.45 $Å^{-1}$ as well as azimuthally along a 60-degree angle from q_z, showing a hexagonal packing superstructure between columns (a = 13.9 Å; c = 3.5 Å). This is shown schematically alongside the scattering pattern and is similar to the structure of a planar aligned equilibrium film of the phenanthroperylene-ester, as shown below. As in the case of the triphenylene-ester system, the schematic for the high temperature sample is representative of one domain-like structure. While film structures accessible in the phenanthroperylene-ester and the triphenylene-ester share some common phenomenology, the phenanthroperylene-ester films show a more continuous transition in structure as $T_{substrate}$ is varied. At intermediate substrate temperatures, highly textured versions of the high temperature hexagonal packing motif can be accessed. These structures will be discussed below and their scattering patterns can be found in Figure 5.

Unlike the two systems discussed above, m-MTDATA (Figure 2 third panel, orange) is a non-mesogen. Films prepared at low $T_{substrate}$ exhibit a slightly face-on packing motif as inferred from the anisotropy in the amorphous halo at q ~ 1.4 $Å^{-1}$ in the top pattern, indicative of some preference for face-on packing with π stacking out-of-plane. A film deposited at $T_{substrate}$ ~ T_g, on the other hand is isotropic and disordered, similar to the structure expected for the equilibrium supercooled liquid of m-MTDATA. Structures trapped into films at intermediate values of $T_{substrate}$ monotonically become more ordered with decreasing $T_{substrate}$. This observation is in qualitative agreement with optical measurements[19] of the molecular orientation of m-MTDATA which showed that the molecules go from isotropically organized to preferentially laying in-plane from high $T_{substrate}$ to low $T_{substrate}$.

Figure 2.

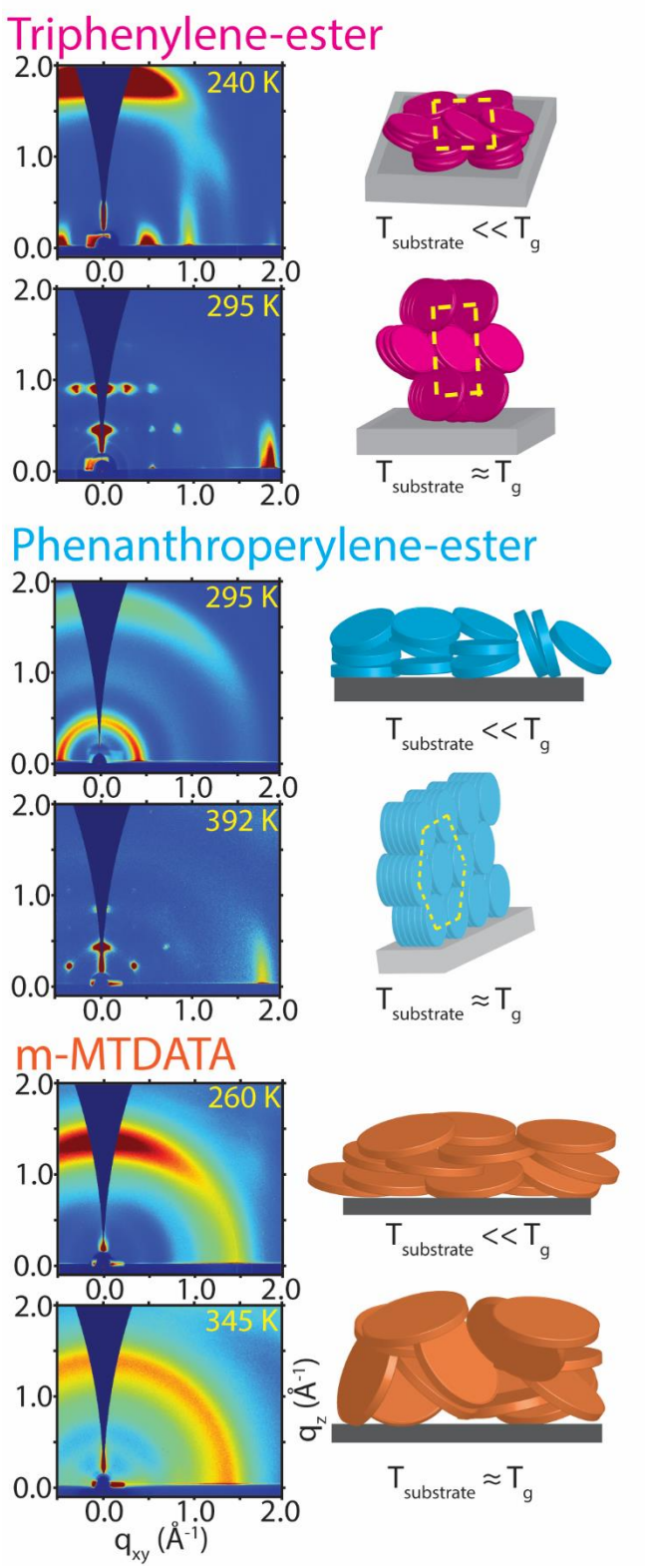

Figure 2. 2D GIWAXS patterns obtained from vapor-deposited films (~ 150 nm thick) of three systems, with schematics describing molecular packing. For each system, data is shown for glasses prepared at $T_{substrate}$ ~ 0.75T_g (upper panel) and $T_{substrate}$ ~ T_g (lower panel). In the schematics, each disk represents one molecule.

Film morphology. Film morphology is important when considering these materials for applications and it provides further insight into the structure and organization of the films that cannot be provided by GIWAXS. We used atomic force microscopy (AFM) to investigate the surface morphology of vapor-deposited films of the three systems. Figure 3 shows AFM micrographs from low $T_{substrate}$ and high $T_{substrate}$ films of the triphenylene-ester, the phenanthroperylene-ester and m-MTDATA. All AFM measurements were performed at room temperature. As discussed above, the highly-ordered films prepared from columnar liquid crystals at $T_{substrate} \sim T_g$ are expected to exhibit domain-like structures in the plane of the substrate. While the surface morphology may not necessarily reflect the bulk morphology, we argue below that the surface features provide a reasonable first approximation to the domain structure in the bulk.

For the triphenylene-ester, films prepared at low $T_{substrate}$ (left micrograph of top panel in Figure 3) are molecularly smooth (R_q = 0.4 nm; where R_q is the root mean square average height deviation from the mean image plane). In contrast, the film prepared at high $T_{substrate}$ (right micrograph) for the same molecule exhibits domains a few 100 nm in size (R_q = 3.0 nm). We interpret the domains observed at high $T_{substrate}$ as highly ordered regions of in-plane columnar structures. This is consistent with a rudimentary Scherrer analysis, based on the peak widths of the columnar scattering peaks ($\Delta q = 0.018$ Å^{-1}), indicating domains of at least 35 nm in the bulk. For films prepared at low $T_{substrate}$, the face-on packing inferred from the scattering pattern does not require the presence of in-plane domains and this is consistent with the smooth nature of the surface.

In vapor-deposited films of the phenanthroperylene-ester, domains are observed in the AFM images for films prepared at both low and high $T_{substrate}$. The domains get smaller as $T_{substrate}$ is lowered, ranging from a few 100 nm (with R_q = 2.8 nm) for $T_{substrate} \sim T_g$ to tens of nm in size (with R_q = 2.2 nm) for $T_{substrate} \sim 0.75\ T_g$ films (AFM micrographs from intermediate substrate temperatures have been excluded for brevity). The domains in the films prepared at high $T_{substrate}$ are similar to those observed in the triphenylene-ester and we imagine that one domain corresponds to a region of uniform in-plane

alignment for the superstructure shown in the schematic in Figure 2, with the domains randomly distributed in-plane on the larger length scale probed by GIWAXS. We interpret the domains observed for the phenanthroperylene-ester film prepared at low $T_{substrate}$ in light of the scattering pattern for this film in Figure 2. The $q \sim 0.45$ $Å^{-1}$ feature indicates the presence of somewhat disorderd columns of molecules. The domain sizes observed in the AFM are smaller for low $T_{substrate}$ films, consistent with the increased disorder.

Films of m-MTDATA are molecularly smooth ($R_{q,345\ K} = 0.6$ nm; $R_{q,260\ K} = 1.1$ nm), and exhibit no significant domain-like structures regardless of $T_{substrate}$. For the film prepared at $T_{substrate} \sim T_g$, this is in agreement with our expectation that this film is identical to a glass prepared by cooling the isotropic liquid. The film prepared at low $T_{substrate}$ is also highly disordered according to Figure 2, in comparison to films prepared from mesogens; domains would not seem to be required in such a disordered material.

Figure 3.

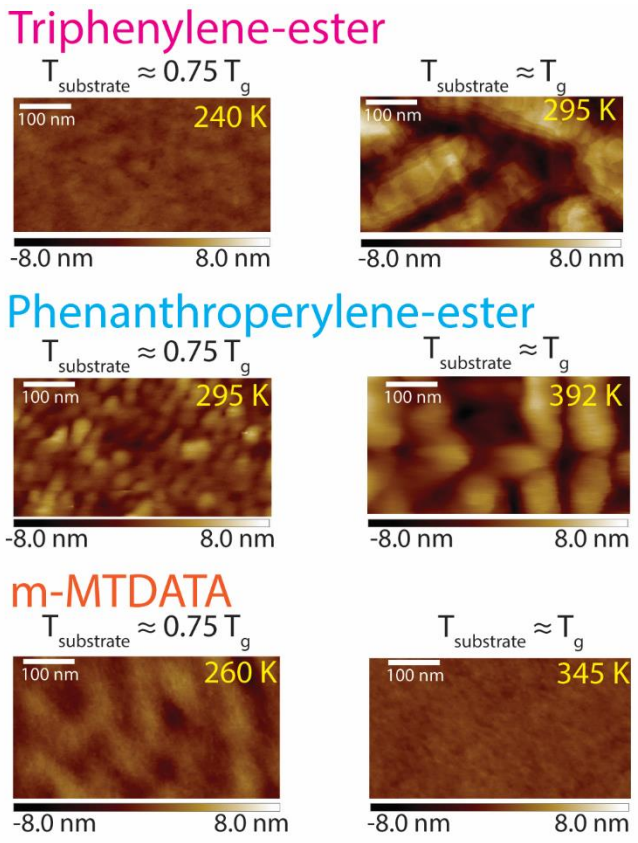

Figure 3. AFM micrographs for glasses vapor-deposited at $T_{substrate} \sim 0.75T_g$ (left) and $T_{substrate} \sim T_g$ (right) for three systems. The height contrast color scale is kept constant at ±8 nm for all the micrographs. The two liquid crystal systems exhibit domain-like structures in the films deposited at $T_{substrate} \sim T_g$ (and the phenanthroperylene-ester shows domain-like structures also in the low $T_{substrate}$ films). The non-mesogen, m-MTDATA, on the other hand, forms molecularly smooth films across the $T_{substrate}$ regime investigated.

Intermolecular π conjugation. For many applications involving organic electronics and optoelectronics, the delocalization of electronic states within the material is highly relevant. Charge carrier mobility in organic materials is controlled by several factors,[5,32–38] and large π-conjugation between molecules is of predominant importance in non-polymeric organic electronic materials.[39] To gain some insight into this, we compared UV/Visible absorption (UV/Vis) spectra obtained from a highly ordered film and a less ordered film of the same system, along with a film prepared by vitrifying the equilibrium liquid crystal state of the system.

Figure 4 shows the UV/Vis spectra as a function of wavelength for three phenanthroperylene-ester films: a film deposited at $T_{substrate}$ = 295 K, a film deposited at $T_{substrate}$ = 387 K, and a film quenched to room temperature from an extending anneal in the equilibrium liquid crystal phase. The position of absorption features in the UV/Vis spectra are indicative of relative electron delocalization: red-shifted (lower energy) absorption features correspond to more delocalization in the system. [40,41] Comparing the as-deposited films, there is a roughly 6 nm red-shift associated with the highest wavelength (lowest energy) absorption at around 460 nm in the film deposited at $T_{substrate}$ = 387 K. We take this to indicate better π-conjugation in the film deposited at the higher temperature and this is consistent with the more ordered structure observed in GIWAXS in Figure 2. Interestingly, the spectrum of the sample prepared by an hour-long anneal at Tg + 10 K of a vapor-deposited film prepared at $T_{substrate}$ =387 K shows no peak shift when compared with the more ordered vapor-deposited glass. This indicates that the extent of conjugation is similar in both films and that, at least on a local level, the extent of ordering in the $T_{substrate}$ ~ T_g vapor-deposited film is similar to that of the equilibrium liquid crystal. As a point of reference, the observed shift of the absorption of the lowest energy electronic state is comparable to shifts in peak absorption between various crystal polymorphs of Alq_3 (aluminum tris(8-hydroxyquinoline), with the red-shifted Alq_3 polymorph believed to exhibit greater π-conjugation between ligands.[42] A larger, roughly 20 nm, shift is seen between an isotropic and nematic polymeric liquid crystal aligned with a polyimide-treated substrate and an external field.[41]

Figure 4.

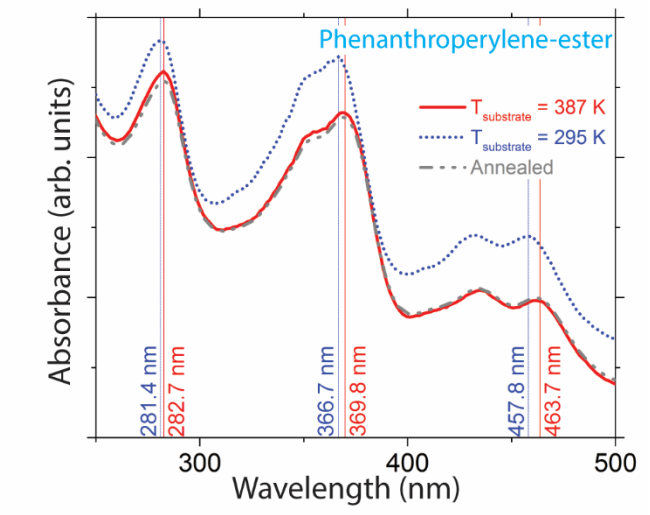

Figure 4. UV/Visible absorption spectra for three films of the phenanthroperylene-ester: a vapor-deposited film ($T_{substrate}$ = 295 K = 0.75T_g, blue dotted line), a highly-ordered vapor-deposited film ($T_{substrate}$ = 387 K = 0.99Tg, red solid line) and a film annealed at 402 K (T_g + 10 K) for an hour before cooling back to room temperature for the measurement (gray dashed line). Three peak positions are labeled with vertical lines to highlight the redshift observed for the highly-ordered vapor-deposited sample.

As-deposited films are not three-dimensional crystalline solids. While most glasses are prepared by cooling an isotropic liquid, glasses have been prepared from many liquid crystalline phases.[43] Glassy states formed from liquid crystals can preserve highly ordered liquid-crystalline packing in the solid state.[10] We can use data on the phenanthroperylene-ester to show that the vapor-deposited films are out-of-equilibrium (glassy) solids as opposed to three-dimensional (3D) crystals.

Figure 5 shows GIWAXS patterns obtained from three phenanthroperylene-ester films, before (left) and after (right) annealing above T_g. On the left, are patterns obtained from films prepared at $T_{substrate}$ = 295 K, 335 K and 360 K ($0.75T_g$, $0.85T_g$ and $0.92T_g$). The patterns on the right were obtained from the same films after a 12 minute anneal at 402 K (= T_g + 10 K = T_m – 118 K). All the patterns shown here were obtained at room temperature; in-situ diffraction patterns obtained during annealing are shown in Supplementary Information. Upon annealing, all three films evolve to some extent towards the columnar hexagonal scattering pattern expected for the equilibrium liquid crystalline phase. The films deposited at $T_{substrate}$ = 335 K and 360 K are initially highly textured forms of the equilibrium edge-on columnar structure that become less textured after annealing. The evolution of the $T_{substrate}$ = 295 K sample upon annealing is and discussed below. *The observation that all three films evolve when held 118 K below the melting temperature indicate that the as-deposited films are not crystalline.* Furthermore, mixed index peaks would be expected for a 3D crystal; the absence of such peaks is a strong general argument that the as-deposited films are not crystals. This conclusion is further supported by comparing the X-ray diffraction pattern of crystalline phenanthroperylene-ester with the vapor-deposited films, shown in the SI.

Figure 5.

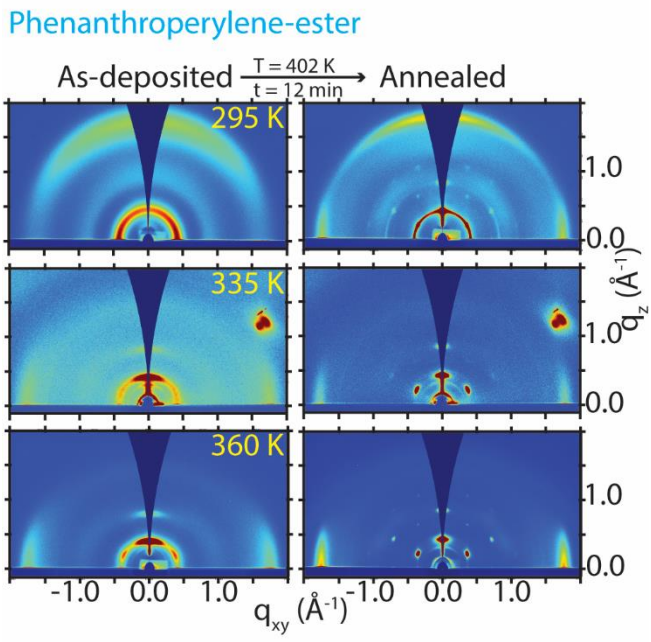

Figure 5. 2D GIWAXS patterns for three vapor-deposited films of the phenanthroperylene-ester before and after annealing at T = 402 K (T_g + 10 K) for 12 minutes, with $T_{substrate}$ values indicated. The left column shows patterns for the as-deposited glasses while the right column shows patterns after annealing. All the films evolve towards the equilibrium structure with homeotropic molecular alignment. In both patterns for the $T_{substrate}$ = 335 K sample, the bright feature at q_{xy} = 1.7 and q_z = 1.2 A^{-1} is diffuse scatter from the underlying silicon substrate and not from the phenanthroperylene-ester film.

The structural evolution of the $T_{substrate}$ = 295 K sample upon annealing is particularly interesting as it gives us a window into the transformation process. After the 12-minute anneal at 402 K, the film is only partially transformed into the preferred planar alignment. An extended anneal of 5 days at the same temperature completely transforms the film into a planar aligned liquid crystal. The GIWAXS patterns in the SI illustrate that this transformation begins at the free surface (vacuum interface) with the molecules anchoring edge-on (planar columnar alignment). During annealing, the bulk of the film initially perfects the pre-existing microstructure (as can be observed, for instance, by the sharpening of the out-of-plane peak at q_z ~1.75 $Å^{-1}$ among other features); eventually the preferred planar column geometry propagates from the free surface through the bulk of the film.

Discussion

The origin of structural anisotropy observed in vapor-deposited films. For each of the three systems investigated here, quite different structures can be prepared by physical vapor deposition, depending upon the choice of substrate temperature during deposition. A mechanism based on molecular dynamics simulations has been proposed to explain how non-mesogens form anisotropic glasses through the physical vapor deposition process.[16,25] Very recent work has utilized this approach to understand the structures prepared by vapor deposition of a smectic mesogen.[20] In this section, we show that this mechanism can also account, at least qualitatively, for the structures observed here for columnar mesogens.

It has been shown that vapor deposition of organic molecules that are not mesogens can produce glasses with higher thermal stability and higher density than glasses of the same system quenched from a liquid;[44,45] at a deposition rate of 0.2 nm/s, the largest effects are often observed for $T_{substrate} \sim 0.85T_g$. The development of these properties is attributed to high mobility near the free surface of the glass that allows molecules near the surface to partially equilibrate as they are being deposited onto the film. During the vapor deposition process, every molecule that lands on the film is, for a short time, part of the highly mobile surface before being buried by the next layers of molecules. During their short residence time at

the free surface (~5 seconds for a typical deposition rate), molecules have enough mobility to find efficient packing arrangements. Further deposition traps these packing arrangements in the bulk material, resulting in high density and high thermal stability.

The structural anisotropy in vapor-deposited glasses can also be traced back to the enhanced surface mobility described above along with one additional feature: the preferred structural packing of the molecules at the free surface of the liquid. Molecular dynamics simulations of coarse-grained[16] and atomistic[19,25] non-liquid crystal forming systems have provided the mechanism to explain anisotropy in vapor-deposited glasses. For example, liquid m-MTDATA was simulated and it was found that at the free surface of the equilibrium liquid, molecules tend to lie flat in the plane of the film, while deeper into the liquid the structure was isotropic. When m-MTDATA is deposited far below T_g ($T_{substrate}$ ~$0.75T_g$, in Figure 2), the anisotropic structure that is preferred at the free surface is trapped into the bulk of the film. In contrast, when m-MTDATA is deposited at high $T_{substrate}$ (just below T_g), the mobility near the free surface propagates deep enough into the film that isotropic packing arrangements are trapped by subsequent deposition (as shown in Figure 2).

The mechanism to explain bulk anisotropy based on free surface structures can also be used to explain the structures prepared by vapor deposition of liquid crystals. Ediger and coworkers vapor-deposited a smectic liquid crystalline system, itraconazole,[20] finding that deposition near T_g resulted in a highly ordered glass with structure similar to a smectic monodomain. In smectic liquid crystals, the free surface structure in equilibrium involves homeotropic anchoring (where the molecular long axis is perpendicular to the vacuum interface) and smectic layers parallel to the interface.[24] When deposited near T_g, high mobility allows each layer to form this equilibrium structure and further deposition traps this structure into the glass.

For columnar systems, the vacuum interface generally induces edge-on molecular alignment (i.e., columns propagating in-plane).[31,46] Thus, the edge-on molecular alignment motif will be assembled during the deposition process if surface mobility is sufficient. For depositions with $T_{substrate}$ ~ T_g, this leads

to the highly-ordered structures shown in Figure 2 for the two mesogens in this study. As each new layer is deposited, the molecules align edge-on along the free surface, with the same director and in registry with the underlying layer, as they would in an equilibrium film, before being trapped in this arrangement by oncoming molecules. This explains why the observed superstructures mimic the equilibrium hexagonal and rectangular columnar structures for the phenanthroperylene-ester and the triphenylene-ester, respectively. Since in-plane structures are being formed simultaneously on all parts of the film and there is no driving force for macroscopic alignment, there should be a domain structure with a uniform distribution of in-plane directors, consistent with our observations. This highly ordered structure is observed when deposition occurs considerably below T_g (down to T_g – 50 K for the triphenylene system) and is an indication that surface mobility is much higher than bulk mobility, as observed previously for glasses of organic molecules that are not mesogens.[26]

For deposition of the columnar liquid crystal systems at $T_{substrate} \sim 0.75T_g$, surface mobility is lower and molecules at the free surface are unable to rearrange into the preferred edge-on molecular alignment before being buried by the next layer of molecules. In this temperature regime, we infer that the molecules deposited on the film initially tend to lie flat in the plane, and are trapped in this motif upon further deposition; this is consistent with observations for low temperature depositions of non-mesogens.[16,19] For both liquid crystalline systems in Figure 2, there is evidence for preferential π-π stacking out-of-plane with columnar structures propagating out-of-plane. For the low temperature depositions, the triphenylene-ester films are more highly ordered than the phenanthroperylene-ester films. We conjecture that this may be due to the high symmetry of the triphenylene-ester molecule; minimal molecular rearrangement would be required to form the in-plane rectangular structures observed in these films.

Previous studies involving columnar liquid crystalline systems have shown there is an order-induced enhancement in charge carrier mobility.[47] Eccher et al., for instance, showed that vapor depositing a discotic derivative of benzo[*ghi*]perylene led to higher charge carrier mobility than a spin-

coated film of the same material, but still higher charge mobility was observed in a highly annealed sample.[22] In that work, the deposited films were prepared by deposition onto a substrate at ambient conditions. We interpret this result to indicate that deposition at a low substrate temperature resulted in a relatively disordered film that, upon annealing, increased in order and electrical performance. In the present work, we have shown that by careful choice of substrate temperature during deposition, the as-deposited film does not need to be annealed to prepare a highly ordered film. Moreover, the substrate temperature can also determine if the ordered structures are packed edge-on or face-on.

Based upon the results presented here for columnar mesogens and those presented previously for a smectic liquid crystal, [20,21] we suggest that vapor deposition can be used generically with various liquid crystalline systems to prepare highly ordered and highly tunable packing motifs in glassy films. In this study we confirmed that the structures of the as-deposited films are identical for deposition onto fused silica and silicon, it has been shown elsewhere that the as-deposited structures are independent of a wider range of underlying substrates.[21] Similarly, preliminary data on thicker films of the columnar systems (300 nm) indicates that the structures of the as-deposited films are independent of thickness; for other vapor-deposited systems, this has been shown for a much wider range of thicknesses and systems, from 20 nm[48] to microns[20]. These findings are consistent with the proposed mechanism since the structure trapped in the solid films is directed by the free surface (and not the substrate).

Potential applications. Manipulating organization and structure in organic solids is a crucial step towards engineering better films for organic electronic and optoelectronic devices. Liquid crystalline moieties have been explored for this purpose and glasses prepared from liquid crystals have been investigated for a variety of applications from thin film transistors to polarizers and optical notch filters.[10] In these studies, however, the ordered layers were prepared by thermal annealing and then quenched to attain the required morphology.

In comparison to thermal annealing, vapor deposition presents a number of potential advantages as a means to prepare solids with liquid crystalline order. Vapor deposition provides access to a large

variety of microstructures independent of the chemical nature of the underlying substrate; for thermal annealing to be successful, the anchoring condition imposed by the substrate must be consistent with the desired structure. In addition, thermal annealing of one layer might degrade the structure of a previously prepared layer. Vapor deposition is already a common thin film fabrication technique in industrial settings, making these findings even more pertinent. The two representative structures formed in the liquid crystalline systems investigated in this study are both potentially useful in devices[46] that require different geometries. For instance, in organic field effect transistors (OFETs) where efficient charge transport is required from a source to a drain (running along the device plane) in-plane columnar structures (i.e., edge-on molecular packing motifs) are beneficial. On the other hand, for organic photovoltaic devices (OPVs) which generally have sandwich device geometries, out-of-plane columnar arrangements (face-on molecular packing) are most efficient to carry charges between the device electrodes. That these structures are accessible without consideration of the underlying substrate chemistry may be valuable in designing devices.

Conclusion

Glasses of three disc-shaped molecular systems were prepared by vapor deposition, including two systems that form columnar liquid crystals. For the liquid crystal systems, a range of potentially useful structural motifs were shown to be accessible by controlling the substrate temperature during deposition ($T_{substrate}$). When deposited at $T_{substrate}$ near T_g, the structures of the columnar systems were closely related to their equilibrium liquid crystal structures. Depositing at $T_{substrate} \sim 0.75\ T_g$, prepared face-on packing motifs of varying levels of organization. The vapor-deposited structures could be rationalized by a mechanism in which glass packing is controlled by surface mobility; if the substrate temperature is close to T_g, molecules at the surface organize into structures preferred at the free surface of the equilibrium liquid crystal and this structure is trapped into a glassy solid.

This work provides a new method to prepare highly organized films of columnar liquid crystalline systems, extending previous work involving a smectic[20] liquid crystal and non-mesogens[16].

This preparation technique may be useful in preparing active layers in organic electronic and optoelectronic devices. One important aspect of the work that needs further investigation is the preparation of highly organized films with controllable in-plane structure (such that all the columns are pointing along a predetermined axis in the device geometry). More work is required to move towards that goal, perhaps with the use of external fields during the deposition process to control in-plane order.

References

(1) Sutton, C.; Risko, C.; Brédas, J.-L. Noncovalent Intermolecular Interactions in Organic Electronic Materials: Implications for the Molecular Packing vs Electronic Properties of Acenes. *Chem. Mater.* **2016**, *28* (1), 3–16.

(2) Yokoyama, D. Molecular Orientation in Small-Molecule Organic Light-Emitting Diodes. *J. Mater. Chem.* **2011**, *21* (48), 19187–19202.

(3) Yokohama, D.; Setoguchi, Y.; Sakaguchi, A.; Suzuki, M.; Adachi, C. Orientation Control of Linear-Shaped Molecules in Vacuum-Deposited Organic Amorphous Films and Its Effect on Carrier Mobilities. *Adv. Funct. Mater.* **2010**, *20*, 386–391.

(4) Mas-Torrent, M.; Hadley, P.; Bromley, S. T.; Ribas, X.; Tarrés, J.; Mas, M.; Molins, E.; Veciana, J.; Rovira, C. Correlation between Crystal Structure and Mobility in Organic Field-Effect Transistors Based on Single Crystals of Tetrathiafulvalene Derivatives. *J. Am. Chem. Soc.* **2004**, *126* (27), 8546–8553.

(5) Diao, Y.; Shaw, L.; Bao, Z.; Mannsfeld, S. C. B. Morphology Control Strategies for Solution-Processed Organic Semiconductor Thin Films. *Energy Environ. Sci.* **2014**, *7* (7), 2145–2159.

(6) Giri, G.; Verploegen, E.; Mannsfeld, S. C. B.; Atahan-Evrenk, S.; Kim, D. H.; Lee, S. Y.; Becerril, H. A.; Aspuru-Guzik, A.; Toney, M. F.; Bao, Z. Tuning Charge Transport in Solution-Sheared Organic Semiconductors Using Lattice Strain. *Nature* **2011**, *480* (7378), 504–508.

(7) Shklyarevskiy, I. O.; Jonkheijm, P.; Stutzmann, N.; Wasserberg, D.; Wondergem, H. J.; Christianen, P. C. M.; Schenning, a. P. H. J.; Leeuw, D. M. D.; Tomovic, Z.; Müllen, K.; Wu, J.; Maan, C. J. High Anisotrophy of the Field-Effect Transistor Mobility in Magnetically Aligned Disotic Liquid-Crystalline Semiconductors. *J. Am. Chem. Soc.* **2005**, *127* (8), 16233–16237.

(8) Karbovnyk, I. D.; Olenych, I.; Kukhta, I. N.; Lugovskii, A.; Sasnouski, G.; Chutora, T.; Luchechko, A. P.; Khalakhan, I.; Kukhta, A. Electric Field Oriented Nanostructured Organic Thin Films with Polarized Luminescence. *Nanoscale Res. Lett.* **2017**, *12* (1), 166.

(9) McCulloch, I.; Heeney, M.; Bailey, C.; Genevicius, K.; MacDonald, I.; Shkunov, M.; Sparrowe, D.; Tierney, S.; Wagner, R.; Zhang, W.; Chabinyc, M. L.; Kline, R. J.; McGehee, M. D.; Toney, M. F. Liquid-Crystalline Semiconducting Polymers with High Charge-Carrier Mobility. *Nat. Mater.* **2006**, *5* (4), 328–333.

(10) Chen, H. P.; Ou, J. J.; Chen, S. H. Glassy Liquid Crystals as Self-Organized Films for Robust Optoelectronic Devices. In *Nanoscience with Liquid Crystals*; Li, Q., Ed.; Springer International Publishing, 2014; pp 179–208.

(11) O'Neill, M.; Kelly, S. M. Liquid Crystals for Charge Transport, Luminescence, and Photonics. *Adv. Mater.* **2003**, *15* (14), 1135–1146.

(12) Wöhrle, T.; Wurzbach, I.; Kirres, J.; Kostidou, A.; Kapernaum, N.; Litterscheidt, J.; Haenle, J. C.; Staffeld, P.; Baro, A.; Giesselmann, F.; Laschat, S. Discotic Liquid Crystals. *Chem. Rev.* **2016**, *116* (3), 1139–1241.

(13) Kumar, S. *Chemistry of Discotic Liquid Crystals: From Monomers to Polymers*; CRC Press, 2016.

(14) Pouzet, E.; Cupere, V. De; Heintz, C.; Andreasen, J. W.; Breiby, D. W.; Nielsen, M. M.; Viville, P.; Lazzaroni, R.; Gbabode, G.; Geerts, Y. H. Homeotropic Alignment of a Discotic Liquid Crystal Induced by a Sacrificial Layer. *J. Phys. Chem. C* **2009**, *113* (32), 14398–14406.

(15) Islam, A.; Rabbani, M.; Bappy, M. H.; Miah, M. A. R.; Sakib, N. A Review on Fabrication Process of Organic Light Emitting Diodes. In *2013 International Conference on Informatics, Electronics and Vision (ICIEV)*; IEEE, 2013; pp 1–5.

(16) Dalal, S. S.; Walters, D. M.; Lyubimov, I.; de Pablo, J. J.; Ediger, M. D. Tunable Molecular Orientation and Elevated Thermal Stability of Vapor-Deposited Organic Semiconductors. *Proc. Natl. Acad. Sci. U. S. A.* **2015**, *112* (14), 4227–4232.

(17) Gujral, A.; O'Hara, K. A.; Toney, M. F.; Chabinyc, M. L.; Ediger, M. D. Structural Characterization of Vapor-Deposited Glasses of an Organic Hole Transport Material with X-Ray Scattering. *Chem. Mater.* **2015**, *27* (9), 3341–3348.

(18) Dalal, S. S.; Fakhraai, Z.; Ediger, M. D. High-Throughput Ellipsometric Characterization of Vapor-Deposited Indomethacin Glasses. *J. Phys. Chem. B* **2013**, *117* (49), 15415–15425.

(19) Walters, D. M.; Antony, L.; de Pablo, J. J.; Ediger, M. D. Influence of Molecular Shape on the Thermal Stability and Molecular Orientation of Vapor-Deposited Organic Semiconductors. *J. Phys. Chem. Lett.* **2017**, *Accepted*.

(20) Gujral, A.; Gómez, J.; Jiang, J.; Huang, C.; O'Hara, K. A.; Toney, M. F.; Chabinyc, M. L.; Yu, L.; Ediger, M. D. Highly Organized Smectic-like Packing in Vapor-Deposited Glasses of a Liquid Crystal. *Chem. Mater.* **2017**, *29*, 849–858.

(21) Gómez, J.; Jiang, J.; Gujral, A.; Huang, C.; Yu, L.; Ediger, M. D. Vapor Deposition of a Smectic Liquid Crystal: Highly Anisotropic, Homogeneous Glasses with Tunable Molecular Orientation. *Soft Matter* **2016**, *12* (11), 2942–2947.

(22) Eccher, J.; Zajaczkowski, W.; Faria, G. C.; Bock, H.; von Seggern, H.; Pisula, W.; Bechtold, I. H. Thermal Evaporation versus Spin-Coating: Electrical Performance in Columnar Liquid Crystal OLEDs. *ACS Appl. Mater. Interfaces* **2015**, *7* (30), 16374–16381.

(23) Gearba, R. I.; Anokhin, D. V.; Bondar, A. I.; Bras, W.; Jahr, M.; Lehmann, M.; Ivanov, D. A. Homeotropic Alignment of Columnar Liquid Crystals in Open Films by Means of Surface Nanopatterning. *Adv. Mater.* **2007**, *19* (6), 815–820.

(24) Sadati, M.; Ramezani-Dakhel, H.; Bu, W.; Sevgen, E.; Liang, Z.; Erol, C.; Taheri Qazvini, N.; Rahimi, M.; Lin, B.; Roux, B.; Schlossman, M.; de Pablo, J. J. Structural Organization of Liquid Crystals at Liquid Crystal-Air Interface: Synchrotron X-Ray Reflectivity and Computational Simulations. *Bull. Am. Phys. Soc.* **2016**, [Access: aps.org/Meeting/MAR16/Session/S37.9].

(25) Antony, L. W.; Jackson, N. E.; Lyubimov, I.; Vishwanath, V.; Ediger, M. D.; de Pablo, J. J. Influence of Vapor Deposition on Structural and Charge Transport Properties of Ethylbenzene Films. *ACS Cent. Sci.* **2017**, *3* (5), 415–424.

(26) Brian, C. W.; Yu, L. Surface Self-Diffusion of Organic Glasses. *J. Phys. Chem. A* **2013**, *117* (50), 13303–13309.

(27) Zhang, Y.; Fakhraai, Z. Decoupling of Surface Diffusion and Relaxation Dynamics of Molecular Glasses. *Proc. Natl. Acad. Sci. U. S. A.* **2017**, *114* (19), 4915–4919.

(28) Hassheider, T.; Benning, S. A.; Kitzerow, H.-S.; Achard, M.-F.; Bock, H. Color-Tuned Electroluminescence from Columnar Liquid Crystalline Alkyl Arenecarboxylates. *Angew. Chemie Int. Ed.* **2001**, *40* (11), 2060–2063.

(29) Kelber, J.; Achard, M.-F.; Durola, F.; Bock, H. Distorted Arene Core Allows Room-Temperature Columnar Liquid-Crystal Glass with Minimal Side Chains. *Angew. Chemie Int. Ed.* **2012**, *51* (21),

5200–5203.

(30) Baker, J. L.; Jimison, L. H.; Mannsfeld, S.; Volkman, S.; Yin, S.; Subramanian, V.; Salleo, A.; Alivisatos, A. P.; Toney, M. F. Quantification of Thin Film Crystallographic Orientation Using X-Ray Diffraction with an Area Detector. *Langmuir* **2010**, *26* (11), 9146–9151.

(31) Grelet, E.; Dardel, S.; Bock, H.; Goldmann, M.; Lacaze, E.; Nallet, F. Morphology of Open Films of Discotic Hexagonal Columnar Liquid Crystals as Probed by Grazing Incidence X-Ray Diffraction. *Eur. Phys. J. E* **2010**, *31* (4), 343–349.

(32) McCulloch, I.; Heeney, M.; Bailey, C.; Genevicius, K.; Macdonald, I.; Shkunov, M.; Sparrowe, D.; Tierney, S.; Wagner, R.; Zhang, W.; Chabinyc, M. L.; Kline, R. J.; McGehee, M. D.; Toney, M. F. Liquid-Crystalline Semiconducting Polymers with High Charge-Carrier Mobility. *Nat. Mater.* **2006**, *5* (4), 328–333.

(33) Kline, R. J.; DeLongchamp, D. M.; Fischer, D. A.; Lin, E. K.; Heeney, M.; McCulloch, I.; Toney, M. F. Significant Dependence of Morphology and Charge Carrier Mobility on Substrate Surface Chemistry in High Performance Polythiophene Semiconductor Films. *Appl. Phys. Lett.* **2007**, *90* (6), 2005–2008.

(34) Chen, C.-W.; Huang, Z.-Y.; Lin, Y.-M.; Huang, W.-C.; Chen, Y.-H.; Strzalka, J.; Chang, A. Y.; Schaller, R. D.; Lee, C.-K.; Pao, C.-W.; Lin, H.-W. Morphology, Molecular Stacking, Dynamics and Device Performance Correlations of Vacuum-Deposited Small-Molecule Organic Solar Cells. *Phys. Chem. Chem. Phys.* **2014**, *16*, 8852–8864.

(35) Tchamba Yimga, N.; Ramanan, C.; Borchert, H.; Parisi, J.; Untenecker, H.; Kirsch, P.; von Hauff, E. Interplay between Long-Range Crystal Order and Short-Range Molecular Interactions Tunes Carrier Mobility in Liquid Crystal Dyes. *ACS Appl. Mater. Interfaces* **2017**, *9* (7), 6228–6236.

(36) Himmelberger, S.; Duong, D. T.; Northrup, J. E.; Rivnay, J.; Koch, F. P. V.; Beckingham, B. S.; Stingelin, N.; Segalman, R. A.; Mannsfeld, S. C. B.; Salleo, A. Role of Side-Chain Branching on Thin-Film Structure and Electronic Properties of Polythiophenes. *Adv. Funct. Mater.* **2015**, *25*, 2616–2624.

(37) Kalb, W. L.; Haas, S.; Krellner, C.; Mathis, T.; Batlogg, B. Trap Density of States in Small-Molecule Organic Semiconductors: A Quantitative Comparison of Thin-Film Transistors with Single Crystals. *Phys. Rev. B* **2010**, *81*, 1–13.

(38) Tsao, H. N.; Cho, D.; Andreasen, J. W.; Rouhanipour, A.; Breiby, D. W.; Pisula, W.; Müllen, K. The Influence of Morphology on High-Performance Polymer Field-Effect Transistors. *Adv. Mater.* **2009**, *21*, 209–212.

(39) Schmidt-Mende, L.; Fechtenkötter, A.; Müllen, K.; Moons, E.; Friend, R. H.; MacKenzie, J. D. Self-Organized Discotic Liquid Crystals for High-Efficiency Organic Photovoltaics. *Science* **2001**, *293* (5532), 1119–1122.

(40) Tsuji, Y.; Morisaki, Y.; Chujo, Y. π-Conjugated Polymer-Layered Structures: Synthesis and Self-Assembly. *Polym. J.* **2017**, *49* (1), 203–208.

(41) Zhu, Z.; Swager, T. M. Conjugated Polymer Liquid Crystal Solutions: Control of Conformation and Alignment. *J. Am. Chem. Soc.* **2002**, *124* (33), 9670–9671.

(42) Brinkmann, M.; Gadret, G.; Muccini, M.; Taliani, C.; Masciocchi, N.; Sironi, A. Correlation between Molecular Packing and Optical Properties in Different Crystalline Polymorphs and Amorphous Thin Films of *Mer* -Tris(8-hydroxyquinoline)aluminum(III). *J. Am. Chem. Soc.* **2000**, *122* (21), 5147–5157.

(43) Suga, H.; Seki, S. Thermodynamic Investigation on Glassy States of Pure Simple Compounds. *J. Non. Cryst. Solids* **1974**, *16*, 171–194.

(44) Swallen, S. F.; Kearns, K. L.; Mapes, M. K.; Kim, Y. S.; McMahon, R. J.; Ediger, M. D.; Wu, T.; Yu, L.; Satija, S. Organic Glasses with Exceptional Thermodynamic and Kinetic Stability. *Science* **2007**, *315* (5810), 353–356.

(45) Zhu, L.; Yu, L. Generality of Forming Stable Organic Glasses by Vapor Deposition. *Chem. Phys. Lett.* **2010**, *499* (1), 62–65.

(46) Sergeyev, S.; Pisula, W.; Geerts, Y. H. Discotic Liquid Crystals: A New Generation of Organic Semiconductors. *Chem. Soc. Rev.* **2007**, *36* (12), 1902–1929.

(47) Eccher, J.; Faria, G. C.; Bock, H.; von Seggern, H.; Bechtold, I. H. Order Induced Charge Carrier Mobility Enhancement in Columnar Liquid Crystal Diodes. *ACS Appl. Mater. Interfaces* **2013**, *5* (22), 11935–11943.

(48) Sakai, Y.; Shibata, M.; Yokoyama, D. Simple Model-Free Estimation of Orientation Order Parameters of Vacuum-Deposited and Spin-Coated Amorphous Films Used in Organic Light-Emitting Diodes. *Appl. Phys. Express* **2015**, *8* (9), 96601.

Chapter 5

Anisotropic molecular orientation near the vacuum interface of organic semiconductor glasses and liquids: Implications for vapor-deposited semiconductor films

Ankit Gujral

Molecular orientation at the interfaces determines important material properties. Orientation at the free surface determines surface charge,[1] surface energy,[2,3] and which functional groups are available for gas phase reactions.[4] At the interface between two organic semiconductors, molecular orientation determines charge injection across the interface. In this work, we show for the first time that molecular orientation at the free surface of organic semiconductors is anisotropic, both in the liquid state and as vapor-deposited glasses. We focus on the relevance of these findings for understanding the anisotropy of vapor-deposited glasses such as those used in the production of OLEDs. In OLEDs, it is understood that anisotropic packing can increase the efficiency of both light emission[5] and charge transport.[6] More generally in organic electronics, it is widely appreciated that anisotropic packing can optimize the performance of a range of devices including OFETs,[7] optical notch filters,[8] and solid-state lasers.[9]

Physical vapor deposition, a common industrial fabrication technique for organic thin films,[10] has been shown to prepare glasses with structural anisotropy and also with high kinetic stability[11]. Vapor deposition of non-mesogenic molecules can form mildly anisotropic glasses while deposition of mesogens can result in highly ordered structures that resemble monodomains of liquid crystals. For any given molecule, a range of anisotropic structures can be formed depending upon the temperature of the substrate during deposition ($T_{substrate}$).[12–17] Understanding the origin of the anisotropic packing in vapor-deposited glasses of such a wide range of molecules is highly relevant, due to the technological importance of controlling molecular packing in solids. Other thin film fabrication methods can also produce anisotropic films but typically utilize external fields[18] or careful control of flow by shearing[19] or blade-coating.[20]

Recently a mechanism[15,16] has been proposed to explain the high kinetic stability and structural anisotropy in vapor-deposited glasses. It is proposed that both effects result from high molecular mobility at the vacuum interface of an organic glass.[21] As the film is deposited below the glass transition temperature Tg, every newly deposited molecule uses the high mobility to partially equilibrate before being buried by additional molecules; once a given molecule is more than a few monolayers from the

interface, it is trapped since it can no longer take advantage of surface mobility. The bulk vapor-deposited glass is, therefore, high stable since all molecules equilibrated to a significant extent below Tg. To explain the anisotropy of vapor-deposited glasses, this mechanism assumes that molecular orientation at the equilibrium vacuum interface of a liquid is generally anisotropic. During deposition, molecules try to equilibrate towards this anisotropic structure, and these configurations are then trapped into the bulk upon further deposition. This mechanism is supported by recent coarse-grained and atomistic molecular dynamics (MD) simulations for rod-shaped[15] and disc-shaped molecules[16]; the simulations indicate significant anisotropic orientation at the free surface of the equilibrium liquids.

To experimentally test this mechanism, we determined the molecular orientation near the vacuum interface and deeper into the bulk of two disc-shaped molecular systems with different equilibrium liquid structures and compared our results to predictions made by the mechanism. We investigated m-MTDATA [T_g = 354 K; 4,4',4"-tris[phenyl(m-tolyl)amino]triphenylamine] that does not exhibit a liquid crystal phase, and phenanthroperylene-ester [T_g = 392 K; 1,16-di(methoxycarbonyl)-6,7,12,13-tetra(ethoxycarbonyl)phenanthro[ghi-1,2,3,4]perylene] which forms a discotic hexagonal liquid crystalline phase above T_g.

The proposed mechanism makes two clear predictions[14,16] of the vacuum interface structure required to achieve the bulk properties of vapor-deposited glasses of the systems investigated: 1) The vacuum interface structure of the equilibrium liquid must be anisotropic (even if the bulk is isotropic and disordered), while the bulk liquid structure must be similar to structure of a glass prepared at $T_{substrate} \sim T_g$. And, 2) even though both systems are disc-shaped, the phenanthroperylene-ester liquid should exhibit edge-on orientation at the vacuum interface while the m-MTDATA liquid should exhibit a preferred face-on orientation to be consistent with the bulk structural properties of the glasses. The results reported here are the first experimental evidence to test the mechanism, and gives us confidence that we understand and can predict anisotropy of vapor-deposited glasses.

We used near-edge X-ray absorption fine structure (NEXAFS) spectroscopy to determine the depth-dependent molecular orientation in films of m-MTDATA and phenanthroperylene-ester. When using a polarized X-ray beam, the absorption intensity near an absorption edge region (up to 30 eV above the edge) depends strongly on the orientation of the bonds the atom is involved in. For an absorption to occur, the polarization state of the incident X-ray beam must align (by a cosine-squared relationship) with the transition dipole associated with the absorption. In the set of experiments shown here, it is not the absorption that is directly measured, but rather the photoelectric emission that occurs upon relaxation following the absorption. Two emission regimes were measured, a surface-sensitive Auger Electron Yield (AEY) originating 1-1.5 nm from the vacuum interface and a bulk-sensitive Total Electron Yield (TEY) penetrating 10 nm from the vacuum interface. NEXAFS has previously been used to determine the molecular orientation of thin organic films[22–24] and adsorption layers,[25–27] and a similar approach will be used here. These are the first reported measurements on low molecular weight organic semiconductor films and vapor-deposited glasses, to the best of our knowledge, providing new insights into the interfacial structures not captured in bulk measurements.

To determine the average molecular orientation, α, spectra are collected at various incidence angles, θ, as described in Figure 1a, inset. Angle-resolved TEY spectra near the carbon K-edge of a phenanthroperylene-ester film are shown in Figure 1a, with a region of interest (ROI) corresponding to the 1s-to-π* excitation (~285 eV). A pre-edge and post-edge normalization was applied to all spectra, as reported previously.[23,28] An expanded view of the ROI is shown in Figure 1b. The absorption intensity is monotonically increasing when the incident angle is increased from 20° to 90°. Qualitatively this means that there is a greater overlap between the incident beam polarization and π-orbital direction when the beam is incident at 90° than 20°. For this sample, there is a larger population of molecules with π-orbitals perpendicular to the substrate than parallel, (and, therefore, more molecules with their benzene ring functionalities standing "edge-on" in the plane of the substrate). To quantify the average molecular orientation,

we integrate the 1s-to-π* response as a function of incident angle, θ (as reported in Figures 2-4). The following equation[24,28] is fit that simulates the angular response of the 1s-to-π* response:

$$I(\alpha,\theta) = A\left\{\frac{1}{3}P\left[1+\frac{1}{2}(3cos^2\theta-1)(3cos^2\alpha-1)\right]+\frac{1}{2}(1-P)sin^2\alpha\right\} \quad (1)$$

In eqn. 1 I is the integrated intensity of the 1s-to-π* response as a function of θ, α, normalization factor, A, and the polarization factor of the beam, P (90%). The equation is used to fit the experimental response with α as the fitting parameter (dashed lines in Figures 2-4). The equation assumes cylindrical symmetry in the system; a reasonable assumption since the films have been shown to be in-plane isotropic, as described elsewhere.[14,16]

We will begin our discussion investigating vapor-deposited glasses of m-MTDATA, the non-mesogen system represented in Figure 2. At the top of the figure are plots representing surface-sensitive AEY (1-1.5 nm depth) and TEY (10 nm depth) 1s-to-π* absorption intensities (nitrogen K-edge ~400 eV) as a function of θ for glasses prepared at $T_{substrate} \sim 0.75T_g$ (left) and $T_{substrate} \sim T_g$ (right). The dashed lines are the best fit to equation (1) with α indicated in the figure. Below the plots are schematics, with every disc representing one molecule of m-MTDATA. The 10-nm depth measurements are consistent with bulk measurements using X-ray scattering and optical observables reported previously. For the film prepared at low $T_{substrate}$, the molecules have a slight tendency to lay "flat" in-plane ($47^\circ < 55^\circ$ isotropic) while the films prepared at high $T_{substrate}$ have a 55° average molecular orientation, consistent with an isotropic response. The high $T_{substrate}$ glass is expected to be essentially identical to the supercooled liquid structure of m-MTDATA based upon optical[16] and X-ray measurements.[14] In addition, we observed that the carbon K-edge spectra collected for the equilibrium supercooled liquid and high $T_{substrate}$ glass were similar, to within 2° uncertainty for TEY orientation measurements (due to time limitations, we were unable to collect nitrogen K-edge spectra on the supercooled liquid). The surface, on the other hand, are similar in both glasses, with AEY spectra indicating identical α values to within 3°, regardless of $T_{substrate}$.

The results from the m-MTDATA glasses discussed above are indicative of two pieces of evidence supporting the proposed mechanism: 1) the surface structures are anisotropic, even for the bulk isotropic glass (and by proxy, the supercooled liquid), and 2) the vacuum interface of all glasses of m-MTDATA are highly mobile, allowing for both the glasses to equilibrate at the vacuum interface to similar structures. During the deposition, molecules arriving at the vacuum interface have a preferred face-on orientation (perhaps to reduce surface area). At low $T_{substrate}$, this preferred orientation is trapped into the bulk of the film upon further deposition. As a new set of molecules arrives at the vacuum interface, the previous set are cannot rearrange due to the limited mobility at low $T_{substrate}$ in the bulk. On the other hand, at high Tsubstrate, there is enough mobility deeper into the film such that even after being buried by continued deposition, the molecules can still rearrange to the preferred bulk orientation (i.e., isotropic or 55°).

Figure 3 shows 1s-to-π* (carbon K-edge ~285 eV) data from vapor-deposited glasses and an equilibrium supercooled liquid film of phenanthroperylene-ester, the columnar mesogen. The 10-nm TEY response is consistent with previously reported bulk measurements. In the bulk, glasses prepared at $T_{substrate} \sim 0.75T_g$ exhibit a tendency for molecules to lie in-plane (50°<55° isotropic), somewhat similar to the non-mesogen. Glasses prepared at $T_{substrate} \sim T_g$, however, show a strong tendency towards "standing" edge-on in the plane of the film, markedly different from the film prepared under equivalent conditions for the non-mesogen. The liquid of phenanthroperylene-ester also shows this strong edge-on molecular orientation in the 10-nm TEY response. The columnar packing motif shown in the schematics cannot be inferred from the NEXAFS spectra, but is based on X-ray scattering results that indicated the formation of highly ordered hexagonal columnar packing motifs present in the high $T_{substrate}$ glass and the equilibrium supercooled liquid. Quite similar to the TEY response, the surface-sensitive AEY response also shows a preferred face-on molecular orientation at the vacuum interface for the low $T_{substrate}$ glass, and an edge-on molecular orientation at the vacuum interface of both, the high $T_{substrate}$ film and the supercooled liquid.

The results from the phenanthroperylene-ester glasses and liquid discussed above are in agreement with the predictions of the mechanism, with the vacuum interface of the liquid being anisotropic. Unlike m-MTDATA, the molecules near the vacuum interface for the high $T_{substrate}$ glass and the liquid of phenanthroperylene-ester, prefer an edge-on orientation. This behavior is phenomenologically similar to other discotic liquid crystal systems.[29] During deposition, the oncoming molecules initially adopt a face-on orientation. At low $T_{substrate}$, this orientation gets trapped into the bulk of the film as the molecules are buried by further deposition into an immobile bulk. At high $T_{substrate}$, however, the mobility is high enough for the molecules during their short residence time, and even deeper into the bulk, to rearrange to the preferred equilibrium orientation. Interestingly, unlike in the films of m-MTDATA, where the film's vacuum interface rearranged to the preferred interface molecular orientation regardless of $T_{substrate}$, phenanthroperylene-ester's vacuum interface structure is kinetically arrested to the as-deposited state. This may be because at room temperature (roughly 100 K below T_g), the molecular mobility, even at the vacuum interface, is limited. However, upon heating the film above T_g, the vacuum interface rearranges to the preferred equilibrium edge-on molecular orientation, while the bulk doesn't have the required mobility to do so, as described below.

Figure 4 summarizes an annealing experiment conducted on the low $T_{substrate}$ phenanthroperylene-ester film to show that, at elevated temperatures, the vacuum interface prefers edge-on molecular alignment, regardless of the underlying material. Previous studies[12] on vapor-deposited glasses have shown that by changing $T_{substrate}$ during deposition, a bilayer film can be formed with the molecular orientation within the 2 layers of the films controlled by $T_{substrate}$ during its deposition. This was inferred to mean that the vacuum interface was templating the structure of the films, regardless of what the underlying material's orientation was (i.e., no substrate/epitaxial effects played a role in the second layers structure). Indeed, this was also observed in the phenanthroperylene-ester film upon annealing. The as-deposited low $T_{substrate}$ phenanthroperylene-ester film exhibits face-on molecular orientation, both, at the vacuum interface and deeper into the film. But after annealing the film for 20 minutes 10 K above T_g (402

K) and quenching back to room temperature, the vacuum interface exhibits preferential edge-on orientation, as indicated by the AEY angular response. Deeper into the film, however, the edge-on orientation was not developed during the anneal, but some changes to the TEY angular response are also observed, indicating that bulk mobility is also present, as expected 10 K above T_g. These results are consistent with a similar annealing experiment conducted and probed using X-ray scattering that showed a small population of the molecules had rearranged to the edge-on orientation post-anneal; with these results, we can confirm that the population involved in the rearrangement is near the vacuum interface.

In conclusion, we used near-edge X-ray absorption fine structure spectroscopy to determine the molecular orientation near the vacuum interface of a non-mesogenic and a mesogenic glass-former, m-MTDATA and phenanthroperylene-ester. We determined that the molecular orientation near the vacuum interface is anisotropic with a preferential face-on orientation for m-MTDATA and edge-on orientation for phenanthroperylene-ester. This study qualitatively confirms the structures predicted in the MD simulation for the non-mesogen and provides experimental evidence to support the mechanism proposed for the origin of anisotropy in vapor-deposited glasses. These results empirically extend the mechanism to mesogenic systems, as well. A deeper understanding of the origin of the observed anisotropy in vapor-deposited glasses will allow for directed engineering of molecular films for organic electronic applications.

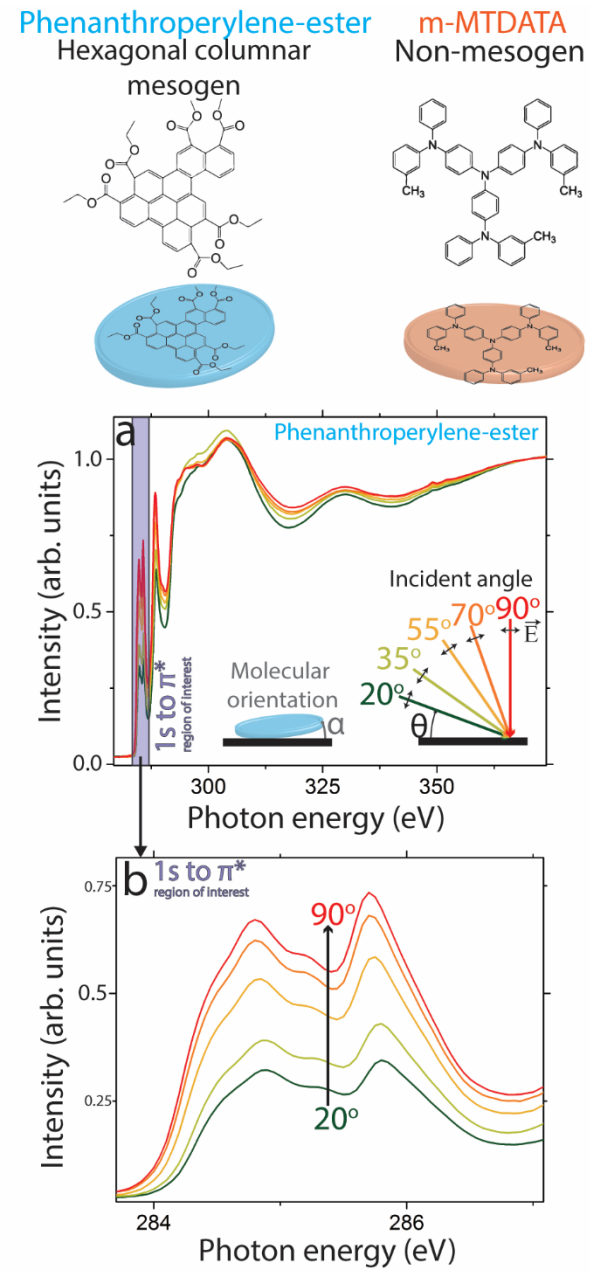

Figure 1. Top: The molecular structures of the two systems investigated. Bottom: a) total electron yield (TEY) spectra near the carbon K-edge collected from a glass of phenanthroperylene-ester prepared at $T_{substrate}$ = 387 K. 5 curves are overlaid, corresponding to spectra collected at different incident angles, θ, as described inset. b) Expanded view of the region-of-interest corresponding to a 1s-to-π* absorption, with monotonically increasing intensity as a function of incident angle.

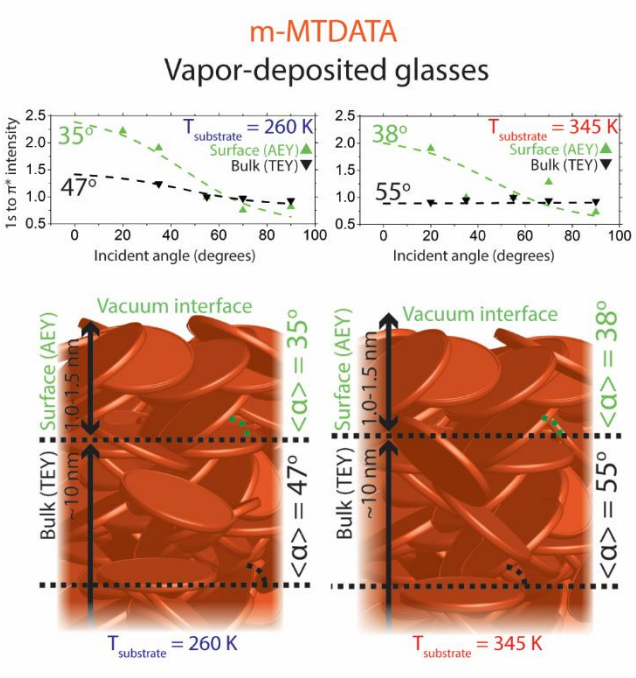

Figure 2. AEY and TEY angular responses for vapor-deposited glasses of m-MTDATA prepared at $T_{substrate}$ = 260 K ~ 0.75 T_g (left) and $T_{substrate}$ = 345 K ~ T_g (right). Schematics are shown below the plots, with one orange disk corresponding to one m-MTDATA molecule, to illustrate the molecular packing in the films.

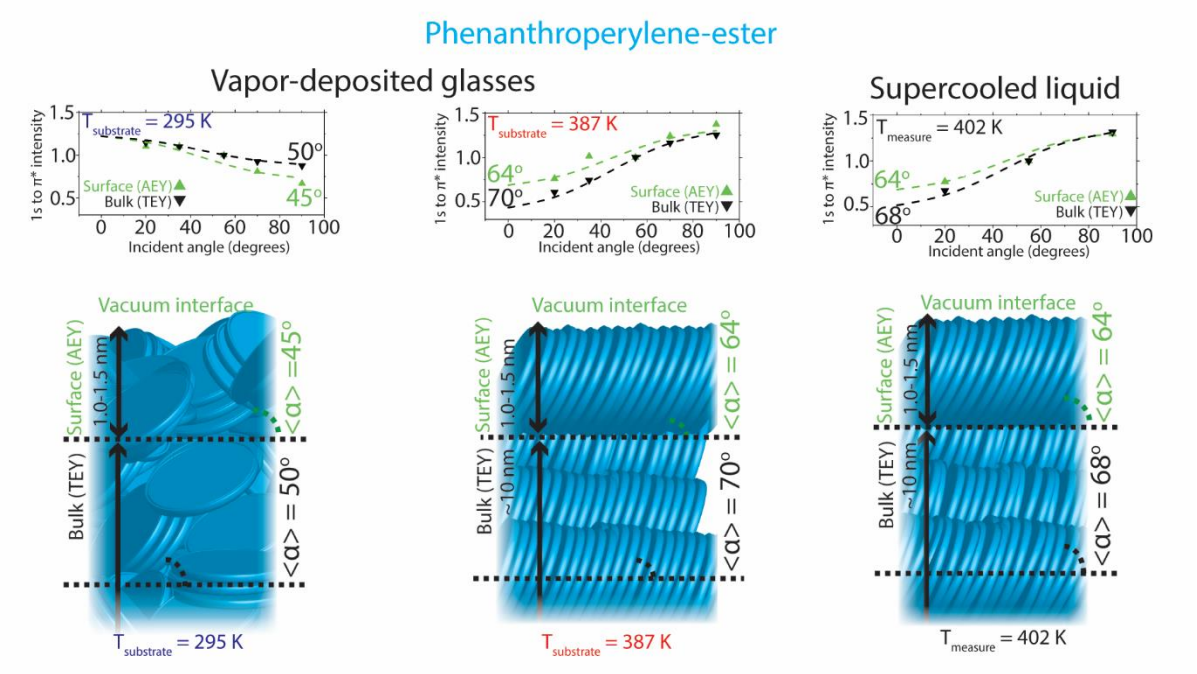

Figure 3. AEY and TEY angular responses for vapor-deposited glasses and the supercooled liquid of phenanthroperylene-ester, prepared at $T_{substrate}$ = 295 K ~ 0.75 T_g (left) and $T_{substrate}$ = 387 K ~ T_g (center) and an equilibrium liquid measured at $T_{measure}$ = 402 K (right). Schematics are shown below the plots, with one blue disk corresponding to one phenanthroperylene-ester molecule, to illustrate the molecular packing in the films.

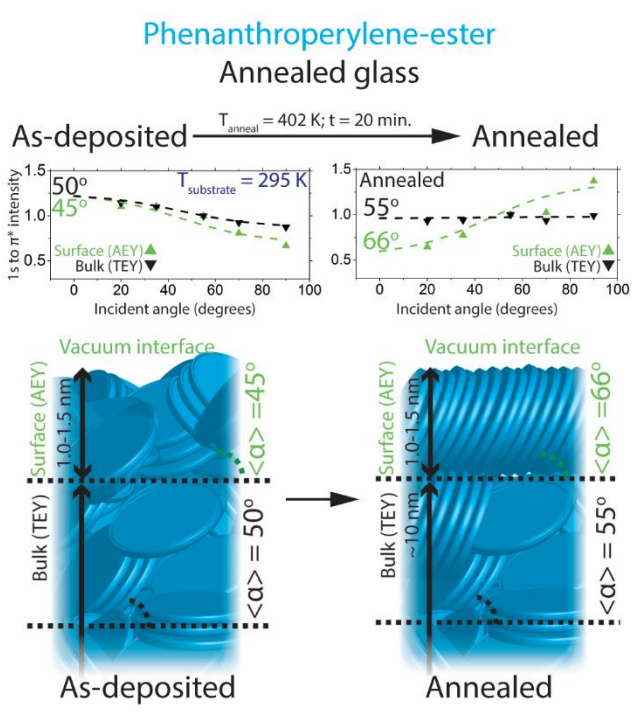

Figure 4. AEY and TEY angular responses for a vapor-deposited glass (left) and an annealed film (right) of phenanthroperylene-ester. The as-deposited film was prepared at $T_{substrate}$ = 295 K ~ 0.75 T_g (left) and exhibited face-on molecular orientation near the vacuum interface and deeper into the film. Upon annealing at T_g + 10 K for 20 min, the molecules near the vacuum interface rearrange to an edge-on orientation. Schematics are shown below the plots, with one blue disk corresponding to one phenanthroperylene-ester molecule, to illustrate the molecular packing in the films.

References

(1) Ohgawara, M.; Uchida, T. Relation between Polarity of Substrate Surface and Liquid Crystal Molecular Orientation. *Jpn. J. Appl. Phys.* **1981**, *20* (3), L237–L240.

(2) Harkins, W. D.; Davies, E. C. H.; Clark, G. L. THE ORIENTATION OF MOLECULES IN THE SURFACES OF LIQUIDS, THE ENERGY RELATIONS AT SURFACES, SOLUBILITY, ADSORPTION, EMULSIFICATION, MOLECULAR ASSOCIATION, AND THE EFFECT OF ACIDS AND BASES ON INTERFACIAL TENSION. [1] (SURFACE ENERGY VI.). *J. Am. Chem. Soc.* **1917**, *39* (4), 541–596.

(3) Kröger, I.; Stadtmüller, B.; Kumpf, C. Submonolayer and Multilayer Growth of Titaniumoxide-Phthalocyanine on Ag(111) Submonolayer Growth of Copper-Phthalocyanine on Ag(111). *New J. Phys* **2016**, *18*, 113022.

(4) Wang, H.; Sapi, A.; Thompson, C. M.; Liu, F.; Zherebetskyy, D.; Krier, J. M.; Carl, L. M.; Cai, X.; Wang, L.-W.; Somorjai, G. A. Dramatically Different Kinetics and Mechanism at Solid/Liquid and Solid/Gas Interfaces for Catalytic Isopropanol Oxidation over Size-Controlled Platinum Nanoparticles. *J. Am. Chem. Soc.* **2014**, *136* (29), 10515–10520.

(5) Yokoyama, D. Molecular Orientation in Small-Molecule Organic Light-Emitting Diodes. *J. Mater. Chem.* **2011**, *21* (48), 19187–19202.

(6) Yokohama, D.; Setoguchi, Y.; Sakaguchi, A.; Suzuki, M.; Adachi, C. Orientation Control of Linear-Shaped Molecules in Vacuum-Deposited Organic Amorphous Films and Its Effect on Carrier Mobilities. *Adv. Funct. Mater.* **2010**, *20*, 386–391.

(7) Sergeyev, S.; Pisula, W.; Geerts, Y. H. Discotic Liquid Crystals: A New Generation of Organic Semiconductors. *Chem. Soc. Rev.* **2007**, *36* (12), 1902–1929.

(8) Chen, H. P.; Ou, J. J.; Chen, S. H. Glassy Liquid Crystals as Self-Organized Films for Robust Optoelectronic Devices. In *Nanoscience with Liquid Crystals*; Li, Q., Ed.; Springer International Publishing, 2014; pp 179–208.

(9) Wei, S. K. H.; Chen, S. H. Spatially Resolved Lasers Using a Glassy Cholesteric Liquid Crystal Film with Lateral Pitch Gradient. *Appl. Phys. Lett.* **2011**, *98* (11), 111112.

(10) Islam, A.; Rabbani, M.; Bappy, M. H.; Miah, M. A. R.; Sakib, N. A Review on Fabrication Process of Organic Light Emitting Diodes. In *2013 International Conference on Informatics, Electronics and Vision (ICIEV)*; IEEE, 2013; pp 1–5.

(11) Swallen, S. F.; Kearns, K. L.; Mapes, M. K.; Kim, Y. S.; McMahon, R. J.; Ediger, M. D.; Wu, T.; Yu, L.; Satija, S. Organic Glasses with Exceptional Thermodynamic and Kinetic Stability. *Science (80-.).* **2007**, *315* (5810), 353–356.

(12) Gómez, J.; Jiang, J.; Gujral, A.; Huang, C.; Yu, L.; Ediger, M. D. Vapor Deposition of a Smectic Liquid Crystal: Highly Anisotropic, Homogeneous Glasses with Tunable Molecular Orientation. *Soft Matter* **2016**, *12* (11), 2942–2947.

(13) Gujral, A.; Gómez, J.; Jiang, J.; Huang, C.; O'Hara, K. A.; Toney, M. F.; Chabinyc, M. L.; Yu, L.; Ediger, M. D. Highly Organized Smectic-like Packing in Vapor-Deposited Glasses of a Liquid Crystal. *Chem. Mater.* **2017**, *29*, 849–858.

(14) Gujral, A.; Gomez, J.; Ruan, S.; Toney, M. F.; Bock, H.; Yu, L.; Ediger, M. D. Preparing Highly

Organized Glasses of Discotic Liquid Crystalline Systems by Vapor Deposition. *Chem. Mater. submitted*.

(15) Dalal, S. S.; Walters, D. M.; Lyubimov, I.; de Pablo, J. J.; Ediger, M. D. Tunable Molecular Orientation and Elevated Thermal Stability of Vapor-Deposited Organic Semiconductors. *Proc. Natl. Acad. Sci. U. S. A.* **2015**, *112* (14), 4227–4232.

(16) Walters, D. M.; Antony, L.; de Pablo, J. J.; Ediger, M. D. Influence of Molecular Shape on the Thermal Stability and Molecular Orientation of Vapor-Deposited Organic Semiconductors. *J. Phys. Chem. Lett.* **2017**, *Accepted*.

(17) Gujral, A.; O'Hara, K. A.; Toney, M. F.; Chabinyc, M. L.; Ediger, M. D. Structural Characterization of Vapor-Deposited Glasses of an Organic Hole Transport Material with X-Ray Scattering. *Chem. Mater.* **2015**, *27* (9), 3341–3348.

(18) Karbovnyk, I. D.; Olenych, I.; Kukhta, I. N.; Lugovskii, A.; Sasnouski, G.; Chutora, T.; Luchechko, A. P.; Khalakhan, I.; Kukhta, A. Electric Field Oriented Nanostructured Organic Thin Films with Polarized Luminescence. *J. Fluoresc.* **2009**, *19* (6), 989–996.

(19) Diao, Y.; Shaw, L.; Bao, Z.; Mannsfeld, S. C. B. Morphology Control Strategies for Solution-Processed Organic Semiconductor Thin Films. *Energy Environ. Sci.* **2014**, *7* (7), 2145–2159.

(20) Diao, Y.; Tee, B. C.-K.; Giri, G.; Xu, J.; Kim, D. H.; Becerril, H. a; Stoltenberg, R. M.; Lee, T. H.; Xue, G.; Mannsfeld, S. C. B.; Bao, Z. Solution Coating of Large-Area Organic Semiconductor Thin Films with Aligned Single-Crystalline Domains. *Nat. Mater.* **2013**, *12* (7), 665–671.

(21) Brian, C. W.; Yu, L. Surface Self-Diffusion of Organic Glasses. *J. Phys. Chem. A* **2013**, *117* (50), 13303–13309.

(22) Stöhr, J.; Samant, M. . Liquid Crystal Alignment by Rubbed Polymer Surfaces: A Microscopic Bond Orientation Model. *J. Electron Spectros. Relat. Phenomena* **1999**, *98–99*, 189–207.

(23) Banerjee, S.; Hemraj-Benny, T.; Sambasivan, S.; Fischer, D. A.; Misewich, J. A.; Wong, S. S. Near-Edge X-Ray Absorption Fine Structure Investigations of Order in Carbon Nanotube-Based Systems †. *J. Phys. Chem. B* **2005**, *109* (17), 8489–8495.

(24) Zhang, W.; Nefedov, A.; Naboka, M.; Cao, L.; Wöll, C. Molecular Orientation of Terephthalic Acid Assembly on Epitaxial Graphene: NEXAFS and XPS Study. *Phys. Chem. Chem. Phys.* **2012**, *14* (29), 10125.

(25) Hoffmann, H.; Zaera, F.; Mark Ormerod, R.; Lambert, R. M.; Lu Ping Wang; Tysoe, W. T. Discovery of a Tilted Form of Benzene Chemisorbed on Pd(111): As NEXAFS and Photoemission Investigation. *Surf. Sci.* **1990**, *232* (3), 259–265.

(26) Himmelhaus, M.; Gauss, I.; Buck, M.; Eisert, F.; Wöll, C.; Grunze, M. Adsorption of Docosanethiol from Solution on Polycrystalline Silver Surfaces: An XPS and NEXAFS Study. *J. Electron Spectros. Relat. Phenomena* **1998**, *92* (1–3), 139–149.

(27) Pedio, M.; Casero, E.; Nannarone, S.; Giglia, A.; Mahne, N.; Hayakawa, K.; Benfatto, M.; Hatada, K.; Felici, R.; Cerdá, J. I.; Alonso, C.; Martin-Gago, J. A. Nexafs Study of Nitric Oxide Layers Adsorbed from a Nitrite Solution onto a Pt(111) Surface. *J. Phys. Chem. C* **2008**, *112* (27), 10161–10166.

(28) Stöhr, J. *NEXAFS Spectroscopy*; Springer Series in Surface Sciences; Springer Berlin Heidelberg: Berlin, Heidelberg, 1992; Vol. 25.

(29) Grelet, E.; Dardel, S.; Bock, H.; Goldmann, M.; Lacaze, E.; Nallet, F. Morphology of Open Films of Discotic Hexagonal Columnar Liquid Crystals as Probed by Grazing Incidence X-Ray Diffraction. *Eur. Phys. J. E* **2010**, *31* (4), 343–349.

Chapter 6

Concluding remarks and future directions

Ankit Gujral

In this chapter, I will summarize the contributions of this body of work within the context of the field at large, divided into technique-based contributions and scientific contributions. I will also propose future directions of work, as well as a re-engineering of chamber components to increase productivity of researchers in the future. Sections 1 and 2 will focus on conclusions, while section 3 will focus on future directions, including (section 3.1) high-throughput NEXAFS measurements, and (section 3.2) determining bulk transformation length scales of glasses into supercooled liquids. And finally, in section 4, I will propose a modification to the vapor-deposition chamber to allow for easier co-deposition of materials from two independently controlled material sources (crucibles).

Adapting new techniques to characterize vapor-deposited organic glasses

X-ray scattering to determine molecular packing in glasses: X-ray scattering is the gold-standard for solid state characterization in crystalline materials. Glasses, however, are generally disordered materials, leading to weak scattering signatures dominated by the so-called amorphous halo,[1] a broad diffraction ring that is azimuthally isotropic in intensity. The origin of the halo is from the distribution of inter-atomic distances that are present in the glassy[2] material (and, as such, the halo is present in the region of reciprocal space corresponding to distance of 3-5 angstroms). Prior work by Ediger and coworkers had shown that some vapor-deposited glasses exhibited structural and optical anisotropy.[3–7] It is important to note that the structural anisotropy was not due to the formation of nanocrystallite-type structures, but rather a manipulation of molecular packing towards anisotropic configurations.[7] Configurations of varying levels of anisotropy could be accessed in vapor-deposited glasses by controlling deposition conditions during film fabrication. These findings were, in large part, the inspiration that led to developing the experiments I undertook.

As proof-of-principle, it needed to be shown that the structural anisotropy seen in a few systems previously was generally true of molecular glasses that exhibited optical anisotropy. Molecular glasses,

however, are poor candidates for X-ray scattering experiments for 2 reasons: 1) they are disordered, so Bragg-type diffraction phenomena that requires periodic structures in the film do not occur and 2) organic molecular systems consisting mainly of atoms with small radii, like carbon, oxygen and hydrogen, are low-Z systems, i.e., have small electron clouds to interact with the X-rays. These factors make determining any X-ray scattering signal on a lab X-ray source particularly challenging. To overcome this, the experimental conditions had to be manipulated, most importantly, with the introduction of a "knife-edge" into the instrument geometry, as shown elsewhere.[8] The knife-edge is a wedge made of Inconel 625, a nickel-based alloy that absorbs X-rays, built in-house. It is placed directly above the thin-film sample, between the source and the detector. In this geometry, it works by blocking stray background scatter of the incident beam as the beam traverses through the air, improving signal-to-noise in the resulting diffraction patterns. Along with the knife-edge, the samples prepared had to be thicker (roughly 1000 nm compared with 100-600 nm used for spectroscopic ellipsometry) to increase scattering volume in the experimental setup. The on-campus setup was also modified to allow for high throughput measurements, using the temperature gradient sample preparation technique developed[4] previously by researchers in the Ediger lab. With this on-campus setup, we could survey glasses prepared over large ranges of substrate temperatures for anisotropic scattering signatures. As preliminary trials, we were successfully able to do this for vapor-deposited glasses of TPD, indomethacin and a subset of the TNBs.

Having developed a screening procedure on-campus, it was possible to shortlist samples of interest to investigate at the Stanford Synchrotron Radiation Lightsource (SSRL). With the assistance of Michael Chabinyc's group at the University of California Santa Barbara and Michael F. Toney's group at SSRL, we optimized the grazing incidence X-ray scattering (GIXS) setup at beamline 11-3 for our requirements: setting detector distance, slit-widths and beamstop positions tailored to investigate organic thin films down to ~100 nm,[9] with periodic feature sizes of d ~ 35 Å to 3 Å, as well as develop in-situ annealing protocols. These parameters have continued to be used by Ediger group members in experiments that have followed. Aside from allowing for thinner films to be investigated, which is

important since functionalizing these materials in devices requires thin geometries, the synchrotron is also equipped with a large 2D detector, allowing for a quick reciprocal space mapping of the film. The reciprocal space map can be used to quantify the extent of anisotropy in highly disordered systems (Chapters 2 and 3), and solve for the structure of 3-dimensional unit cell-type structures (Chapter 4) of highly organized glassy materials.

X-ray scattering has proven to be useful, especially when combined with optical techniques to gain deeper insight into the molecular packing configurations accessible by vapor deposition. As researchers in the Ediger lab continue to make strides towards preparing films with more complex structures GIXS will grow in its usefulness to characterize the films.

X-ray Absorption Spectroscopy to determine depth-dependent molecular orientation in glasses and supercooled liquids: A mechanism for the origin of structural and optical anisotropy in vapor-deposited glasses was posited based on atomistic and coarse-grained molecular dynamics (MD) simulations on supercooled liquids of a few molecular systems.[10,11] The systems were rod-shaped and disc-shaped non-mesogens. The mechanism relies on the fact that the vacuum interface of the supercooled liquid has anisotropic molecular orientation.

With the assistance of Dennis Nordlund at SSRL, a Near-Edge X-ray Absorption Fine Structure (NEXAFS) spectroscopy protocol was developed at beamline 8-2, allowing for automated sample alignment and in-situ temperature control, to get experimental evidence of a monolayer of molecules with anisotropic orientation near the vacuum interface supercooled liquids and glasses. (This setup may be modified such that the high-throughput temperature gradient sample geometry may be adopted for NEXAFS runs in the future; detailed description in 6.3.1). NEXAFS spectroscopy to determine molecular orientation works on the "search-light effect" principle. When a polarized incident beam is used, the absorption spectrum depends on the angular relationship between the polarization state of the incident beam and the transition dipole of the excitation, by a cosine-squared law (i.e., an absorption occurs when the polarization state and the transition "line up" and does not occur when they are perpendicular to each

other).[12] This anisotropic absorption can be used to determine an average tilt angle of the transition dipole.[13,14] In the case of a 1s-to-π* transition in a benzene moiety, the absorption maximum occurs perpendicular to the plane of the benzene ring. Therefore, qualitatively, if a higher absorption is seen when the sample is illuminated with X-rays at the 1s-to-π* energy at a glancing incidence than a normal incidence with the polarized beam, it can be inferred that there is a larger population of benzene rings laying in-plane.

Scientific contributions of this body of work

A recent push in materials science has been towards preparing organic films with controllable microstructures for organic electronic and optoelectronic applications. Depending on the application, preferential face-on or edge-on packing arrangements can be advantageous. In non-mesogenic systems, the extent of structural anisotropy is relatively small, but still quantifiable by X-ray scattering anisotropy, as shown in Chapter 2. To prepare films that were highly anisotropic, we turned to liquid crystal-forming mesogens, with their penchant to self-assemble into highly ordered structures in equilibrium. We investigated how substrate temperature during deposition ($T_{substrate}$) affects the structure in vapor-deposited glasses of calamitic (rod-shaped; section 6.2.1) and discotic (disc-shaped) mesogens (section 6.2.2) in Chapters 3 and 4, respectively. In 6.2.3, I briefly discuss the experimental evidence collected to verify a mechanism proposed to explain the origin of structural anisotropy in vapor-deposited glasses as described in Chapter 5.

Calamitic liquid crystals form highly tunable structures by vapor deposition. Itraconazole, a model smectic liquid crystal former, was shown to exhibit not only highly organized structures upon vapor-deposition, but also exhibit structures that could not be accessed in equilibrium or by long annealing.[15] In equilibrium, itraconazole forms smectic layers above the glass transition temperature. When deposited at or above T_g, monodomain films of layered itraconazole were prepared that would maintain the smectic-like layering even after the film was cooled to below T_g, with an average tilt angle of 27 degrees from the

substrate normal. Decreasing $T_{substrate}$ found that layer-spacing could be monotonically decreased as well, until the average molecular tilt angle was roughly 55 degrees (at a $T_{substrate}$ ~ 307 K). In films prepared at $T_{substrate}$ less than roughly 307 K, the molecules were almost exclusively face-on with an average tilt angle of 76 degrees. Perhaps most remarkably, the vapor-deposited films prepared above T_g were more highly organized than a film of similar thickness annealed above T_g for one week, showcasing the potential advantages of vapor deposition over thermal annealing.

Discotic liquid crystals form highly organized columnar structures by vapor deposition. In equilibrium, columnar discotic mesogens molecular columns that further aggregate into either hexagonal or rectangular (distorted hexagonal) superstructures.[16] The direction of these columns, either perpendicular or parallel to the substrate, in equilibrium systems is dependent on the boundary conditions at the substrate (and/or vacuum) interfaces.[17] We showed for two mesogen systems that, by controlling $T_{substrate}$ during deposition, glasses with columns propagating in- or out-of-plane could be formed. At $T_{substrate}$ ~ $0.75T_g$, the columns propagate out-of-plane and the molecules are laying face-on, while at $T_{substrate}$ ~ T_g, the columns propagate in-plane (albeit randomly propagating in-plane. The films prepared at high $T_{substrate}$ were particularly highly ordered with domain-like formations observed on the free surface, as well. These results were in stark contrast to the non-mesogen disc-shaped system investigated that showed no domain-like structures and did not exhibit any sharp diffraction peaks associated with long range columnar packing motifs.

Molecular orientation near the vacuum interface. To explain the motivation behind this study, it is illustrative to revisit the mechanism[10,11] proposed in the literature on the origin of anisotropy in vapor deposited films. The mechanism proposes that the anisotropic nature and the high kinetic stability of vapor-deposited glasses can be traced by to the enhanced surface mobility observed at the vacuum interface of organic glasses. As molecules are vapor-deposited, they land at the vacuum interface where they can have up to 8 orders of magnitude higher molecular mobility to rearrange than when trapped in the bulk of a glass. During the short residence time at the vacuum interface, the molecule partially

equilibrates, before getting buried by the next set of molecules to be deposited. The extent of equilibration depends on the length of residence time (controlled by deposition rate) and the mobility at the surface (controlled by the substrate temperature during deposition, $T_{substrate}$). The anisotropy arises because the partial equilibration leads the molecules to rearrange in an anisotropic configuration because, as per the molecular dynamics simulations[10,11] of the liquids, these are the preferred configurations at a vacuum interface in equilibrium. Experimentally measuring the molecular orientation near the vacuum interface would let us test the validity of the mechanism.

NEXAFS spectroscopy was used to determine the molecular orientation near the vacuum interface and deeper into the bulk of the film for 2 systems: m-MTDATA and phenanthroperylene-ester, a non-mesogen and columnar mesogen, respectively. We experimentally verified that the MD simulations were a reasonable picture for the nature of the vacuum interface of the liquids, providing evidence towards verifying the proposed mechanism. We also empirically extended the proposed mechanism to mesogens by determining molecular orientation near the vacuum interface for liquid crystalline systems, as well, that exhibit very different bulk anisotropy upon vapor-deposition than non-mesogenic systems. Based on the mechanism, one would predict an opposite anisotropy near the vacuum interface of supercooled liquids (and by proxy, liquid-cooled glasses) for mesogens (edge-on orientation) as opposed to non-mesogens (face-on orientation). We determined this to be true, and the results are shared in Chapter 5.

Future directions

6.3.1 High-throughput NEXAFS experiments

The pre-existing hardware at beamline 8-2 can be easily adapted to be used for temperature gradient samples. A change in the command line that controls the instrument is enough to modify the protocol to be used. In Figure 1, I have provided an example of what the modified SPEC command line

would look like along with a schematic showing the experimental setup if using a temperature gradient sample. Every command allocates a certain area defined by positions on the NEXAFS sample holder "stick," and the measurement occurs at the center of that allocated area, as described in Figure 1.

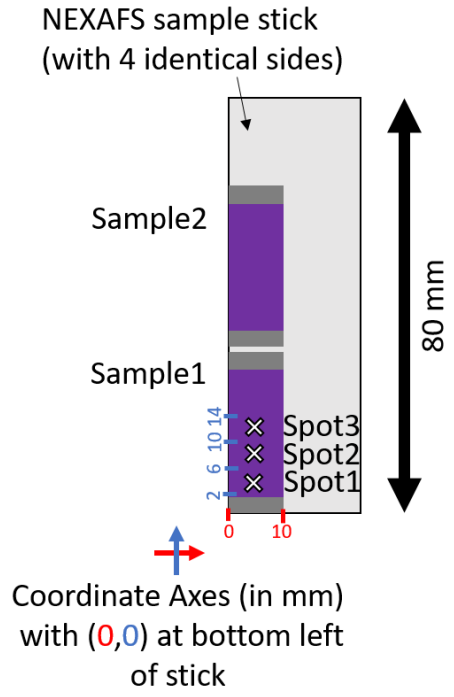


```
# Everything between "#" is a comment (not code) #
htxs_set_sample_info 1 1 "sample1 spot1"  0 -0.5 2  10 -0.5 6

# The above command defines an area with filename "sample1 spot1"
section 101 (6-2=)4 by (10-0=)10 mm area (0.5 mm thick substrate)#

htxs_set_sample_info 1 2 "sample1 spot2"  0 -0.5 6  10 -0.5 10
htxs_set_sample_info 1 3 "sample1 spot3"  0 -0.5 10  10 -0.5 14
# This can be run with smaller limiting dimensions if needed, keeping
in mind spot size is about 1 mm#
.
.
.
```

Figure 1. One of the NEXAFS sample holders available at beamline 8-2 is shown above, with two temperature gradient samples shown mounted on. The SPEC code shown below will execute the measurements indicated by the white X marks. The demarcations of spot position are not to scale for

illustrative purposes, and are representative of the areas of interest on the sample as defined by the code below. Measurements occur at the center of an area of interest.

Determining the length-scales associated with bulk vapor-deposited stable glass transformations

Stable glasses, unlike liquid-cooled glasses, transform via a growth front mechanism[18] when annealed above the glass transition temperature, T_g. (Liquid-cooled glasses, on the other hand, inherit dynamic heterogeneity from the liquid, and so transform via a bulk mechanism where some regions transform sooner than others, but on a scale of 5 nm or larger looks homogeneous). The growth-front transformation of stable glasses is related to the high molecular mobility[19] at the free surface of a film, and the very efficient molecular packing of the bulk of a stable glass. When the stable glass is annealed above T_g, the molecules in the bulk are very densely packed (compared with the packing efficiency in a liquid-cooled glass) but the molecules at the free surface are able to rearrange (due to enhanced mobility/free volume at the free surface). This leads to the transformation of the top layer of the film into a supercooled liquid, and the layer of glass right below it has a liquid-glass interface, where it too can transform. And so, this front of enhanced mobility cascades through the rest of the film.

By reducing mobility at the free surface (by capping the film with a higher T_g material or sputtering a metal on top), the growth front mechanism can be impeded. In this case, the glass may begin to transform from within the bulk. This is also observed in very thick (uncapped) films of stable glasses where, it is inferred that, both a bulk and a growth front process occur. One way to think about this is that the bulk transformation process is stochastic, and the larger the volume of bulk the higher the chances of this process being initiated.

The bulk transformation process in stable glasses described above has not been characterized. Small angle X-ray scattering (SAXS) may allow us to gain insight into the size and dynamics of the growth of supercooled liquid regions within a glassy matrix as a glass is transformed. Scattering relies on

fluctuations in electron density, and the density changes between the supercooled liquid and the glass can be about 1.5-2% (depending on glass preparation and annealing temperature). Similar studies have previously been shown in cases of polyamorphism of an organic system[20] and transformation kinetics of a metallic glass,[21]. It has been observed in vapor-deposited glasses of indomethacin that for films about 1 micron or thicker,[18] the bulk process competes with the growth front mechanism. Assuming a roughly 1-micron distance between supercooled liquid-initiation sites in a thicker vapor-deposited indomethacin film (on the order of 10s of microns), a $q \sim 0.01$ $Å^{-1}$ would be required to measure such density fluctuations. This is accessible, for instance, at the Advanced Photon Source in Argonne, IL. Beamline 8-ID-I could be setup with a detector distance of about 3.5 m, and a photon energy of 7.35keV, allowing for the small-angle reciprocal space mapping. SSRL beamline 1-5, also optimized for SAXS measurements, is equipped with a variable 4.6-16 keV source, a variable detector distance and a temperature-controlled stage, required for annealing the sample during the run. A similar geometry may be setup there. Aside from just the size of the density fluctuations, R_g, the shape and dispersity of the regions can also be determined as described schematically in Figure 2.[22] The plot is a schematic of the dataset expected from a sample with polydisperse (in shape and size) set of density fluctuations. The plot can be divided into 2 regimes:[1] 1) The plateau of intensity at low q values, or the Guinier regime ($q*R_g < 1$). Where the plot "rolls over" (short dashed line) is representative of the average size, R_g. 2) At higher q, the intensity goes as q^{-P} where P is the Porod exponent. This provides information about the shape of the fluctuations, with extremes at $P = 4$ corresponding to perfectly spherical and $P = 1$ corresponding to rod-shaped fluctuations.[22]

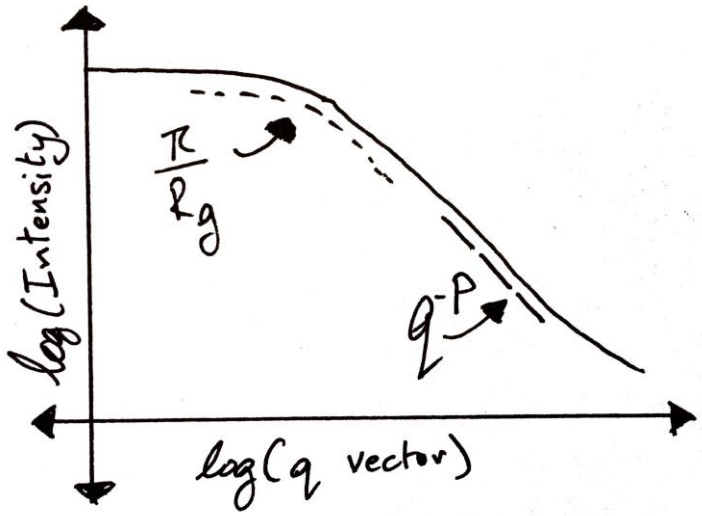

Figure 2. Schematic of small angle X-ray scattering data from a sample with polydisperse density fluctuations. The low q Guinier regime describes the average size of fluctuations, R_g, while the high q Porod exponent, P, describes the shape of the fluctuations as described in the text. Schematic based on data presented in Sinha et al.[22] and Cherny et al.[23]

New crucible shield design for two-component co-depositions

Two-component glasses with carefully controlled composition are of fundamental and application interest. Previous work in the Ediger group has shown that preparing films with two components with controllable composition is possible.[3] There are two approaches to achieving this: 1) pre-mixing a known composition into a single crucible and running a single-source deposition, and 2) having two independently controlled crucibles of pure material and maintaining their relative rates of deposition to achieve the desired composition. The second of the two strategies allows for much more experimental flexibility and less wasted material. However, when designing such experiments with colleagues, some recurring engineering issues impeded progress. Most crucial of these was the fact that the crucibles had to be rotated around a fixed axis to measure independent rates of deposition before exposing the substrates to the vapor. The crucibles are connected to the vacuum feedthrough via crimp connectors, and upon rotating, these connectors would often come lose due to the tension applied to them when the crucibles were moved. To work around this, I have designed a shield that can be mounted on the same rotational axis that the crucible holders are currently mounted on while the crucibles will be set at the bottom of the chamber (it may help to add weight to the bottom of the crucible holder for stability). The shield would allow for 3 positions, as shown in Figure 3, that expose either crucible one at a time, or both crucibles simultaneously, allowing for a precise determination of rate of deposition from both sources before beginning the deposition by dropping the substrate shield. Figure 4 includes a blueprint to construct the shield.

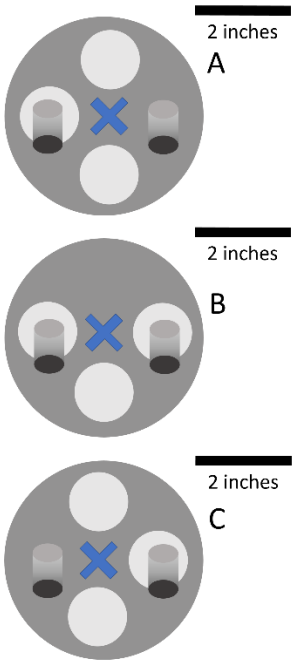

Figure 3. Top-down view of the proposed shield shown relative to position of crucibles in the vacuum chamber. The rotation axis of the shield is denoted by the blue X. Positions A, B and C allow for deposition from only the left crucible, both crucibles and only the right crucible, respectively.

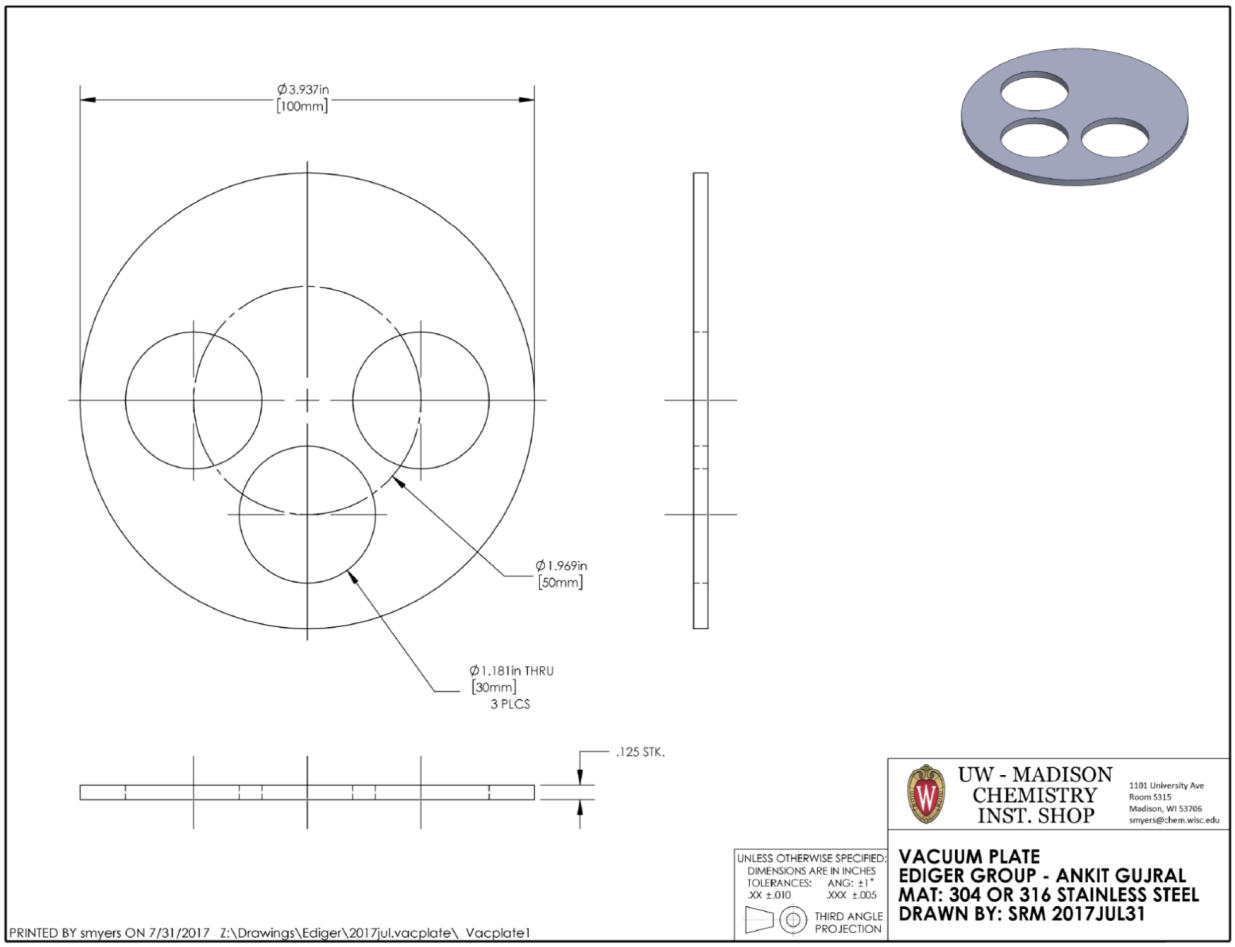

Figure 4. A blueprint for the proposed shield. Note the screw hole in the center of the disk has not been specified, and should be added once the correct mount has been identified (a 1/8th inch screw will be compatible with the current feedthrough setup, but may need to be modified depending on user need).

References

(1) Guinier, A. *X-Ray Diffraction in Crystals, Imperfect Crystals and Amorphous Bodies*; W.H. Freeman: San Francisco, 1963.

(2) Finney, J. L. Bernal's Road to Random Packing and the Structure of Liquids. *Philos. Mag.* **2013**, *93* (31–33), 3940–3969.

(3) Jiang, J.; Walters, D. M.; Zhou, D.; Ediger, M. D. Substrate Temperature Controls Molecular Orientation in Two-Component Vapor-Deposited Glasses. *Soft Matter* **2016**, *12* (13), 3265–3270.

(4) Dalal, S. S.; Fakhraai, Z.; Ediger, M. D. High-Throughput Ellipsometric Characterization of Vapor-Deposited Indomethacin Glasses. *J. Phys. Chem. B* **2013**, *117* (49), 15415–15425.

(5) Dawson, K. J.; Zhu, L.; Yu, L.; Ediger, M. D. Anisotropic Structure and Transformation Kinetics of Vapor-Deposited Indomethacin Glasses. *J. Phys. Chem. B* **2011**, *115* (3), 455–463.

(6) Dalal, S. S.; Ediger, M. D. Molecular Orientation in Stable Glasses of Indomethacin. *J. Phys. Chem. Lett.* **2012**, *3* (10), 1229–1233.

(7) Dawson, K.; Kopff, L. A.; Zhu, L.; McMahon, R. J.; Yu, L.; Richert, R.; Ediger, M. D. Molecular Packing in Highly Stable Glasses of Vapor-Deposited Tris-Naphthylbenzene Isomers. *J. Chem. Phys.* **2012**, *136* (9), 94505.

(8) Renaud, G.; Lazzari, R.; Leroy, F. Probing Surface and Interface Morphology with Grazing Incidence Small Angle X-Ray Scattering. *Surf. Sci. Rep.* **2009**, *64* (8), 255–380.

(9) Baker, J. L.; Jimison, L. H.; Mannsfeld, S.; Volkman, S.; Yin, S.; Subramanian, V.; Salleo, A.; Alivisatos, A. P.; Toney, M. F. Quantification of Thin Film Crystallographic Orientation Using X-Ray Diffraction with an Area Detector. *Langmuir* **2010**, *26* (11), 9146–9151.

(10) Dalal, S. S.; Walters, D. M.; Lyubimov, I.; de Pablo, J. J.; Ediger, M. D. Tunable Molecular

Orientation and Elevated Thermal Stability of Vapor-Deposited Organic Semiconductors. *Proc. Natl. Acad. Sci. U. S. A.* **2015**, *112* (14), 4227–4232.

(11) Walters, D. M.; Antony, L.; de Pablo, J. J.; Ediger, M. D. Influence of Molecular Shape on the Thermal Stability and Molecular Orientation of Vapor-Deposited Organic Semiconductors. *J. Phys. Chem. Lett.* **2017**, *Accepted*.

(12) Stöhr, J. *NEXAFS Spectroscopy*; Springer Series in Surface Sciences; Springer Berlin Heidelberg: Berlin, Heidelberg, 1992; Vol. 25.

(13) Stöhr, J. Liquid Crystal Alignment on Carbonaceous Surfaces with Orientational Order. *Science (80-.).* **2001**, *292* (5525), 2299–2302.

(14) Wegner, H.; Weiss, K.; Grunze, M.; Wöll, C. Determination of Molecular Orientation in Ultrathin Liquid Crystal. Films on Solid Substrates Using X-Ray Absorption Spectroscopy. *Appl. Phys. A Mater. Sci. Process.* **1997**, *65* (3), 231–234.

(15) Gujral, A.; Gómez, J.; Jiang, J.; Huang, C.; O'Hara, K. A.; Toney, M. F.; Chabinyc, M. L.; Yu, L.; Ediger, M. D. Highly Organized Smectic-like Packing in Vapor-Deposited Glasses of a Liquid Crystal. *Chem. Mater.* **2017**, *29*, 849–858.

(16) Sergeyev, S.; Pisula, W.; Geerts, Y. H. Discotic Liquid Crystals: A New Generation of Organic Semiconductors. *Chem. Soc. Rev.* **2007**, *36* (12), 1902–1929.

(17) Grelet, E.; Dardel, S.; Bock, H.; Goldmann, M.; Lacaze, E.; Nallet, F. Morphology of Open Films of Discotic Hexagonal Columnar Liquid Crystals as Probed by Grazing Incidence X-Ray Diffraction. *Eur. Phys. J. E* **2010**, *31* (4), 343–349.

(18) Kearns, K. L.; Ediger, M. D.; Huth, H.; Schick, C. One Micrometer Length Scale Controls Kinetic Stability of Low-Energy Glasses. *J. Phys. Chem. Lett.* **2010**, *1* (1), 388–392.

(19) Brian, C. W.; Yu, L. Surface Self-Diffusion of Organic Glasses. *J. Phys. Chem. A* **2013**, *117* (50),

13303–13309.

(20) Alba-Simionesco, C.; Tarjus, G. Experimental Evidence of Mesoscopic Order in the Apparently Amorphous Glacial Phase of the Fragile Glass Former Triphenylphosphite. *Europhys. Lett.* **2007**, *52* (3), 297–303.

(21) Matsuura, M.; Fukunaga, T.; Mizutani, U. Evolution of Medium-Range Order of Mg0.5Ni0.3La0.2 Metallic Glass at a Supercooled Liquid Temperature. *Mater. Sci. Eng.* **1994**, *A179/A180*, 464–468.

(22) Sinha, S. K.; Sirota, E. B.; Garoff, S. X-Ray and Neutron Scattering from Rough Surfaces. *Phys. Rev. B* **1988**, *38* (4), 2297.

(23) Cherny, A. Y.; Anitas, E. M.; Osipov, V. A.; Kuklin, A. I. Small-Angle Scattering from Multiphase Fractals. *J. Appl. Crystallogr.* **2014**, *47* (1), 198–206.